(2)

AEFA PROJECT NO. 83-13

US ARMY
AVIATION
SYSTEMS COMMAND

JUH-1H REDESIGNED PNEUMATIC BOOT DEICING SYSTEM FLIGHT TEST EVALUATION

MATTHEW S. GRAHAM
PROJECT OFFICER/ENGINEER

LORAN A. HAWORTH
CPT, AV
PROJECT PILOT

JACK L. KIMBERLY
CPT, AV
PROJECT PILOT/ENGINEER

AUGUST 1987

FINAL REPORT

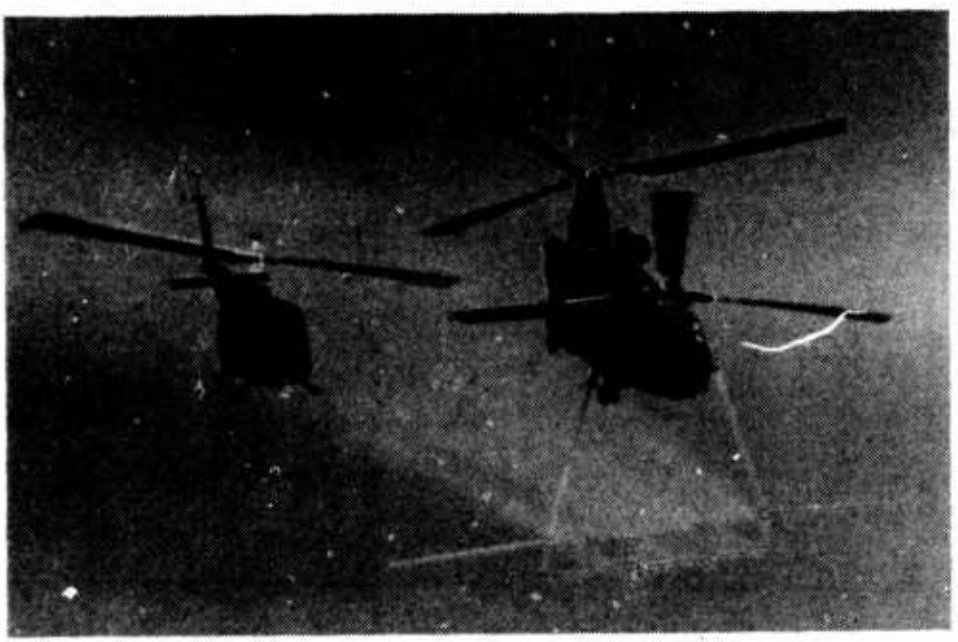

Approved for public release; distribution unlimited.

AVIATION ENGINEERING FLIGHT ACTIVITY
EDWARDS AIR FORCE BASE, CALIFORNIA 93523 - 5000

DISCLAIMER NOTICE

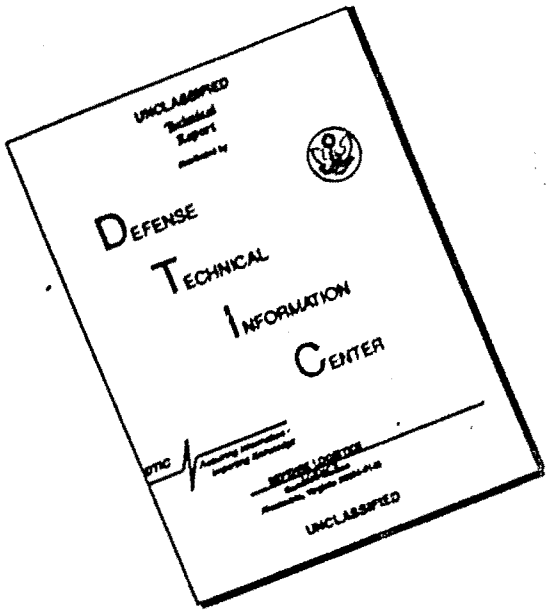

THIS DOCUMENT IS BEST QUALITY AVAILABLE. THE COPY FURNISHED TO DTIC CONTAINED A SIGNIFICANT NUMBER OF PAGES WHICH DO NOT REPRODUCE LEGIBLY.

DISCLAIMER NOTICE

The findings of this report are not to be construed as an official Department of the Army position unless so designated by other authorized documents.

DISPOSITION INSTRUCTIONS

Destroy this report when it is no longer needed. Do not return it to the originator.

TRADE NAMES

The use of trade names in this report does not constitute an official endorsement or approval of the use of the commercial hardware and software.

UNCLASSIFIED
SECURITY CLASSIFICATION OF THIS PAGE

REPORT DOCUMENTATION PAGE

Form Approved OMB No. 0704-0188

1a. REPORT SECURITY CLASSIFICATION UNCLASSIFIED	1b. RESTRICTIVE MARKINGS
2a. SECURITY CLASSIFICATION AUTHORITY U.S. ARMY AVIATION SYSTEMS COMMAND	3. DISTRIBUTION/AVAILABILITY OF REPORT Approved for public release, distribution unlimited.
2b. DECLASSIFICATION/DOWNGRADING SCHEDULE	
4. PERFORMING ORGANIZATION REPORT NUMBER(S) AEFA PROJECT NO. 83-13	5. MONITORING ORGANIZATION REPORT NUMBER(S)
6a. NAME OF PERFORMING ORGANIZATION U.S. ARMY AVIATION ENGINEERING FLIGHT ACTIVITY 6b. OFFICE SYMBOL (If applicable)	7a. NAME OF MONITORING ORGANIZATION
6c. ADDRESS (City, State, and ZIP Code) EDWARDS AIR FORCE BASE, CALIFORNIA 93523-5000	7b. ADDRESS (City, State, and ZIP Code)
8a. NAME OF FUNDING/SPONSORING ORGANIZATION U.S. ARMY AVIATION SYSTEMS COMMAND 8b. OFFICE SYMBOL (If applicable)	9. PROCUREMENT INSTRUMENT IDENTIFICATION NUMBER
8c. ADDRESS (City, State, and ZIP Code) 4300 GOODFELLOW BLVD. ST. LOUIS, MO 63120-1998	10. SOURCE OF FUNDING NUMBERS PROGRAM ELEMENT NO. 97633 / PROJECT NO. / TASK NO. / WORK UNIT ACCESSION NO.

11. TITLE (Include Security Classification)
JUH-1H Redesigned Pneumatic Boot Deicing System Flight Test Evaluation. Unclassified

12. PERSONAL AUTHOR(S)
Matthew S. Graham, Loran A. Haworth, Jack L. Kimberly

13a. TYPE OF REPORT	13b. TIME COVERED	14. DATE OF REPORT (Year, Month, Day)	15. PAGE COUNT
FINAL	FROM 83/11/15 TO 86/3/7	August 1987	144

16. SUPPLEMENTARY NOTATION

17. COSATI CODES			18. SUBJECT TERMS (Continue on reverse if necessary and identify by block number)
FIELD	GROUP	SUB-GROUP	Artificial & Natural Icing Conditions, Feasibility Testing, Limited Artificial Rain Erosion Tests, Pneumatic Boot Deicing System (PBDS), Performance & Handling Qualities

19. ABSTRACT (Continue on reverse if necessary and identify by block number)

The U.S. Army Aviation Engineering Flight Activity conducted an evaluation of the Pneumatic Boot Deicing System (PBDS) with two pneumatic deicer boot designs, referred to as second and third generation. These designs were refinements intended to rectify problem areas identified in an earlier (first generation) design. The objective of the test was to conduct feasibility testing of the pneumatic system concept for deicing helicopter rotor blades in forward flight, and to assess any changes to aircraft performance and handling qualities. The test was conducted in four phases from 15 November 1983 to 7 March 1986. Phase 1 consisted of a ground and inflight structural loads survey which established an operational envelope. This phase was further subdivided into Phase 1A (second generation) and Phase 1B (third generation). The third generation design exhibited high pitch link loads in unaccelerated forward flight. An attempt was made to correct this, but failure of instrumentation to transmit rotor system loads caused termination of testing of the third generation configuration. Phase 2 consisted of forward flight testing in artificial and natural icing conditions of the second generation

20. DISTRIBUTION/AVAILABILITY OF ABSTRACT	21. ABSTRACT SECURITY CLASSIFICATION
☐ UNCLASSIFIED/UNLIMITED ☒ SAME AS RPT. ☐ DTIC USERS	UNCLASIFIED

22a. NAME OF RESPONSIBLE INDIVIDUAL	22b. TELEPHONE (Include Area Code)	22c. OFFICE SYMBOL
SHEILA R. LEWIS	(805)277-4024	SAVTE-PR

DD Form 1473, JUN 86 — Previous editions are obsolete. — SECURITY CLASSIFICATION OF THIS PAGE
UNCLASSIFIED

A

Block No. 19

design only. A total of 7.2 hours were flown in artificial icing conditions and 5.1 in natural conditions. The PBDS successfully deiced the main rotor blade under all conditions tested. Phase 3 consisted of limited artificial rain erosion tests of the second generation design. A total of 6.1 hours were flown in the artificial rain environmert. Only small, almost imperceptible pitting was noted on the outboard, non-inflatable section of the boots. Phase 4 consisted of performance and handling qualities evaluation of the second generation design. Hover and level flight performance were greatly improved over the first generation, but a significant performance penalty still exists. Handling qualities were essentially unchanged from the standard UH-1H. Two unsatisfactory and six undesirable reliability and maintainability characteristics were identified.

TABLE OF CONTENTS

INTRODUCTION

BACKGROUND

1. In 1979, the National Aeronautics and Space Administration (NASA) in cooperation with the B. F. Goodrich Company (BFG) initiated a program to evaluate the feasibility of pneumatic deicing systems for helicopter rotor blades. The concept was revived by development of an erosion resistant polyurethane elastomer (trade name ESTANE). Wind tunnel icing tests conducted by NASA's Lewis Research Center and BFG indicated that it might be feasible to produce a pneumatically deiced rotor blade using ESTANE for the deicer (ref 1, app A). To flight test the concept, NASA-Ames Research Center requested the assistance of the U.S. Army Aviation Systems Command (AVSCOM) (ref 2, app A). AVSCOM subsequently tasked the U.S. Army Aviation Engineering Flight Activity (AEFA) to conduct flight tests to further evaluate the feasibility of the pneumatic deicing concept for helicopter rotor systems. Limited artificial icing tests during the 1982-83 winter were conducted at a hover with pneumatic deicers installed on a JUH-1H (AEFA Project No. 81-11) helicopter. Icing tests showed that the pneumatic deicers successfully deiced the rotor blades under all conditions tested (ref 3). Several problem areas were identified during these tests which were corrected by design change and component replacement (ref 3).

2. Overall support of the pneumatic testing and research for pneumatic deicer was transferred to NASA-Lewis from NASA-Ames in 1983 while NASA-Ames still provided technical assistance. AEFA was tasked through AVSCOM by NASA-Lewis to test and evaluate the pneumatic concept for helicopter rotor system during the 1983-1984 icing season in artificial and natural icing conditions during forward flight. After completion of forward flight icing tests BFG further refined the design of the deicer boots in an effort to reduce performance penalties and solve the problem of internal bleeder material breakdown.

TEST OBJECTIVE

3. The objectives of this test were to conduct feasibility testing of the pneumatic system concept for deicing helicopter rotor blades in forward flight, and to assess any changes to aircraft performance and handling qualities.

DESCRIPTION

4. The test JUH-1H is a thirteen-place, single-engine helicopter using a single two-bladed teetering main rotor and pusher anti-torque rotor. The maximum gross weight of the helicopter is

9500 pounds. Power is provided by a Lycoming T53-L-13B free turbine engine rated at 1400 shaft horsepower (shp) on a sea level standard day. The helicopter is limited by the transmission to 1100 shp. A more detailed description may be found in reference 4, appendix A. The test JUH-1H helicopter USA S/N 70-16318 manufactured by Bell Helicopter Textron, Incorporated (BHTI) has been modified to incorporate a partial ice protection system (Kit A) described in reference 5, a rotor brake, cabin mounted and hub mounted video cameras and the Pneumatic Boot Deicing System (PBDS). Video cameras were only mounted during Phase 2 icing tests.

5. The second (and later, third) generation prototype ESTANE® deicer boot and leading edge airfoil nose piece were applied to the leading edge of a standard UH-1H rotor blade and were intended to remove accumulated ice through pneumatic expansion (inflation) of chordwise and spanwise tubes. A cross-section of the second generation deicer is shown in figure 7, appendix B. A cross-section of the third generation deicer is shown in figure 9. The PBDS also includes a modified main rotor mast, electrical and pneumatic slip rings, associated controllers, electrical components, and air supply components for providing engine bleed air to the PBDS components as shown in the simplified drawing in figure 10. Compressor bleed air from the engine is routed to the deicers in a single inflation activation cycle. A normal activation cycle consists of inflation of the deicer boots for approximately two seconds, followed by subsequent deflation of 12 to 16 seconds. A more detailed description of non-standard features of the test aircraft and the pneumatic deicing boots is contained in appendix B.

TEST SCOPE

6. The PBDS evaluation consisted of four basic phases (table 1). The flight loads survey for the second prototype PBDS (Phase 1A) was conducted at Edwards Air Force Base (EAFB), California during the period of 15 November through 15 December 1983. The flight loads survey for the third prototype PBDS (Phase 1B) was conducted at EAFB during the period 16 June through 12 September 1985 and 1 to 7 March 1986. Artificial and natural icing tests (Phase 2) were conducted from 3 January through 19 March 1984 in Duluth, Minnesota. Phase 3, rain erosion tests were conducted at EAFB, California from 12 through 27 June 1984, and Phase 4, performance and handling qualities tests on the second prototype PBDS were conducted at EAFB, California during 10 through 28 August 1984 and at Bakersfield, California during 31 March through 6 April 1985.

Table 1. Test Phases

Test Phase	Test	Blade Configuration
1A	Structural Loads Survey	Second Generation Deicer
1B		Third Generation Deicer
2	Forward Flight Artificial and Natural Icing Tests	Second Generation Deicer
3	Artificial Rain Erosion Tests	Second Generation Deicer
4	Performance and Handling Qualities	Clean Blades
		Second Generation Deicer

7. AEFA had overall responsibility for conduct of the test to include maintenance and instrumentation of the test helicopter. The main rotor system was instrumented for structural loads by BHTI. BFC furnished technical assistance and deicer maintenance expertise during the four phase test cycle. NASA-Lewis provided funding for the evaluation. Technical and engineering support was provided by NASA-Ames, AVSCOM and AEFA. NASA-Ames provided a dynamicist to monitor structural loads during Phase 1A and 2 testing. AVSCOM provided a dynamicist for Phase 1B testing.

8. The test aircraft was operated within the limitations of the operator's manual (refs 4 through 7, app A) as amended by the airworthiness release (ref 8). Flight tests were conducted at the general test conditions shown in table 2.

TEST METHODOLOGY

9. Established flight test techniques (refs 9 and 10) were used wherever possible throughout this evaluation. Test methods used are briefly discussed in the Results and Discussion section of this report, while unique and performance test methods are discussed in detail in appendix E. The Handling Qualities Rating Scale (HQRS) (fig. 1, app E), and the Vibration Rating Scale (VRS) (fig. 2) were used to supplement pilot's qualitative comments. Flight test data were recorded by hand, video and still cameras, and on-board magnetic tape. Six rotor system component loads were monitored real-time via telemetry (TM) during Phases 1A, 1B, and 2 to verify that loads were within allowable limits. A detailed listing of test instrumentation is contained in appendix D. Data analysis methods used are presented in appendix E.

Table 2. Test Conditions[1]

Test	Average Gross Weight (lb)	Average Density Altitude (ft)	Trim Calibrated Airspeed (kts)	Remarks	Deicer Boot Configuration
Loads Survey (Phase 1A)	7040-9500	300-7100	0-100	Second generation PBDS[2] ground and inflight structural tests	Deflated, inflated and vented
Loads Survey (Phase 1B)	7550-8600	4350-10,200	0-80	Third generation PBDS ground and inflight structural tests	Deflated, inflated and vented
Forward Flight Icing	7100-8100	0-10,600	70-90	Artificial and natural icing conditions	Deflated and inflated
Rain Erosion	7100-8000	7300-9300	80	Behind modified HISS[3]	Deflated
Hover Performance	N/A	1450	0	Standard blades. In-ground effect (5-foot skid height), tethered method	None
		4180	0	PBDS deflated. In-ground effect (5-foot skid height), tethered method	Deflated
Level Flight Performance	7380 8010 7190 8360 8980	5860 7180 10,790 11,170 11,730	35-110 35-90 35-80 35-80 35-80	Standard blades Zero sideslip	None
	7710 7950 8280	6030 8630 11,470	35-110 35-90 35-80	PBDS deflated Zero sideslip	Deflated
Low Speed Flight	7150-8000	300	0-20 KTAS[4] sideward and rearward 0-50 KTAS forward	9, 90, 180, 270 degree azimuths.	Deflated and vented
Control Positions in Trimmed Forward Flight	7580	6460	38-110		Deflated
Controllability	7700-7900	8360	80	Lateral and longitudinal	Deflated
Maneuvering Stability	7960	8740	80	Windup turns	Deflated

NOTES:

[1]Normal utility configuration, mid center of gravity.
[2]PBDS: Pneumatic Boot Deicing System.
[3]HISS: Helicopter Icing Spray System.
[4]KTAS: Knots true airspeed.

RESULTS AND DISCUSSION

GENERAL

10. The JUH-1H redesigned Pneumatic Boot Deicing System evaluation tested two prototype pneumatic deicer designs, referred to as second and third generation. The program was conducted in four phases (table 1) under the conditions shown in table 2. Phase 1 (divided into Phases 1A and 1B) was a ground and inflight structural loads survey which established an operational envelope. Monitored structural loads during Phase 1A demonstrate that the test helicopter with the second generation PBDS installed may be safely flown through the established envelope. During Phase 1B, however, excessive pitch link loads were encountered in unaccelerated forward flight. Phase 2, conducted in the vicinity of Duluth, Minnesota, consisted of artificial and natural icing conditions tests of the second generation deicers. These tests demonstrated that the PBDS satisfactorily deiced the main rotor blades under all conditions tested. Phase 3 consisted of limited rain erosion tests. This testing showed a minor, almost imperceptible pitting of the outboard section of the deicer boots. Phase 4 consisted of performance and handling qualities testing of the second generation only. Performance testing of the test helicopter were also conducted with standard clean blades to provide a baseline for comparison. These tests demonstrated that the second generation PBDS showed a significant reduction in drag from earlier reported testing of a previous PBDS design (ref 3, app A). Handling qualities were essentially unchanged from the standard UH-1H helicopter. System reliability and maintainability were documented throughout the evaluation. Eight problem areas were identified.

PHASE 1 STRUCTURAL LOADS SURVEY

General

11. Loads survey tests were conducted to establish a flight envelope for the UH-1H helicopter with the redesigned PBDS installed and were evaluated at the test conditions listed in tables 3 and 4.

12. For test purposes three blade deicer configurations were used: (1) deflated with vacuum, (2) inflated, representing the pneumatically expanded boot condition reached just after PBDS activation (a PBDS activation cycle is transient and consists of a single deicer inflation immediately followed by deflation), and (3) vented, representing a failure mode caused by loss of engine bleed air allowing the boots to partially inflate. PBDS temperatures were monitored at selected locations as described in

Table 3. Loads Survey Test Conditions (Phase 1A)

Test	Average Gross Weight (lb)	Average Density Altitude (ft)	Trim Calibrated Airspeed (kts)	Rotor Speed (rpm)	Pneumatic Boot Configuration
Dynamic System Engine Compatibility (Tied Down)	8710-9500	920	0	294 324	Deflated Inflated Air Supply Shutoff
Rapid Throttle Reductions (Tied Down)	8960-9000	1400	0	324	
Hover Dynamic System Engine Compatibility	7880-8000	1850	0	324	Deflated Inflated Air Supply Shutoff
Low Speed Flight	7150-8000	300	0-20 KTAS Sideward and Rearward 0-40 KTAS Forward	294 310 324	
Level Flight	7080-8000	7060	50-100	324	
Climbs and Descents	7010-8000	980-7800	60,90		
Maneuvering Turns	7040-7950	7100	90		
Auto Entry, Delay	7500-7610	5200	70,80,90		
Stabilized Autorotations	7500-7950	1000-5200	60,90		Air Supply Shutoff

Table 4. Loads Survey Test Conditions (Phase 1B)

Test	Average Gross Weight (lb)	Average Density Altitude (ft)	Trim Calibrated Airspeed (kts)	Rotor Speed (rpm)	Pneumatic Boot Configuration
Static Ground Runs	8400-8600	4350	0	310 320	Deflated Inflated Air supply shutoff
Hover	7550-7800	4600	0	322	Deflated Inflated Air supply shutoff
Forward and Sideward Accelerations and Declerations			0-40 Forward 0-20 Sideward		Deflated Inflated
Level Flight	7800-8000	10,200	0-80	310	Deflated Inflated Air supply shutoff

appendix D to determine if temperatures were in excess of system component qualification values. For Phase 1A a structural dynamicist from NASA-Ames monitored loads via TM to verify that loads during each test point were within allowable limits and would predictably remain so during the next test point. Further structural loads and dynamic analysis was completed by AVSCOM engineers. Monitoring of measured loads demonstrated that the test helicopter with the second generation PBDS from a structural loads standpoint may be flown through the established test envelope. No unusual or unexpected dynamic responses of the main rotor or control systems were noted as a result of the redesigned PBDS installation. Since aerodynamic changes to the boot were minimal for the third generation, discussions with the AVSCOM structural dynamicist led to the conclusion that only a limited loads survey was required. However, during forward flight testing with third generation boots, pitch link loads were encountered in excess of the endurance limit in unaccelerated forward flight in all three boot conditions. After modifications to the boot installation, further tests were begun but had to be terminated due to failure of instrumentation sliprings.

Ground Structural Tests

13. Phase 1A ground tests were conducted at a 9500 pound aircraft gross weight with the aircraft lightly secured by a clevis to a tie-down anchor. Rotor loads associated with the three boot conditions were monitored via TM during starting and acceleration to engine idle, to normal operating speed and to the maximum governing speed. The engine was shutdown and the rotor system inspected at the end of each acceleration to the different rotor speed settings. Once safe operation was established, engine power was then increased in increments of approximately 5 pounds per square inch (psi) of engine torque within allowable limits of engine power and tether load at the above rotor speeds. All loads monitored during Phase 1A ground structural tests remained below endurance limits as shown in tables 1 and 2, appendix F.

14. Dynamic system/engine compatibility tests were completed during Phase 1A at main rotor speeds of 294 and 324 rpm at three power settings (minimum, mid range and maximum) by cycling the collective control and antitorque pedals at the critical frequency of the dynamic system. For each power setting at 324 rpm the boots were inflated and deflated during an activation cycle, and throttle reductions were made. No unusual dynamic response was noted throughout these tests.

15. Phase 1B ground tests were conducted at an 8600 pound gross weight with the rotor at flat pitch. Rotor loads were monitored

during start, acceleration, and over the governing range of operating speeds. All three boot configurations were tested at 310 and 320 rpm. All loads monitored remained below the endurance limits, as shown in tables 3 and 4, appendix F.

16. During the ground runs, an activation cycle of the second generation PBDS at flat pitch resulted in an engine torque pressure increase of 1.2 psi over the baseline of 8.9 psi required to maintain constant rotor speed of 322 rpm. Elapsed time required for engine torque to return to the baseline (deicer boot deflation time) was 12 to 16 seconds as shown in figure 1, appendix F. The third generation PBDS displayed a 1.2 psi increase over the 12.7 psi baseline. Boot deflation time was the same as for the second generation PBDS.

Inflight Structural Tests

17. Phase 1A inflight structural load tests (second generation PBDS) were conducted at the conditions shown in table 2. Dynamic system/engine compatibility tests at a hover included collective control and antitorque pedal inputs and deicer boot inflations similar to those of the ground tests. Forward flight testing involving PBDS activation cycles, as well as the deflated and vented configurations, were conducted. All inflight loads monitored during phase 1A were below endurance limits except for pitch change link load during steady state climbs at 60 knots indicated airspeed (KIAS) at 38 psi torque, and 90 KIAS at 35 to 37 psi torque. The steady state endurance limit was exceeded by 20% at these conditions. Rotor system loads are shown in tables 3 through 9, appendix F. Phase 1B inflight structural loads tests (third generation PBDS) were conducted at the conditions presented in table 3. All loads remained below endurance limits during hover, sideward accelerations, forward accelerations and decelerations. Main rotor pitch link endurance limits were reached or exceeded in level flight at 80 KIAS in the deflated configuration, 80 KIAS in the inflated configuration, and 60 KIAS in the vented configuration. Rotor system loads are shown in tables 10 and 11, appendix F. Testing was halted to determine the cause of excessive loads. Examination of the installation revealed an approximately 1/16th inch high ridge corresponding to the aft edge of the nose piece on the upper surface of both blades (fig. A). It is suspected that this ridge disturbed the airflow enough to cause the excessive loads. BFG fabricated another set of deicers and installed them, paying particular attention to the centering of the nose piece. Testing was resumed, but failure of the electrical slipring that transmitted blade loads to the instrumentation caused termination of testing before any useful data could be gathered. The high pitch link loads in

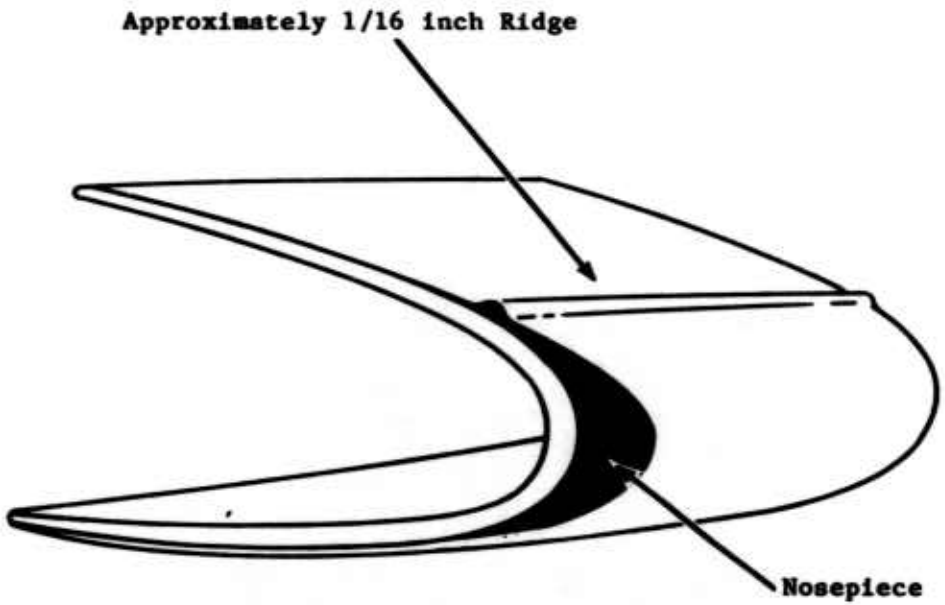

Figure A. Ridge at Leading Edge of Boot

unaccelerated flight are unsatisfactory. Future tests are planned to investigate this problem.

Pneumatic Boot Deicing System Temperatures

18. PBDS temperatures were monitored at selected locations to determine if temperatures were in excess of system component qualification values. Monitored temperatures were below component qualification values during Phase 1 testing. Representative system temperatures are shown in table 5.

PHASE 2 ARTIFICIAL AND NATURAL ICING TESTS IN FORWARD FLIGHT

General

19. Test flights in the icing environment were conducted during January through March 1984 in the vicinity of Duluth, Minnesota. The temperatures of interest for these tests were from -5° to -20° C, with liquid water content (LWC) values from 0.25 gm/m^3 to 1.0 gm/m^3. The deicing capabilities of the PBDS were evaluated at the conditions shown in tables 6 and 7 and figures B and C. Ice accretion and deicing action of the PBDS were documented by video and still cameras (app D). Overall the PBDS successfully deiced the main rotor blades at conditions shown in figures B and C in the artificial and natural icing environment, however, deicing action at lower ice accretion levels resulted in incomplete ice removal from the main rotor blades leaving areas of residual accreted ice on the rotor blades. These areas were, however, removed upon additional ice accretion and subsequent pneumatic deicer activation.

Artificial Icing Tests

20. Artificial icing tests behind the Helicopter Icing Spray System (HISS) as shown in photo 1, appendix G, were conducted during January and February 1984 in the vicinity of Duluth, Minnesota. Artificial icing test conditions are presented in table 6 and figure C. A total of 36 individual artificial icing cloud immersions and 66 PBDS activation cycles were completed.

21. The artificial icing procedure involved immersing the helicopter main rotor blades in the HISS cloud for a time interval sufficient to accrete an estimated minimum of 0.25 inches at the mid span point on the rotor blades. Previous UH-1H test data of immersion times that resulted in a 0.25 inch ice thickness are available in reference 7, appendix A. Immersion times and chase

Table 5. Maximum Recorded Bleed Air Temperatures

Flight Condition	Outside Air Temperature (°C)	Bleed Air Temperature at Engine Deck (°C)	Bleed Air[1] Temperature at Regulator (°C)	Bleed Air[2] Temperature at Ejector Flow Control Valve (°C)
Ground Run	29.8	86	39	31
Hover	31.9	89	42	33
Low Speed Flight	35.5	105	47	36
Level Flight	19.5	59	30	32

NOTES:

[1]Maximum qualification temperature of regulator = 288°C.
[2]Maximum qualification temperature of ejector flow control valve = 71°C.

Table 6. Artificial Icing Test Conditions

LWC at Aircraft (gm/m^3)	OAT (°C)	Immersion Time (min)	Observed[1] Ice	Observed Ice Remaining After Deice Cycle
0.22	-15.5	0	Ice to 60% span	N.A.[2]
	-15.5	20	Ice 80 to 90% span	N.A.
	-15.7	6.4	Ice to 75% span	N.A.
	-15.7	4.5	Ice to 80% span	N.A.
	-15.5	4	Ice to 80% span	N.A.
0.25	-10.5	12.8	Thin line to 70% span	Trace on inboard 2 ft
	-10.0	22.5	70% coverage. 1/2" to 1" thick to 60%	Clean except for 1 ft section at 55% one blade
	-9.3	8.4	Ice to 75% span	Trace on inboard 2 ft
	-9.5	5.4	Ice to 75% span	Small pieces on inboard 2 ft
	-9.9	3	Thin line to 50%	Small pieces on inboard 2 ft
	-10.3	3.5	Uniform thin coat to 80%	Small pieces on inboard 2 ft
	-19.5	12	Ice 90 to 95% span	Small pieces on inboard 2 ft
	-18.5	16.3	Ice 90 to 95% span	Small pieces on inboard 10%
	-18.8	8.8	Ice to 80% span	Small patches on underside to 30%
		5	Ice to 80% span	Clean blade
		3.3	Thin ice to 80% span	Large patches on inboard 3 ft
		3	Trace ice to 60% 1/16" thick	Large patches on inboard 3 ft
0.36	-19.3	13	Ice to 90%. Asymmetric shed 1.5 ft one blade	Slight residue on inboard 20%
		17.4	Ice to 90%. Asymmetric shed at 55% span one blade, 10% in length	Slight residue on inboard 20%
		22.5	Ice to 95%. Asymmetric shed 2 ft long from tip of one blade, 5 ft from other	Very small pieces on inboard 20%
		5	Ice to 95% span	Small patches on inboard 30%
0.45	-11.7	16	Ice to 70% span. Extends to 10% chord at 60% span	Small piece near grip
	-10.3	9	Ice to 80% span span	Small piece near grip
	-11.5	5.2	Thin ice to 80% span	First 2 ft did not shed for approximately 3 rpm. Small pieces remaining to 20%
	-11.6	3.4	Thin ice to 70% span	Frost remaining from 20 to 40%
	-11.6	4	Thin ice to 70% span	Frost remaining from 20 to 40%
	-17.0	9.5	Ice to 95% span. Asymmetric shed of 1.5 ft at 60% span	Small patches 30% span
0.47	-5.1	14.4	Approximately 1/4" thick to 60% span	Clean blade
	-5.0	20	Ice to 70%. Most dense 20 to 60%. Asymmetric shed 10% long at 60%	Clean blade
	-5.2	3.3	Ice to 70% span	Small pieces to 40%
	-5.2	3.6	Ice to 75% span	Some ice to 30% span
0.50	-14.1	3.3	Lumpy ice to 75% span	Large pieces to 40%
	-14.1	3.4	Thin lumpy coat to 75%	Small pieces to 30%
0.53	-14.3	18.4	Ice to 85%. 1 ft asymmetric shed	Clean blade
	-14.6	12.8	Ice to 80%. 2 ft asymmetric shed	Clean blade
	-14.7	17.1	Ice to 80%. 1.5 ft asymmetric shed	Clean blade
	-15.0	5	Ice to 80% span	Small patches on upper surface to 30%
0.73	-9.8	3.4	Ice to 60% span	Very small pieces to 20%
	-9.6	3.4	Ice to 70% span	Very small pieces to 20%
	-10.5	2.5	Thin lumpy ice to 70%	Pieces to 25% span
	-10.5	3.4	Lumpy ice to 70%	Large ragged patches to 70% span
	-10.5	3.4	Thin ice to 60%	Small patches on underside to 40%
	-9.8	3.5	Thin ice to 60%	Patches from 20 to 50% span
	-9.9	3.4	Approximately 1/8" thick to 50%	Large patch from 20 to 50%
	-9.9	3.4	Frost coat to 70%	Frost from 20 to 50% span
	-9.1	3.4	Frost coat to 70%	Patch of frost from 20 to 60%
	-9.3	3	Thin ice to 75%	Patch of frost from 20 to 30%
	-9.3	3.4	Ice to 70%	Clean blade
	-10.0	3.4	Ice to 70%	Frost from 20 to 40%
	-9.7	3.4	Ice to 65%	Slight frost from 20 to 30%
	-10.3	3.3	Thin ice to 60%	Pieces at 30% span
	-10.5	2.4	Patch ice to 60%	Pieces at 30% span
	-10.1	3.4	Thin ice to 75%	Pieces from 20 to 50% span
0.78	-9.9	3.5	Ice to 70% span	Clean blade
	-9.8	3	Ice to 70%	Clean blade
	-9.8	2	Thin ice to 70%	Small pieces to 10% span
	-9.8	3	Thin ice to 70%	Ice remaining to 30% span
	-9.1	3	Thin ice to 70%	Small amount remaining at 50% span
	-10.5	3.4	Thin ice to 75%	Some ice to 20% span
0.80	-5.8	0	Approximately 1/4" thick to 60%	Approximately 6 in. remaining at 50%, one blade
	-5.2	3	Ice to 55% span	Small ragged pieces to 20%
	-5.5	3.5	Ice to 50% span	Clean blade
1.10	-5.4	3.1	Ice to 65% span	Clean blade
	-5.9	6.5	Ice to 65% span	Small pieces 20 to 30%. One large piece at 30%, one blade
	-5.8	7.3	Ice to 55% span	Clean blade

NOTES:

[1]From chase pilot comments, still photographs, chase and test aircraft mounted video.
[2]N.A. = Data not available.

Table 7. Natural Icing Conditions

Average LWC Measured by U-21 (g/m^3)	Average LWC at Aircraft (gm/m^3)	OAT (°C)	Immersion Time (min)	Observed Ice[1]	Observed Ice Remaining After Deice Cycle
0.07	N.A.	-13.4	15.8	Ice to 70% span	Some ice inboard on one blade
		-12.8	13.8	Ice to 70% span asymmetric shed at 60%	Some ice on inboard one foot
0.20	N.A.	-14.2	17	1/4" thick	N.A.[2]
		-12.2	17	N.A.	N.A.
		-12.5	6	Thin ice to 80% span	Small pieces to 50% span
0.90	0.15	-2.6	20	Very thin coat to 50%	Thin line remaining inboard 2 ft
		-2.5	7	Very thin coat to 50%	Small pieces to 20%
0.273	0.32	-4.3	14.5	N.A.	N.A.
		-5.6	7	Ice to 50%	
		-5.4	3.9	N.A.	
		-4.7	5.4	N.A.	
		-5.6	3.5	Ice to 60%	
		-5.6	3.7	Ice to 60%	
		-6.1	1.7	N.A.	
		-6.4	2	Ice to 50%	
		-5.7	3.8	Ice to 60%	
		-5.5	3.7	Ice to 60%	
		-5.7	4.8	Ice to 50%	Frost to 30%
0.26	0.3	-1.0	12	Frost to 60%	N.A.
		-1.6	17	Frost to 50%	Clean
		-3.5	29	Ice to 30%, frost line to 50%	1/2" piece at 40%
		-5.0	8.5	Frost to 50%	N.A.
		-1.5	4.5	Frost to 50%	N.A.
0.1	0.2	-13.0	39.5	Ice to 70%, then from 50 to 70%	Clean
		-13.0	6	N.A.	N.A.
0.034	0.07	-20.5	38	Ice to 95%	Very small patches to 30% small piece on one non-inflatable section

NOTES:

[1]From chase pilot comments, still photographs and chase test aircraft mounted video.
[2]N.A. = Data not available.

FIGURE 8
ARTIFICIAL
ICING TEST CONDITIONS

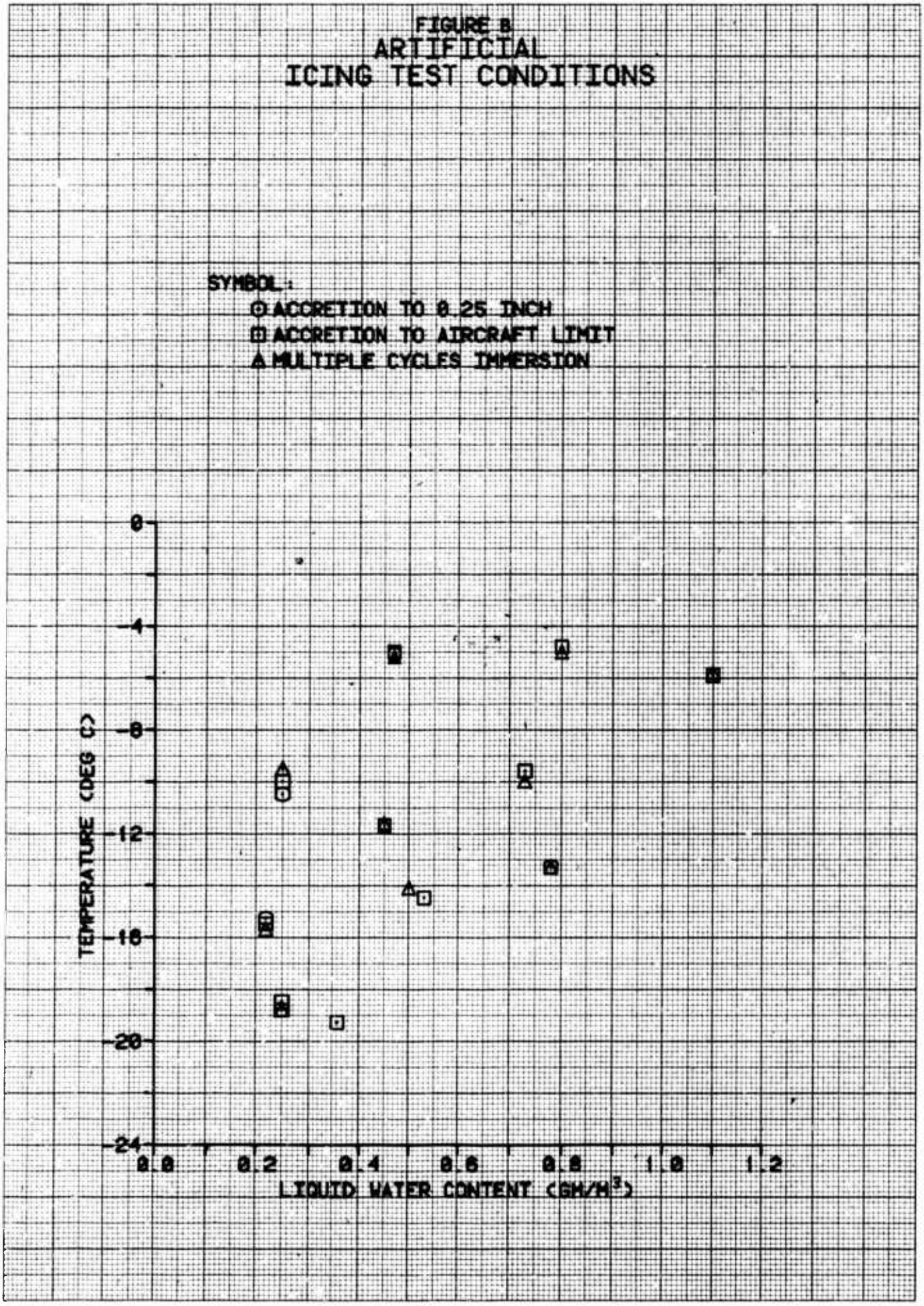

FIGURE C
NATURAL
ICING TEST CONDITIONS

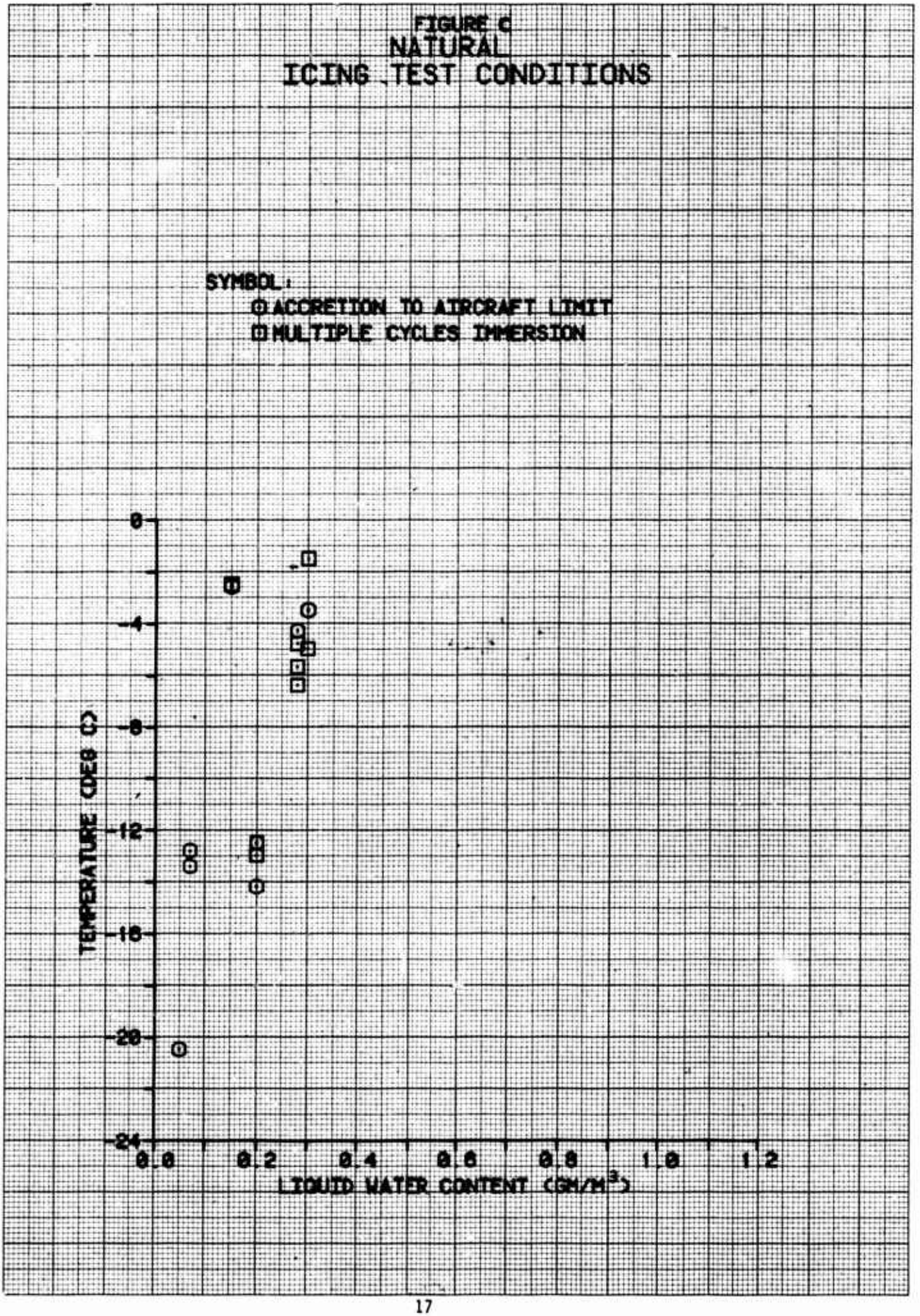

pilot reports of blade ice accretion were used to estimate 0.25 inches at the midspan point. A 0.25 inch ice accretion is the minimum thickness typically recommended by BFG for cycling pneumatic deicing boots on fixed-wing aircraft. It was felt that the accretion level would not cause aircraft limits to be reached or result in high vibrations or loads if an asymmetrical blade ice shed occurred. The limits on monitored parameters were: an increase in engine inlet differential pressure of 10 inches of water; or, an increase of 5 psi engine torque. After a clean deice cycle the rotor blades were immersed in the cloud until engine torque increased 5 percent or moderate vibration levels were encountered. The blades were then deiced. Once this "endurance time" was defined for a particular condition the time to the next deice cycle was reduced to examine the effects of lower accretion levels. Baseline power checks were performed periodically prior to and after the deice cycle. Multiple deice cycles were also accomplished while remaining in the HISS cloud to study deicer effectiveness at both high and low accretion levels.

22. At accretion levels estimated to be greater than 0.25 inches at midspan, activation of the PBDS normally resulted in complete removal of the ice cap from the leading edge of the main rotor blade. Any ice remaining was usually in the form of small ice patches or a frost like residue on the inboard blade section. As shown on the video systems, ice fracturing normally began inboard (photos 2 through 5, app G) as the pneumatic deicer inflated at accretion levels greater than the estimated 0.25 inches. At the lower accretion levels, ice of less than 0.06 inches thickness was sometimes retained especially in areas near the blade grip, as shown in photo 6. Subsequent deicer cycles after further ice accretion removed these small accumulations (photo 7). The coverage of ice remaining after a single deice cycle was documented by cabin mounted high speed video, hub mounted video and chase high speed video cameras in addition to the chase aircraft crew. Attempts were made to document the increase in power required over clean deicers when accreted ice was retained after a single deice cycle. These were reasonably successful when the test aircraft moved far enough away from the HISS so as not to be influenced by its downwash. Ice retention after a single deice cycle under conditions of low ice accretion is due to a limitation of the pneumatic deicing system to fracture and remove thin ice accretions. Fixed wing aircraft using pneumatic deicers have the same problem. While subsequent deicer action will remove these accumulations as discussed above, the pilot does not have complete freedom in choosing the deicer interval. Retention of small, thin areas of ice accretion after a single deice cycle under conditions of minimal ice accretion reduces helicopter

range and performance. Additional artificial icing tests should be conducted to optimize time between deicer cycles and study performance losses associated with ice retention if the pneumatic design is to be pursued.

23. During the immersion times intended to reach an aircraft icing endurance limit, the 5 psi torque rise limit caused by ice accretion as imposed by the airworthiness release (ref 8, app A) was the limiting factor approximately 70% of the time. The 5 psi torque rise was difficult to estimate because of torque fluctuations caused by the HISS wake and the collective movements required to maintain formation flight. Naturally occurring asymmetrical ice sheds resulting in moderate vibration levels became the other limiting factor. Engine inlet screen ice accretion was not a factor limiting icing exposure time. Immersion times required to reach a 5 psi torque increase or moderate vibration levels are included in table 6.

24. All deice cycles performed after reaching the above described conditions resulted in successful deice cycles (complete or near complete removal of the ice cap from the leading edge of the main rotor blades). PBDS activations resulted in symmetrical ice sheds with slight increases in vertical vibrations during the activation cycle as shown in figure 2, appendix F. Naturally occurring ice sheds were sometimes asymmetrical and resulted in increased lateral and vertical vibrations. Activation of the pneumatic deicer boots reduced the associated vibration level within two seconds (fig. 3, app F) and is a desirable characteristic.

25. Increases in torque (power) required during deice activation following low ice accretion levels on the main rotor were similar to power increases during dry air testing. However, with a large quantity of ice on the blades when the PBDS was activated, the torque decrease due to shedding offset the torque increase due to boot inflation. Nevertheless, when the test aircraft is operated near the power limit of 50 psi of torque, caution must be exercised to avoid possible overtorque during the PBDS activation. This condition may be avoided by momentarily reducing collective pitch slightly prior to PBDS activation. The torque (power) increase experienced during activation of the PBDS when operating near maximum torque limits due to the potential for overtorque is unsatisfactory.

26. In forward flight at approximately -19°C and 0.25 gm/m^3 LWC ice accreted to 90% to 95% span on the main and tail rotor blades and at -15°C to 80-85% span. With higher temperature the spanwise accretion was reduced. At -10°C ice accreted to approximately 70% to 75% of the main rotor blade span and 50% to 75% at -5°C.

27. The outboard section of the main rotor blade (outboard of blade station 244) which included the non-inflatable portion of the deicer boot was naturally self shedding (photo 8, app G). Ice accretion on the non-inflatable section of the deicer was only observed at temperatures below -15°C. Self shedding of the non-inflatable area occurred without buildup of vibration levels. This was probably due to the lower ice adhesion characteristics of the ESTANE® deicer surface when compared to the standard UH-1H metal airfoil. The lowered adhesion level would allow the accreted ice to self-shed prior to ice accretion of sufficient mass to result in significant lateral vibration. Reduction of the span wise pneumatics should be further investigated since this would reduce profile drag, vibration levels, susceptibility to pneumatic tube impact damage, and improve handling qualities during PBDS activation.

28. Overall, the deicing capability of the deicer boots was satisfactory at all conditions tested in the HISS cloud. One unsatisfactory and one undesirable characteristic were identified during artificial icing tests: (1) the aircraft engine torque (power) increase experienced during activation of PBDS when operating near maximum torque limits is unsatisfactory. (2) retention of small, thin areas of ice accretion after a single deice cycle especially under conditions of minimal ice accretion is undesirable. One desirable characteristic of the PBDS is the capability of the pneumatic deicer to reduce the vibrations associated with a natural assymetrical ice shed from the main rotor blade within two seconds.

Natural Icing Tests

29. Test flights in the natural icing environment were conducted during February and March 1984 in the vicinity of Duluth, Minnesota, after the icing envelope had been expanded under artificial conditions. A total of 7 natural icing flights were accomplished for a total of 5.1 hours in the natural icing environment. Twenty-six PBDS activations were accomplished. The deicing capability of the PBDS in the natural icing environment were evaluated at the conditions shown in table 7 and figure C. The natural icing procedure involved immersing the aircraft in the natural icing environment until a torque rise of 3 to 5 psi was noted due to ice accretion. Ice accretions and deicing action of the PBDS were documented above or below the cloud deck by still and video cameras when possible. Overall, the PBDS successfully deiced the main rotor blades in forward flight. At lower blade accretion levels, the deicing action of the PBDS resulted in only partial removal of the ice cap leaving

some small areas of residual ice on the main rotor blades, however, further accretion of ice on the main rotor blades to the level shown in table 7 would result in complete removal of the ice cap. The deicing action of the pneumatic boot in natural icing conditions was very similar to that found in artificial icing conditions and was satisfactory.

PHASE 3 ARTIFICIAL RAIN EROSION TESTS

30. Rain erosion tests were conducted during May and June of 1984 at EAFB to evaluate the rain erosion characteristics of the pneumatic deicer. The test flights in the artificial rain environment were flown behind the HISS for a total of 6.0 hours. Spray nozzles and operating pressures were modified to produce droplet sizes as large as 3.5 mm with a median drop size of approximately 1-2 mm. The only apparent erosion of the deicer surface was a very slight, almost undetectable, pitting of the outer ESTANE® surface near the blade tip as shown in figure D, which was discovered after 5.1 hours exposure to the artificial rain cloud. This erosion was so slight that it did not pose a problem to operation of the deicers. Additional rain erosion testing should be accomplished in natural rain conditions to further access rain erosion characteristics and the potential to repair eroded deicer surfaces.

PHASE 4 PERFORMANCE AND HANDLING QUALITIES

Performance

General:

31. Hover, level flight, and autorotational descent performance testing were conducted at EAFB and Bakersfield, California at the conditions listed in table 2. Performance data were obtained with the PBDS in the deflated configuration for the second generation design. The performance data obtained with the second generation PBDS installed was compared to standard blade UH-1H data generated during phase 4 and data from the first generation PBDS in reference 3, appendix A.

Hover Performance:

32. Hover performance with deicer boots in the deflated configuration was evaluated using the tethered hover technique at a 5-foot skid height in winds of less than 5 knots. A comparison of nondimensional hover performance for the deflated boot configuration

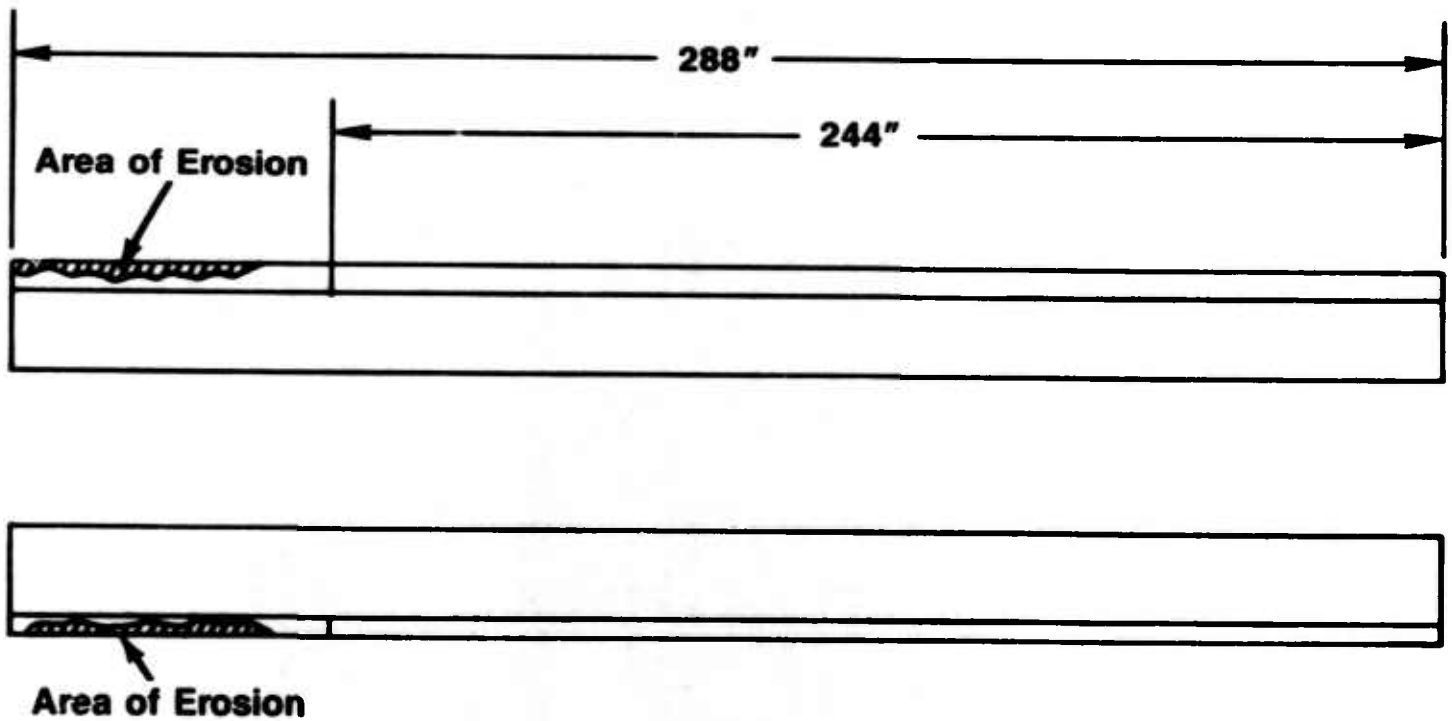

Figure D. Areas of Rain Erosion

to standard-blade hover data and deflated boot configuration data for the first generation PBDS from reference 3, appendix A, is presented in figure 4, appendix F. In dimensional terms, the performance penalty caused by the deflated second generation PBDS on a UH-1H at 9000 pounds on a standard day at sea level is 54 shp. This represents 46% less penalty than with the deflated first generation PBDS. Although performance with the second generation deicer boot is improved over the first generation, the incurred hover performance penalty is undesirable. Additional hover performance testing should be conducted with the third generation boot design to document any performance improvement.

Level Flight Performance:

33. Level flight performance of the test UH-1H with the second generation PBDS installed was evaluated in the deflated configuration, in zero sideslip level flight at thrust coefficients (C_T) of 0.0032, 0.0037 and 0.0043 (figs. 5 through 9, app F) using the constant gross weight to air pressure ratio (w/δ) method. Additionally, C_T's of 0.0031, 0.0036, 0.0041, 0.0045, and 0.0048 (figs. 10 through 16) were flown with standard (clean) blades to generate baseline data for comparison purposes. Test results are compared in figure E with standard bladed UH-1H data.

34. At 90 knots calibrated airspeed (KCAS), at a C_T of 0.003633, and a referred rotor speed of 320 rpm, approximately 85 additional shp over standard UH-1H blades is required with PBDS deflated. Under the same conditions, but with a referred rotor speed of 331 rpm, the first generation PBDS required 170 additional shp (ref 3, app A). Although not directly comparable to first generation data due to the difference in referred rotor speed, there appears to be a significant reduction in power required over the first generation PBDS. Nonetheless, the incurred level flight performance penalty is undesirable. Additional level flight performance testing should be conducted with the third generation boot design to document any performance improvement.

Autorotational Descent Performance:

35. Autorotational descents were evaluated in conjunction with the Phase 1A (structural) testing in the vented configuration. The vented boot configuration would occur with an engine failure and subsequent loss of the engine bleed air pressure needed to provide the vacuum which keeps the boots deflated. After establishing a stable autorotational descent, the PBDS air supply was shut off at the regulator-reliever/shut-off valve to establish the vented configuration which allowed the deicer boot to auto-inflate. Auto-inflation in this configuration results from

FIGURE E

LEVEL FLIGHT PERFORMANCE COMPARISON

THRUST COEFFICIENT = 0.003633
PNEUMATIC BOOTS DEFLATED

NOMINAL CONDITIONS: GROSS WEIGHT = 8140 LB
DENSITY ALTITUDE = 8020 FT
REFERRED ROTOR SPEED = 320 RPM

NOTE: CURVES DERIVED FROM FIGS. 5-6 AND 10-11, APPENDIX F

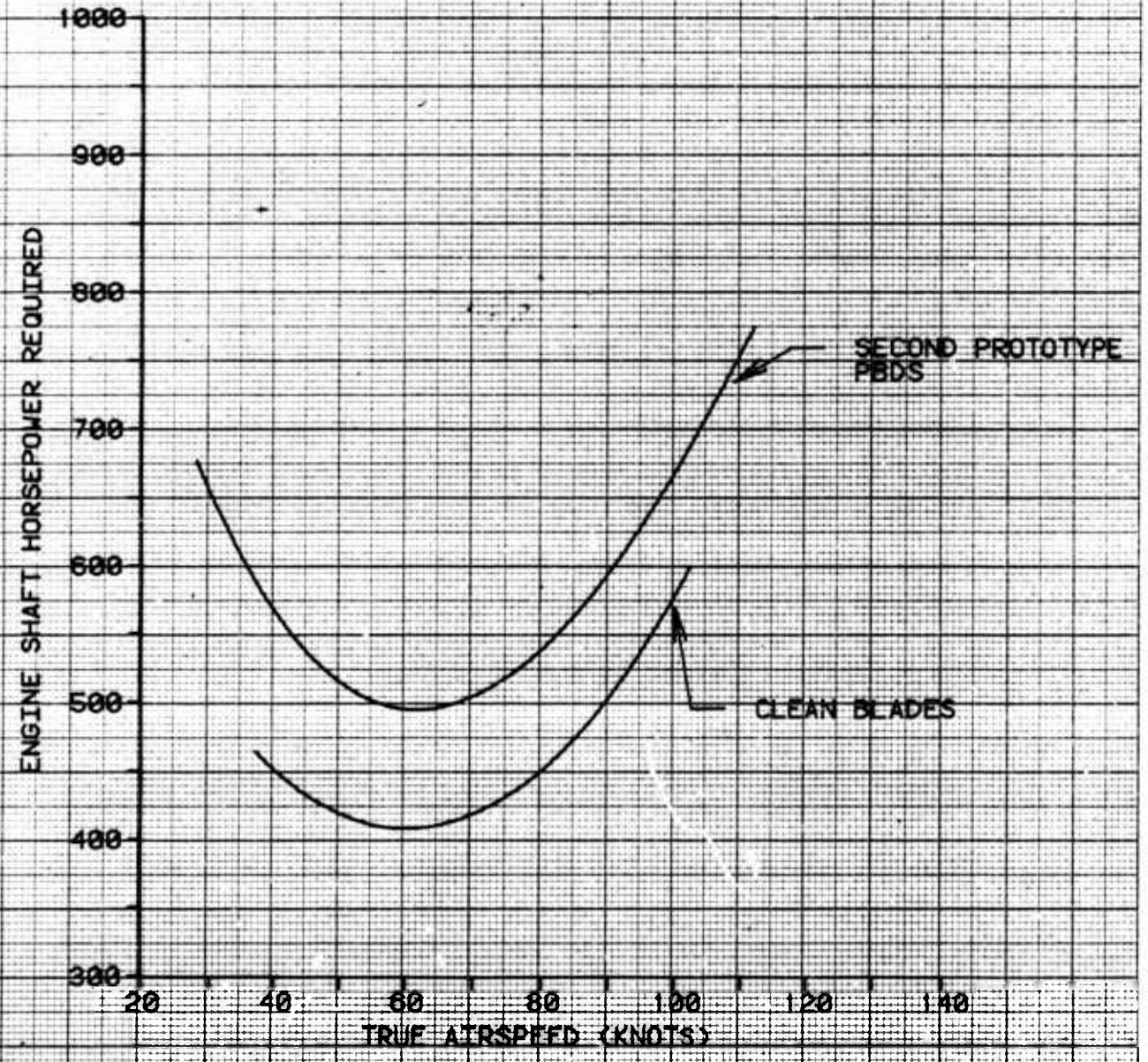

differential air pressures and centrifugal forces acting on the boot. During the 5 to 10 second period of auto-inflating, the autorotative rotor speed decreased by 4 to 6 rpm, but remained above the lower limit of 294 rpm (collective full down). Steady state descent rates were approximately 200 to 400 feet per minute greater than those reported for standard blades reference 12. Prevention of deicer boot auto-inflation (vented condition) in case of engine failure would prevent rpm loss and lower descent rates during autorotation. Further autorotational performance evaluations should be conducted during icing tests to study the combined effects of auto-inflation and blade ice accretion.

Handling Qualities

General:

36. Handling qualities evaluations were conducted in conjunction with Phase 1 (structural) testing and Phase 4 (handling qualities and performance) testing. The handling qualities of the UH-1H helicopter with the PBDS installed were also qualitatively evaluated throughout the dry air testing. Results of these tests were compared with the standard UH-1H data reported in reference 10.

Control Positions in Trimmed Forward Flight:

37. Control positions in trimmed ball-centered forward flight were evaluated from 38 to 110 KCAS with the PBDS in the deflated condition. Tests were conducted in conjunction with the airspeed calibration at the conditions presented in table 2. Test results are presented in figure 17, appendix F. The control position characteristics in trimmed forward flight are satisfactory and similar to standard UH-1H helicopters.

Maneuvering Stability:

38. Maneuvering stability was conducted using the windup turn method at the conditions shown in table 2. Data for maneuvering stability are presented in figure 18. Maneuvering stability characteristics are satisfactory and similar to the standard UH-1H.

Controllability:

39. Longitudinal and lateral controllability were evaluated in forward flight at the conditions shown in table 2. Data for controllability are presented in figures 19 and 20. Longitudinal and lateral controllability characteristics are satisfactory and similar to the standard UH-1H.

Low-Speed Flight Characteristics:

40. The low-speed flight characteristics of the UH-1H helicopter with the PBDS installed were evaluated at the conditions listed in table 1. Tests were performed at a constant skid height of 10 feet in winds of 5 knots or less. A ground pace vehicle with a calibrated fifth wheel was used as a speed reference. Data were recorded at 5-knot increments from a hover to 40 knots true airspeed (KTAS) forward and 20 KTAS sideward and rearward. The low-speed flight data were obtained with the PBDS in the deflated and vented conditions and are presented in figures 21 through 24. Variations in the control positions during low-speed flight with the boot vented or deflated are essentially the same as results previously reported for a standard UH-1H (ref 13, app A) and are satisfactory.

RELIABILITY AND MAINTAINABILITY

General

41. The reliability and maintainability of the PBDS were evaluated during all testing phases. Two unsatisfactory characteristics were identified: (1) abrasion of damper control tube by pneumatic hose (second generation); (2) impact damage to tail rotor blade due to ice shed from deicer during natural icing tests (second generation). Six undesirable characteristics were identified: (1) debonding of hose and flap assembly (second generation); (2) debonding of deicer boot from main rotor blades (second and third generation); (3) internal debonding of deicer boot (third generation); (4) breakdown of internal bleeder material (second generation); (5) impact damage to inflatable section of deicer (second generation); (6) formation of water pockets between deicer boot and blade during artificial icing test (second generation).

Phase 1A:

42. Debonding of a small area of the pneumatic boot and flap assembly from the main rotor blade occurred during the first ground run due to a suspected lack of bonding adhesive in these areas. Debonding of a small circular area as shown in photo 9, appendix G, occurred in the noninflatable section of the deicer boot. A four inch area of the hose and flap assembly as shown in photo 10, also debonded from the top of the main rotor blade in the doubler area. The above areas were easily rebonded by BFG personnel using Minnesota Mining and Manufacturing (3M) 1300L rubber cement prior to further ground operations. Time of repair was approximately 1.5 manhours. Debonding of the

deicer from the main rotor blade (while not critical in the above described occurences) is undesirable and requires close inspection of the deicers during preflight and post flight inspections to determine airworthiness. Reliability of the deicer bonding should be improved.

Phase 1B:

43. During initial ground runs with the first set of third generation deicers, an approximate 4 inch long section of the inflatable portion at midspan of one blade and a 3 inch section of the noninflatable section debonded. This was repaired by BFG personnel in the manner previously described. After the initial ground run of the second set of third generation deicers, a 4 inch long rupture occurred in the surface of the boot at the outboard end of the inflatable section on one blade (photo 11). Only the external ESTANE® surface was ruptured and the deicer boot was still functional. Additionally, a 3.75 inch long bubble was observed between the inner fabric plies and the ESTANE® surface on the second blade. BFG personnel repaired the rupture by trimming the affected area and cementing on an ESTANE® patch. The bubble was repaired by injecting cement between the fabric plies and the ESTANE® surface. During test inflations, conducted prior to reinstalling the blades on the aircraft, numerous small bubbles (approximately 1/16 to 1/8 inch in diameter) appeared with every inflation. BFG recommended that the boots be restricted from inflated or vented operations. The internal debonding of the deicer boot is undesirable. The reliability of deicer bonding should be improved.

Phase 2:

44. After a 20 minute icing flight damage to the damper control tubes as shown in photo 12, appendix G was discovered. The steel-wire wrapped pneumatic hose (photo 13) leading from the pneumatic slip ring assembly to the main rotor blade flap assembly rubbed against the damper control tube causing damage which required replacement of the control tube. A combination of factors such as a loosened plastic fastener, accreted ice on the hose and centrifugal force probably contributed to the rubbing action. Use of steel wire wrapped pneumatic hose is a potential problem area when placed near moveable control surfaces as in the current test installation, and is unsatisfactory. Extreme caution should be used during the pneumatic tube installation. Preflight and postflight inspections of the damper control tube area should be emphasized.

45. During Phase 2 testing, small lumps (photo 14) developed under the spanwise tube surface. As reported in reference 3, appendix A these lumps were caused by a breakdown of the internal ventilation material (manifold) as shown in photo 15, appendix G. Most pieces of this manifold material were forced into the chord wise tubes creating small bulges at the outboard tip of the inflatable boot, applying shop air to keep the boot inflated and then manually removing the pieces of manifold material out of the boot. These cuts were then repaired (photo 17) as described in paragraph 43. This breakdown of the internal ventilation material is undesirable and continues to be a problem area even though the ventilation material was reportedly improved to prevent breakdown. The third generation boot incorporated a new ventilation material design to eliminate this breakdown.

46. Damage to the lower span wise tube of the pneumatic deicer boot occurred during the third artificial icing flight. The damage was in the form of a semi-circular cut, 3/4 inches in length through the surface of the ESTANE®, and bottom ply and stretch fabric of the inflatable tube as shown in photo 18. Based on post flight analysis, damage was suspected to have occurred during formation lift off with the HISS helicopter which created a considerable amount of flying debris. Review of the hub-mounted video camera recorded five minutes after take off shows a 5 to 8 inch area of the upper boot surface at the outboard section of the inflatable area that was auto-inflated presumably due to lack of effective vacuum caused by the cut. Additionally, very slight lateral vibration (VRS 3) was noted during takeoff. Pressure and vacuum gauges indicated slightly lower pressure and vacuum during flight. The cut did not seem to functionally impair operation of the deicer in artificial icing conditions at -10°C. Susceptibility of the pneumatic deicer to impact damage is undesirable. Investigation of impact damage properties of the pneumatic boot should be conducted.

47. Two small areas between the main rotor blade and the boot at 40% span filled with water as shown in photo 19. The largest of the two pockets of water was 0.75 inch diameter where debonding of the back side of the deicer from the blade surface had occurred. Suspected cause of the water deposit was moisture entering and traveling to the above area along the leading edge nose piece by centrifugal force when the main rotor was rotating. The area where the deicer boot is bonded to the doubler section of the blade was sealed. This prevented further accumulations of water during the remainder of the icing tests. Water was removed from the pockets and areas rebonded. Water entering

under the surface of the deicer at the deicer root of the boot during main rotor blade rotation is undesirable. Water accumulation between the main rotor blade and internal pneumatic deicer surface should be prevented prior to further testing.

48. One problem area was noted during natural icing tests. The leading edge of a tail rotor blade was damaged as shown in photo 20. This damage was discovered after a 38 minute natural icing flight at -20°C in which a deicing cycle had been accomplished. Probability of tail rotor damage increases when time between deice cycles is lengthened due to the greater ice accretion on the main rotor blades and is independent of the deice method. Time between deice cycles should be optimized during further icing tests to reduce the potential of blade damage. Damage to the tail rotor blade is unsatisfactory.

CONCLUSIONS

GENERAL

49. The following conclusions were reached upon conclusion of testing:

a. The second generation PBDS successfully deiced the main rotor blades under all conditions tested.

b. Handling qualities with the boots in the deflated or vented condition are essentially unchanged from the standard UH-1H.

c. Four unsatisfactory and nine undesirable characteristics were identified.

DESIRABLE CHARACTERISTICS

50. The pneumatic deicer reduced vibrations associated with a natural asymmetric ice shed from the main rotor within two seconds (para 24).

UNSATISFACTORY CHARACTERISTICS

51. The following unsatisfactory characteristics were identified:

a. Pitch link loads exceeded the endurance limit in unaccelerated forward flight with the third generation boot design (para 17).

b. The torque increase experienced during activation of the PBDS when operating near maximum torque limits creates the potential for overtorque (para 25).

c. The abrasion of the damper control tube by the pneumatic hose (para 44).

d. Impact damage to the tail rotor blade due to ice shed from the deicer (para 48).

UNDESIRABLE CHARACTERISTICS

52. The following undesirable characteristics were identified:

a. Retention of small, thin areas of ice accretion after a single deice cycle, especially under conditions of minimal ice accretion (para 22).

b. The performance penalty in a hover of the second generation boot design, although reduced from the first generation boot design (para 32).

c. The performance penalty in level flight of the second generation boot design, although reduced from the first generation boot design (para 34).

d. Debonding of the hose and flap assembly (second generation) (para 42).

e. Debonding of the deicer boot from the main rotor blade (second and third generation) (para 43).

f. Internal debonding of the deicer boot (third generation) (para 43).

g. Breakdown of internal bleeder material (second generation) (para 45).

h. Impact damage to inflatable section of deicer (second generation) (para 46).

i. Formation of water pockets between the deicer boot and the main rotor blade during artificial icing tests (second generation) (para 47).

RECOMMENDATIONS

53. Modify the design of the third generation deicer boot to reduce high pitch link loads in forward flight (para 17).

54. Conduct additional artificial icing tests to optimize time between deicer cycles and document performance losses associated with ice retention (para 22).

55. Investigate reduction of spanwise coverage of the inflatable section, as this has the potential of reducing profile drag, vibration levels, susceptibility of pneumatic tube impact damage, and handling qualities degradation during PBDS activation (para 27).

56. Conduct further erosion testing in actual rain and sand conditions (para 30).

57. Conduct further performance testing of the third generation boot design to document any performance improvement from previous designs (paras 32 and 34).

58. Conduct further autorotational performance studies during icing tests to study combined effects of boot auto-inflation and blade ice accretion (para 35).

59. Improve reliability of deicer bonding (para 43).

60. Emphasize that extreme caution should be used during pneumatic hose installation and pre-flight and post-flight inspection of the damper control tube area (para 44).

61. Investigate impact damage properties of the pneumatic boot (para 46).

62. Prevent accumulation of water between the rotor blade and the internal pneumatic deicer surface (para 47).

APPENDIX A. REFERENCES

1. Report, NASA Lewis CP-2170, *1980 Aircraft Safety and Operating Problems, Pneumatic Boot for Helicopter Rotor Deicing,* undated.

2. Letter (reference number FH1: 237-4 (64/LAH)) from NASA requesting AVSCOM Support, subject: Pneumatic Boot Concept for Rotors, undated.

3. Final Report, AEFA Project No. 81-11, *JUH-1H Pneumatic Boot Deicing System Flight Test Evaluation,* May 1983.

4. Technical Manual, TM 55-1520-210-10, *Operator's Manual, US Army Model UH-1D/H Helicopters,* with change 13, 25 August 1971.

5. Technical Manual, TM 55-1520-210-10, *Operator's Manual, US Army Model UH-1D/H and EH-1H Helicopters,* 18 May 1979, with change 19, 14 March 1984.

6. Technical Manual, TM 55-1520-210-10, *Operator's Manual, US Army Model UH-1H/V Helicopter,* 15 July 1985.

7. Supplement to Technical Manual, TM 55-1520-210-10, *Operator's Manual, UH-1H Helicopter, Serial No. 70-16318, Incorporating an Advanced Ice Protection System and UH-1H Kit A Ice Protection,* 19 July 1978.

8. Letter, AVSCOM, DRSAV-E, 28 November 1983, with revision 1 dated 2 December 1983, subject: Experimental Airworthiness Release for JUH-1H S/N 70-16318 with Main Rotor Pneumatic Boot Deicing System (PBDS) and Main Rotor Brake Installed.

9. Engineering Design Handbook, Headquarters, U.S. Army Materiel Command, AMCP 706-204, *Helicopter Performance Testing,* August 1974.

10. Naval Test Pilot School Flight Test Manual, Naval Air Test Center, USNTPS-FTM-No. 101, *Helicopter Stability and Control,* June 1968.

11. Technical Report, USAAMRDL-TR-32, *Ottawa Spray Rig Tests of an Ice Protection System Applied to the UH-1H Helicopter,* July 1980.

12. Report, AFFTC, TR-73-35, *Category II Performance and Flying Qualities Evaluation of the HH-1H Helicopter,* August 1973.

13. Final Report, AEFA Project No. 80-06, *Preliminary Airworthiness Evaluation of UH-1H with Hot Metal Plus Plume Infrared Suppressor and Infrared Jammer,* June 1981.

14. Engineering Design Handbook, Army Material Command, AMC Pamphlet 706-203, *Qualification Assurance*, 3 April 1972.

APPENDIX B. DESCRIPTION

GENERAL

1. The test helicopter, U.S. Army S/N 70-16318, was a production CH-1H modified to accommodate test instrumentation, the prototype Pneumatic Boot Deicing System (PBDS), rotor brake, video camera, and a partial ice protection system (Kit A). The principal modifications included the PBDS components installed within the cabin area, routing of bleed air through the mast and rotor assembly, and the pneumatic deicers installed on the main rotor blades. Photos 1 and 2 show the test aircraft with the PBDS and test instrumentation installed.

PNEUMATIC BOOT DEICING SYSTEM

General

2. The PBDS installation consisted of six major components: the PBDS regulator-reliever/shut-off valve (fig. 1), ejector flow control valve (fig. 2), timer (fig. 3), rotary union (fig. 4), hose and flap assembly (fig. 5) and the pneumatic deicer (figs. 6 through 9). A simplified drawing of the system showing major components is shown in figure 10. Schematics of the pneumatic deicer system layout designed for evaluation purposes are presented in figure 11.

3. Customer bleed air from the aircraft engine is routed through a check valve to the regulator-reliever/shut-off valve, which is manually adjusted to the system operating pressure of 25 pounds per square inch (psi). The solenoid-operated ejector flow control valve (electrically energized by the timer) directs bleed air through the pneumatic rotary union, through the nose and flap assembly to the pneumatic deicers in a single inflation activation cycle. A normal activation cycle consists of inflation of the deicer boots for approximately two seconds, followed by subsequent deflation of 12 to 16 seconds. With the solenoid de-energized, the ejector flow control valve provides the vacuum necessary to keep the deicers deflated by directing bleed air overboard. A shop air test connection is installed downstream of the check valve for leak and maintenance checks. An electrical/manual gate valve is provided upstream of the rotary union to capture pressure or vacuum in the deicer boots and prevent deflation during performance testing or leak checks. The pressure gauge downstream of the regulator-reliever/shutoff valve displays regulated pressure of the ejector control valve. A vacuum/pressure gauge downstream of the gate valve displays the vacuum or pressure of the deicer boots. To evaluate a degraded mode that would occur with engine failure or damage to the PBDS, vacuum to the

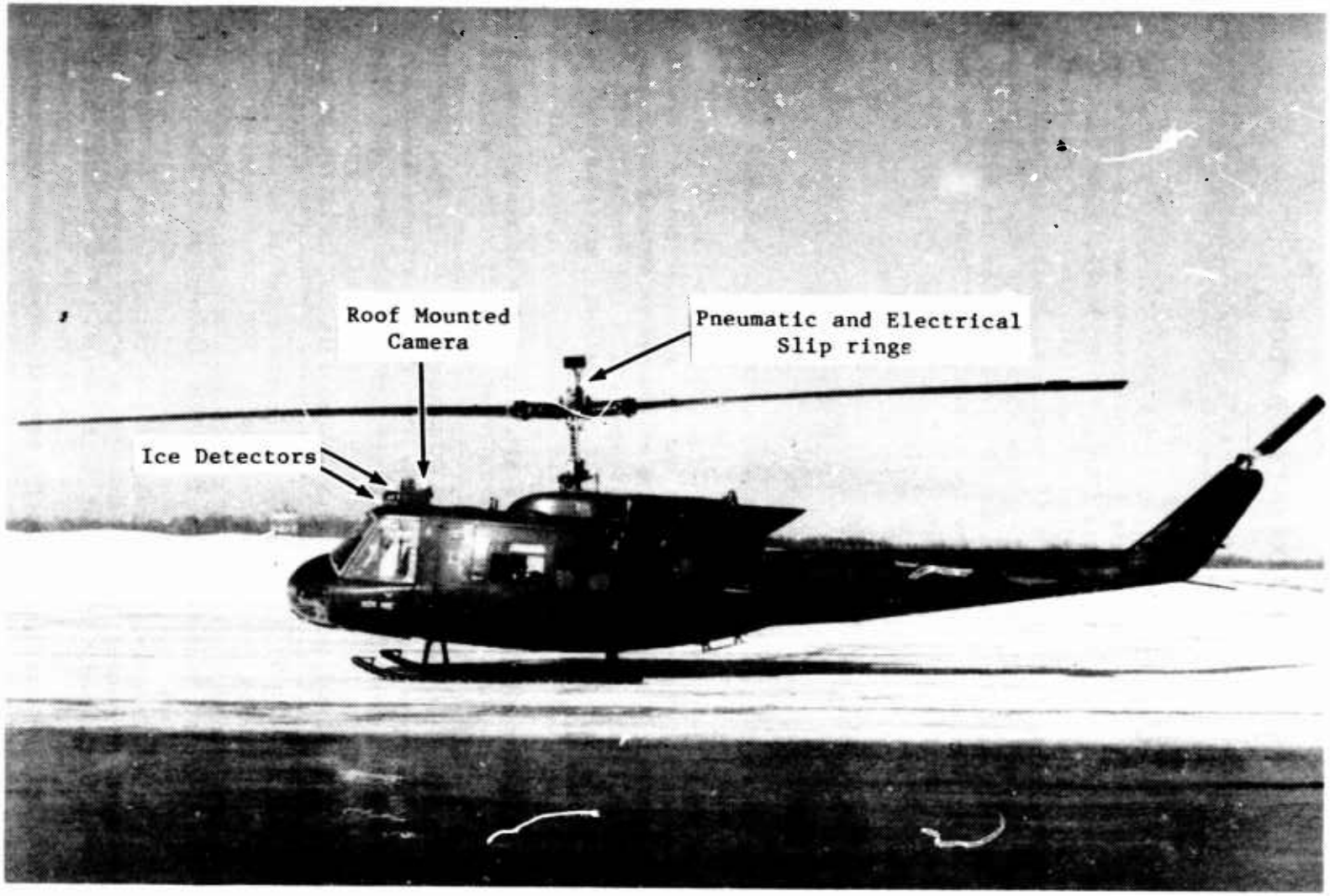

Photo 1. Test Aircraft

Photo 2. Test Aircraft

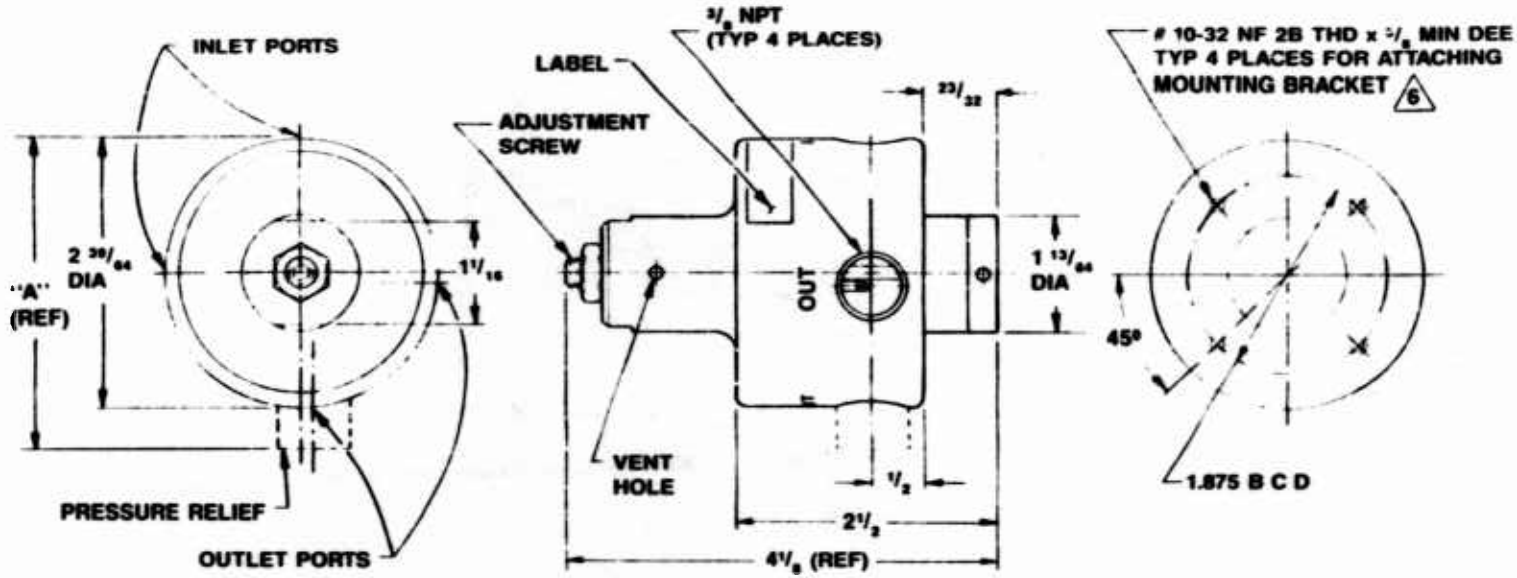

Figure 1. Regulator-Reliever/Shut-off Valve

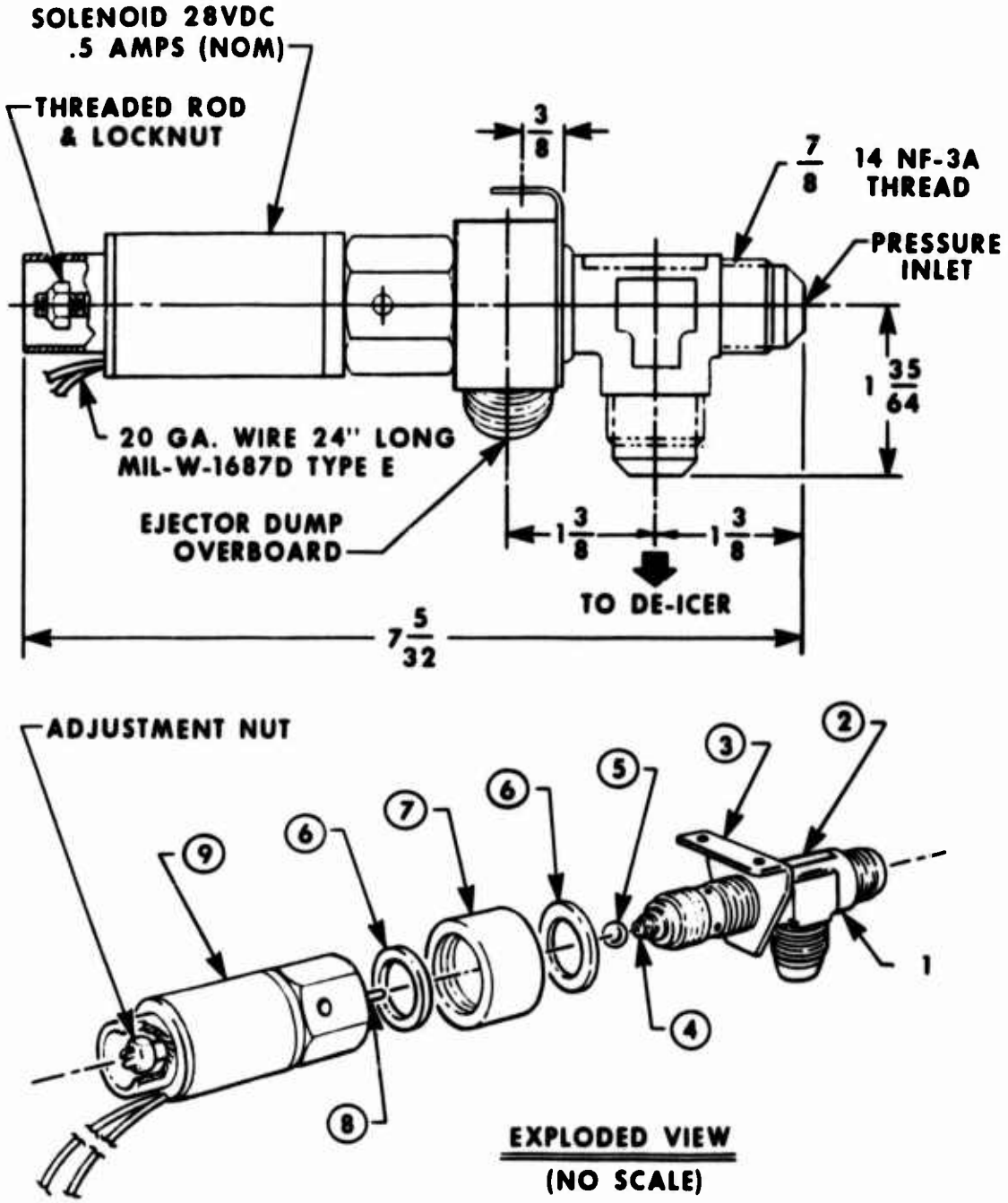

Figure 2. Ejector Flow Control Valve

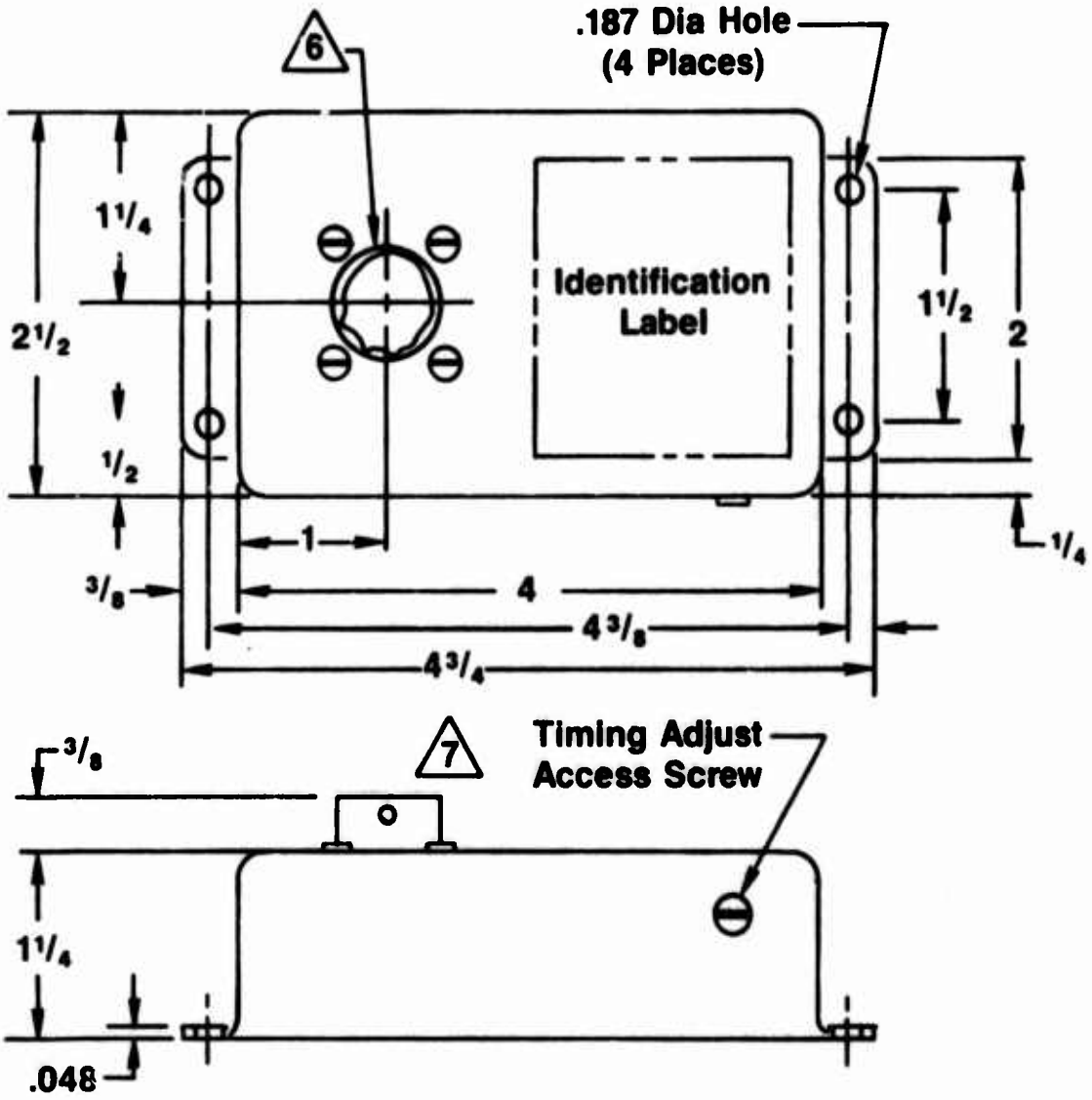

Figure 3. Timer

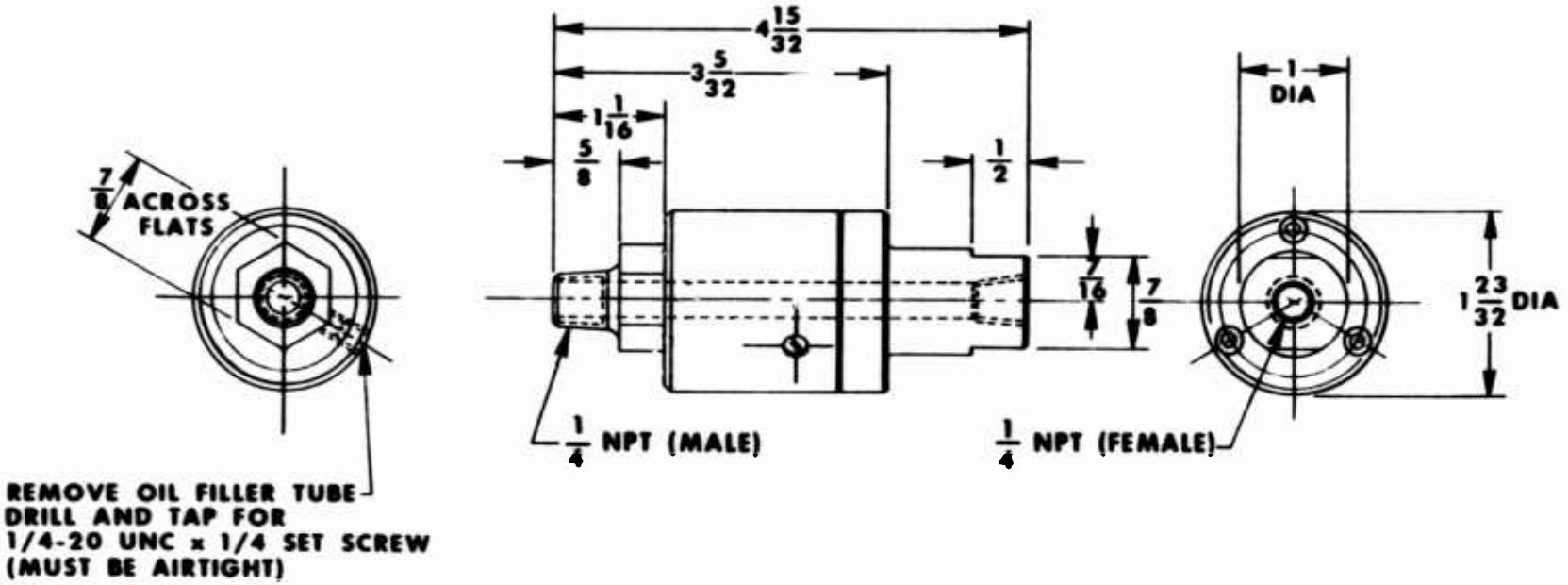

Figure 4. Rotary Union

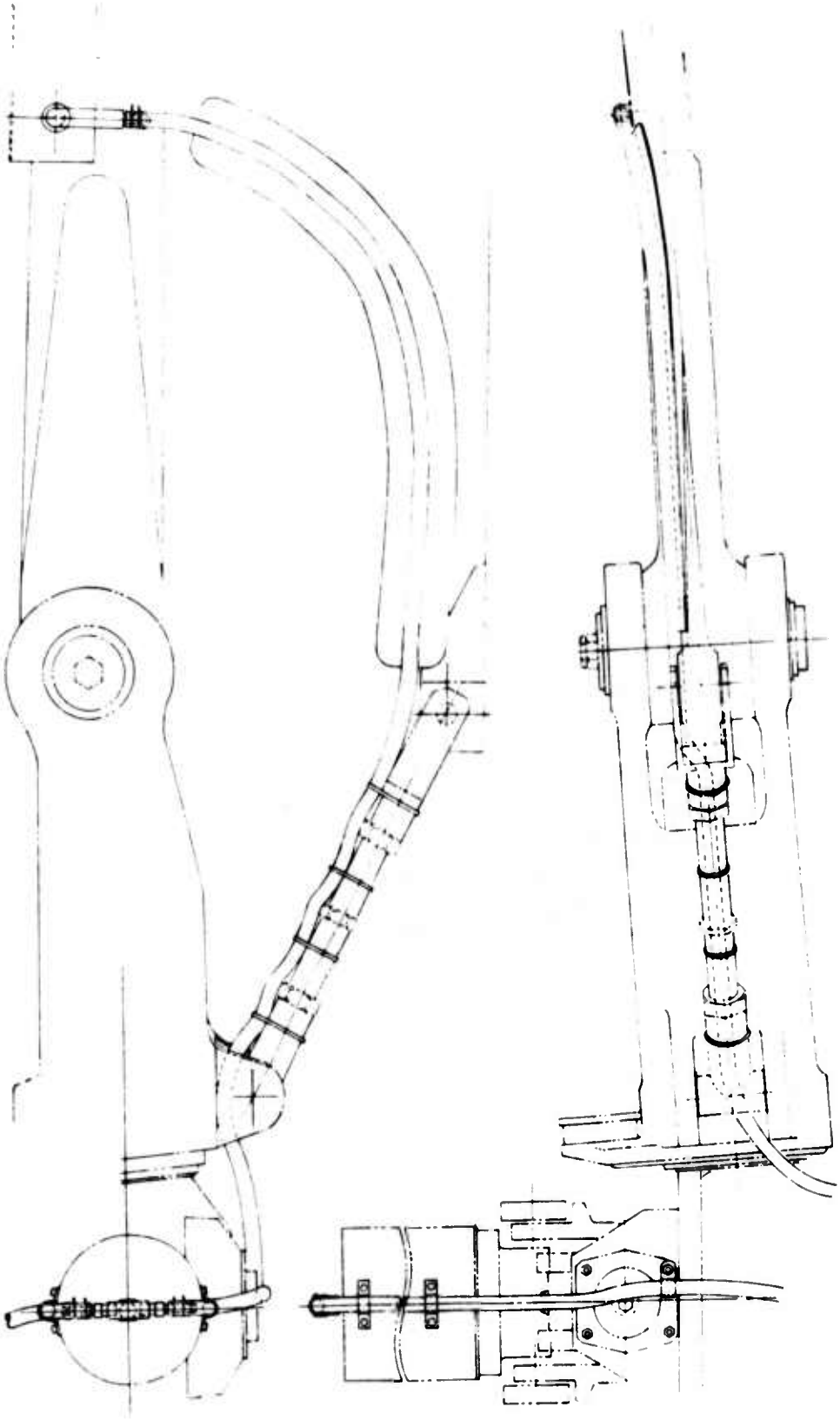

Figure 5. Hose and Flap Assembly

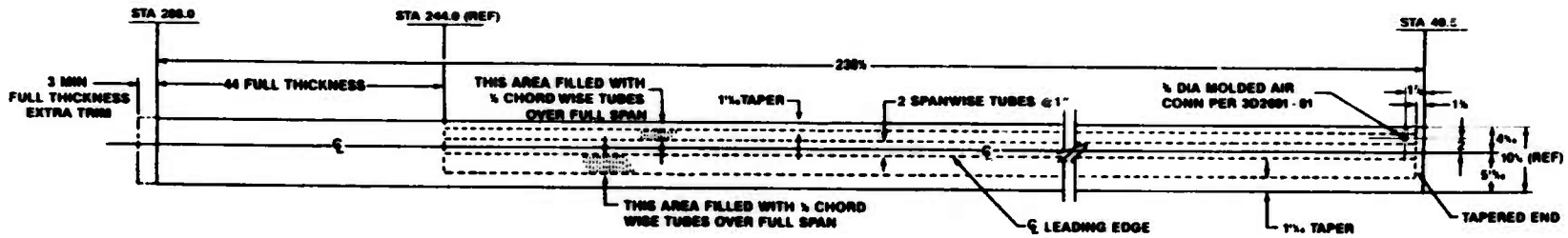

Figure 6. Second Generation PBDS

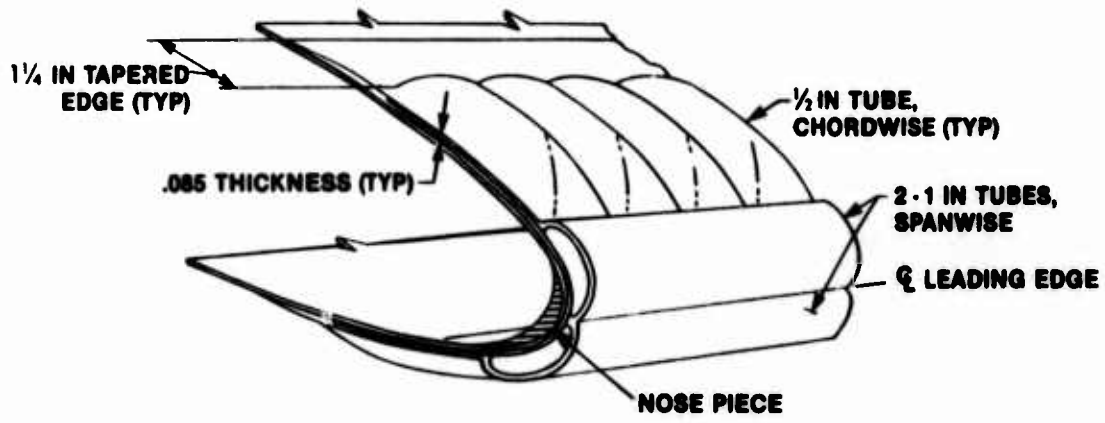

Figure 7. Typical Cross-Section (Second Generation)

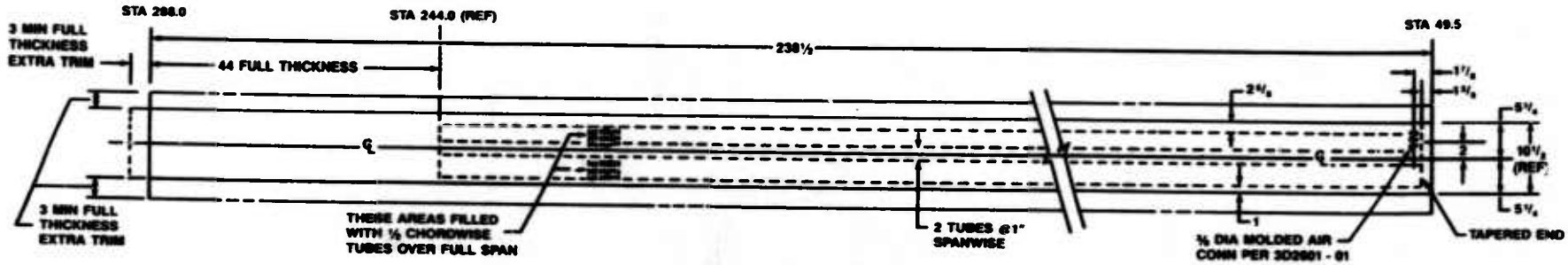

Figure 8. Third Generaion PBDS

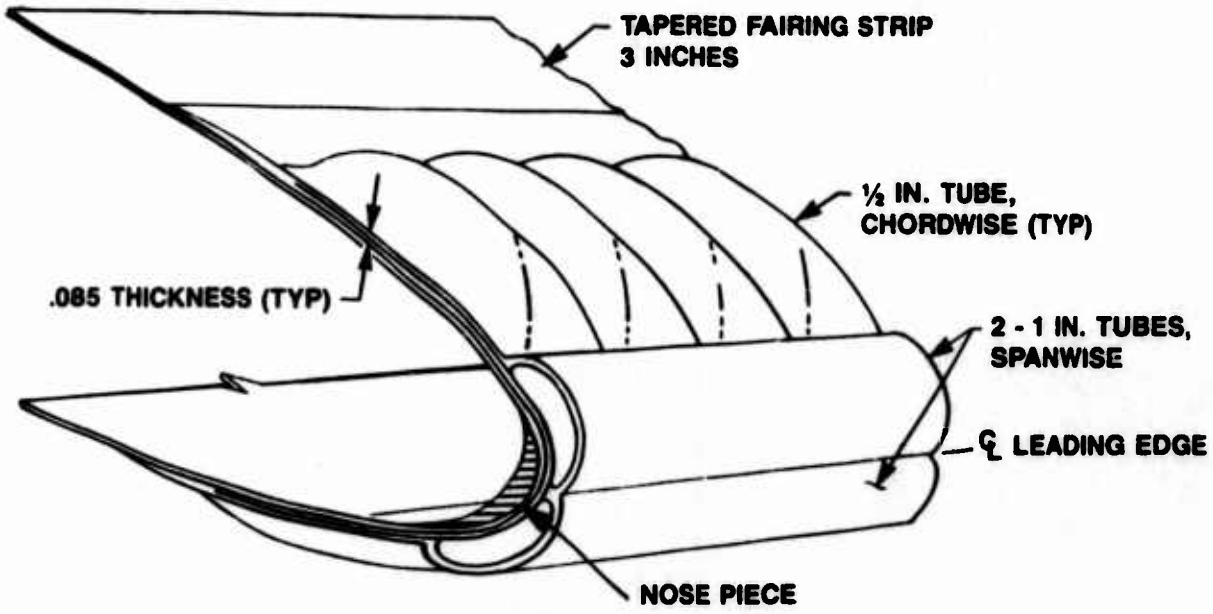

Figure 9. Typical Cross-Section (Third Generation

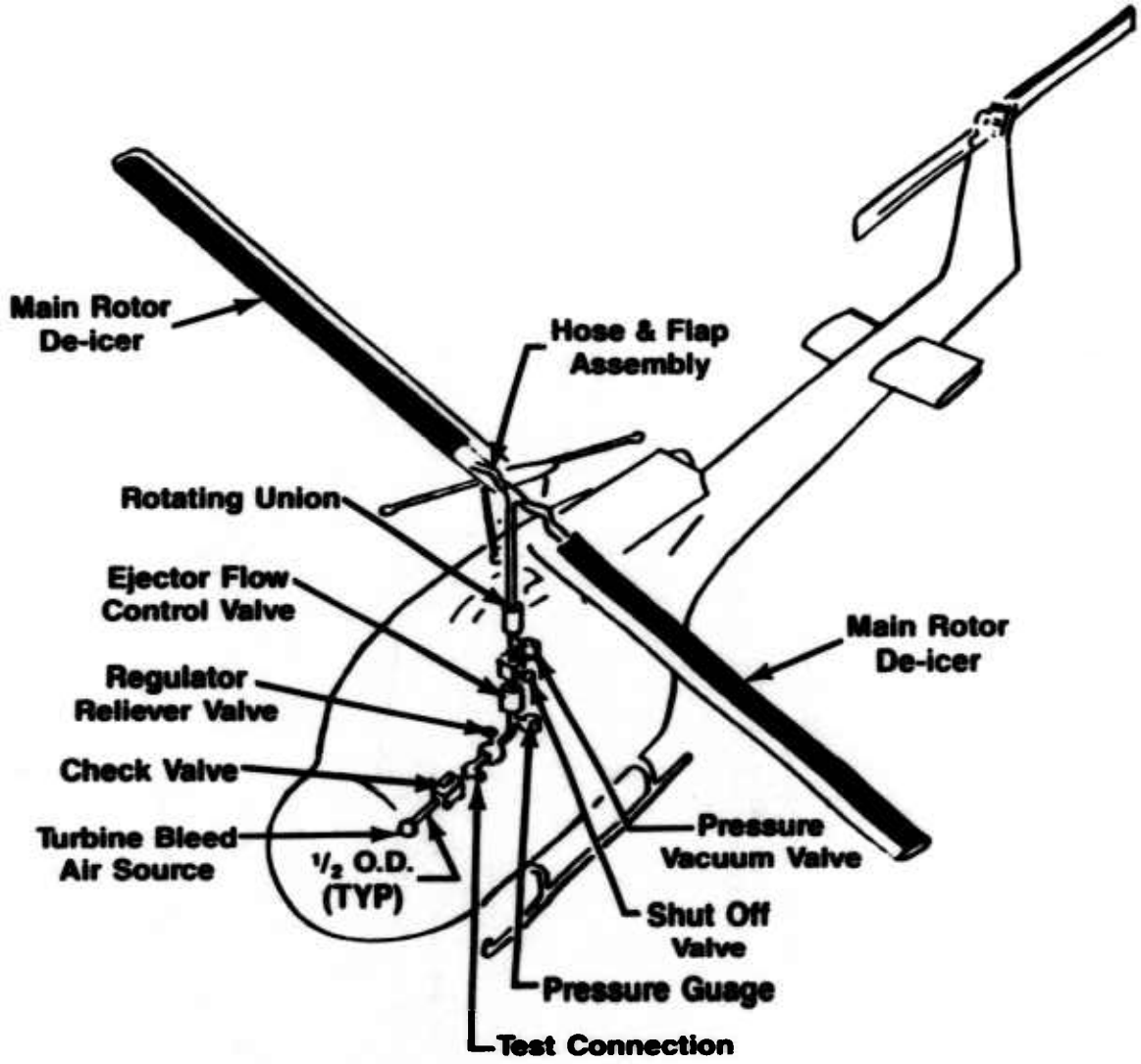

Figure 10. Piping Schematic

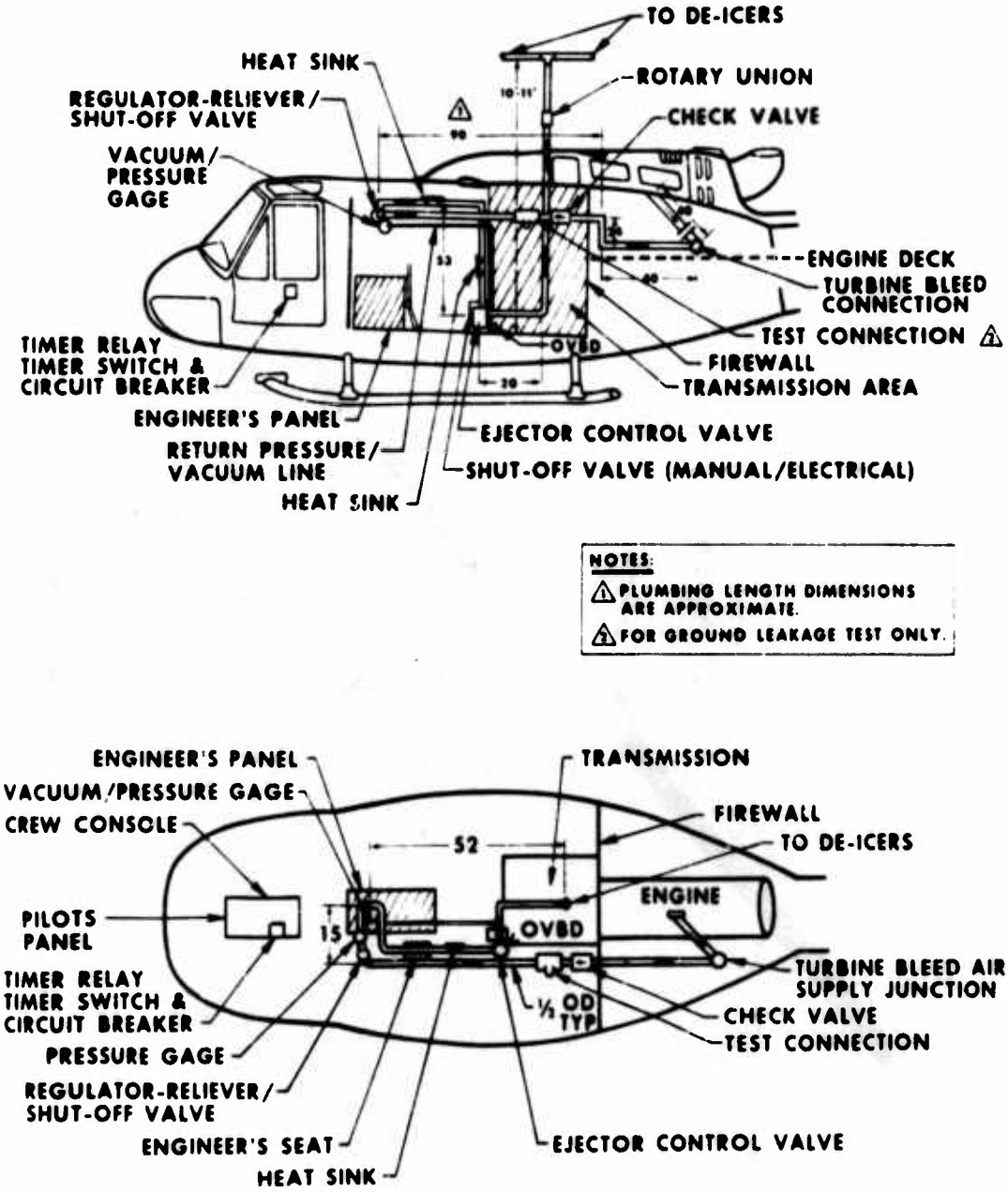

Figure 11. Schematic of Pneumatic Deice System

deicer boots could be removed by use of the regulator-reliever/ shut-off valve. This allows the deicer boots to vent to ambient atmospheric conditions through the de-energized ejector control valve, resulting in partial boot inflation (auto-inflation) from differential air pressures and centrifugal forces on the rotor blades.

Check Valve

4. The check valve is a axial flow, spring loaded, poppet type unit. During normal operation, the valve poppet is open and has low resistance to flow of air from the engine compressor bleed air supply connection. The valve poppet closed to prevent leakage when the direction of air flow through the valve reversed during ground test only.

Regulator-Reliever/Shut-Off Valve

5. The regulator portion is a single-stage, diaphragm-type unit. When the regulated pressure reaches the regulator set point, the pressure on a diaphragm closes a port, shutting off inlet flow of air or preventing system pressure from rising above the system set point. The pressure-reliever is a separate spring-loaded poppet connected to a common system pressure port. The reliever is set to open and relieve pressures slightly above the system nominal pressure level. The regulated pressure was set to 25 psi and the reliever set to open at 27 psi. The regulator-reliever/ shut-off valve is shown in photo 3.

Ejector Flow Control Valve

6. The ejector flow control valve is a three-way solenoid valve (photos 4 and 5) with the deicer connected to the common port. In the de-energized condition, the deicer port is connected to the exhaust port through an internal ejector. System air pressure is connected to the inlet port which has an orifice that operates the ejector to supply vacuum to the deicer. When electrical power is applied to the valve's direct acting solenoid, the valve mechanism shifts to shut off vacuum supply air and to direct inlet air through the deicer port to inflate the deicer. When electrical power is removed from the valve solenoid, the valve mechanism shifts to connect the deicer port to the exhaust port and vacuum is reapplied to the deicer. Modifications were made to a #3D2331 ejector flow control valve to increase the vacuum to 18 inches of mercury with a 25 psi inlet pressure.

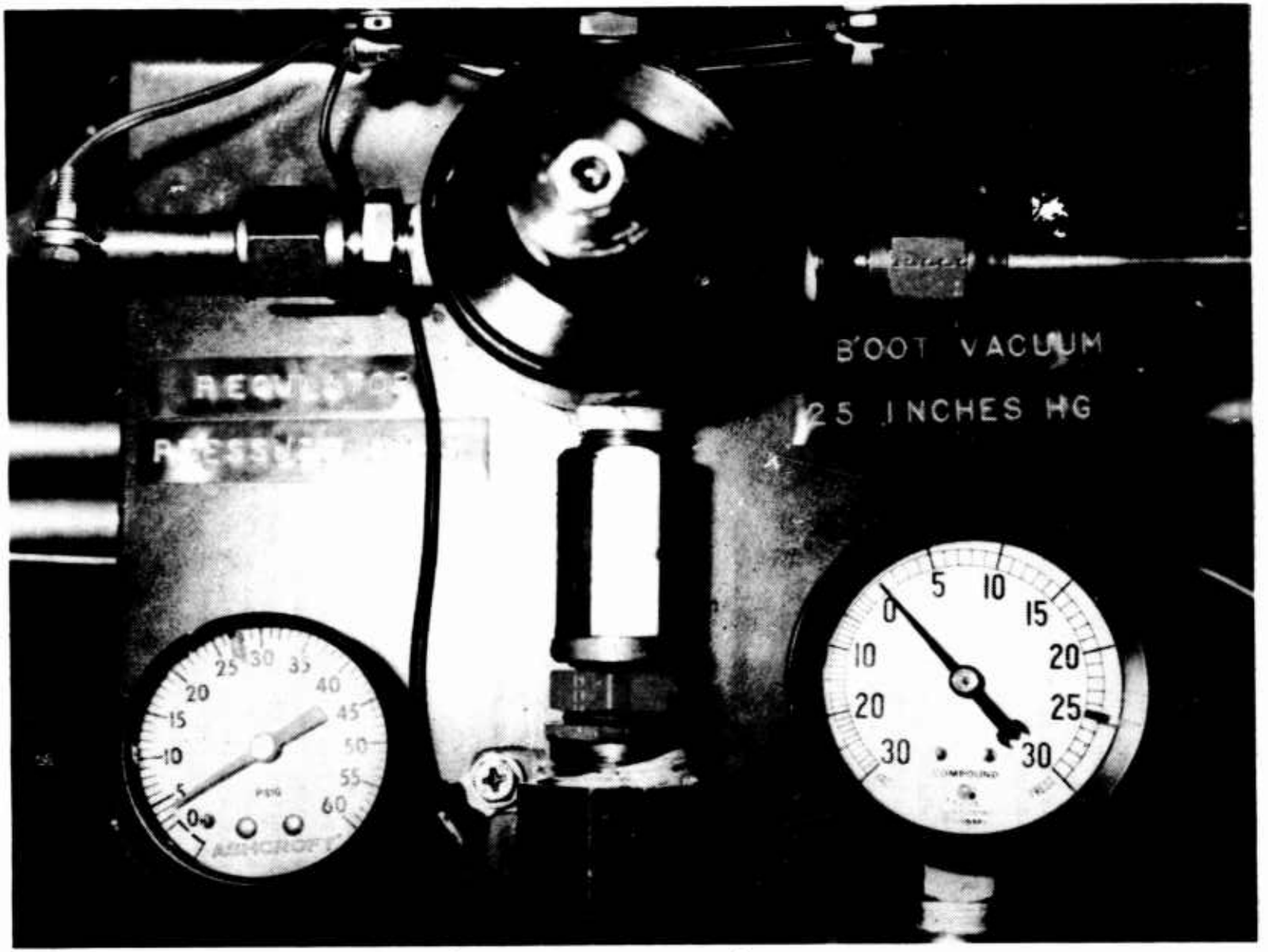

Photo 3. Regulator-Reliever/Shutt-off Valve

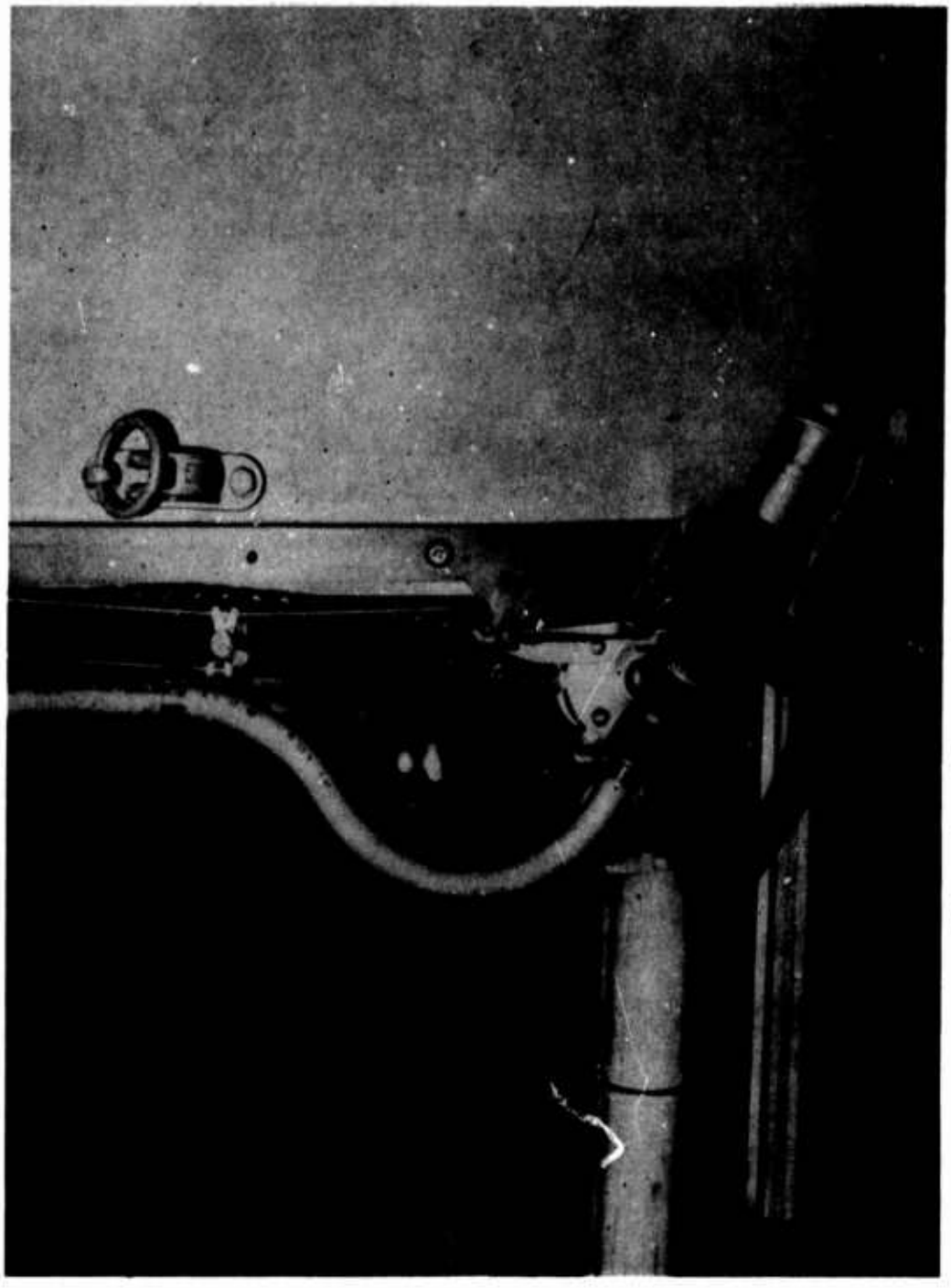

Photo 4. Ejector Flow Control Valve

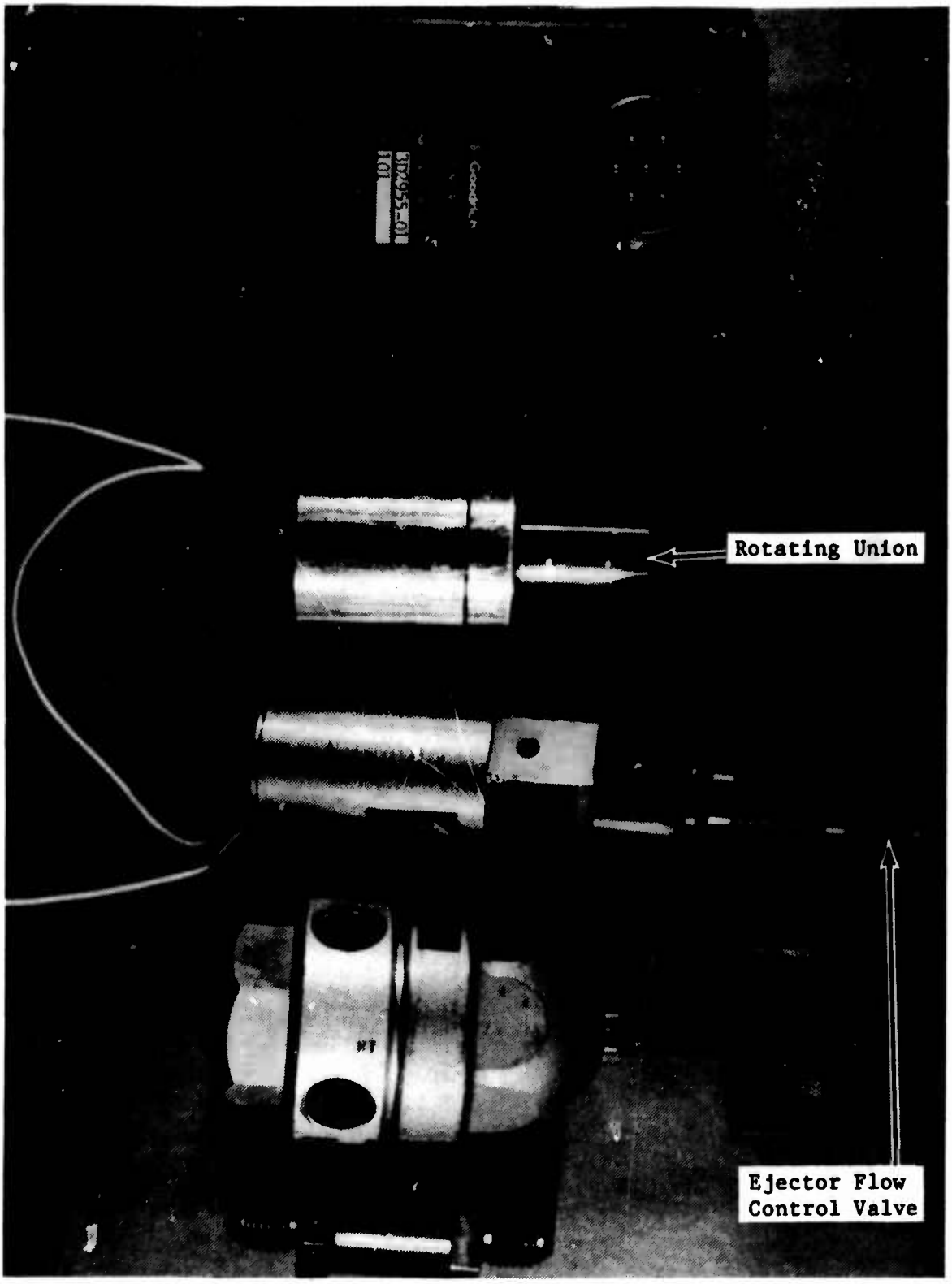

Photo 5. PBDS Components

Timer

7. The pneumatic deicer timer is a solid-state electrical timing device providing a single timed output of electrical power to the ejector control valve solenoid. The timer is actuated through the control switch which causes the solenoid in the ejector flow control valve controlling air flow to immediately energize for the inflation period. At the end of the deicer inflation period, the solenoid is de-energized allowing the air to be evacuated from the deicers.

Control Switch

8. The control switch (photo 6) is a single pole, momentary contact, toggle switch rated for 15 amps @ 125 VAC or 10 amps @ 250 VAC. This switch starts the timer for the single deicer inflation period.

Rotating Union

9. The rotating union (photo 5) is a single pass, straight through air union, with two single row ball bearings. The union utilizes a balanced carbon steel to carbon graphite floating seal with "O" ring. The union is rated by the manufacturer at 1000 rpm and 150 psi maximum.

Deicer Hose and Flap

10. The deicer hose is of wire reinforced neoprene and fabric construction. The hose is modified with a flap constructed of rubber with fabric covering top and bottom. The flap is used to attach the hose to the rotor blade surface. The deicer hose is attached to the drag link using nylon cable ties (TY-RAP, P/N TY-527M, Per MIL-S-23190 and MIS17332).

11. If the control switch is depressed for more than the preset deicer inflation period, the timer will de-energize at the end of the period and the control switch must be released and depressed again to start another inflation period.

Pneumatic Deicer

12. The pneumatic deicer consists of a smooth rubber and fabric blanket containing two small spanwise deicing tubes along the leading edge, with the balance of the deicer consisting of small chordwise deicing tubes as shown in figure 9. Due to self shedding at the outboard section of the blade, the last 44 inches of each blade is non-inflatable. This area is still covered with BF Goodrich Company (BFG) polyurethane erosion material. All tubes

Photo 6. Control Switch

in each deicer are simultaneously inflated through a single air connection located on the "breeze side" of the deicer. The deicer is cement-bonded to the airfoil leading edge.

13. Deicing action is provided by pressurizing the stretchable deicing tubes with compressed air. The inflation of the tubes produces cracking and shearing stresses in the ice causing it to be broken into pieces and break its bond with the deicer surface. The scavenging effect of the air stream and centrifugal forces then removes the ice particles.

14. When the ejector flow control valve is de-energized, vacuum is applied to the deicer tubes. This is necessary to resist negative aerodynamic pressures and to maintain the tubes in a flat or deflated condition. The "breeze side" of the deicer incorporates a 0.025 ply of "ESTANE®" (BFG ploy urethane) to resist weathering and abrasion. The deicers are designed to operate at 25 psi (nominal) and to be installed over the basic airfoil.

Nose Piece

15. A molded nose piece was installed to the leading edge of the UH-1 blade under the pneumatic deicer. The purpose of the nose piece is to keep the airfoil section contour as close to that of a standard UH-1 blade as possible. Weight of the nose piece is approximately 0.121 lbs/ft. With deicer length equal to 19.875 ft each nose piece weighed 2.4 pounds.

Third Generation Deicer

16. Several changes were made to the boot design in an attempt to reduce the performance penalties of the installation and to eliminate the breakup of the internal bleeder material.

17. To improve the aerodynamics of the boot installation, BFG equalized the chord length of the upper and lower boot surfaces, then added a 3.0 in. wide tapered fairing strip cemented behind the boot along the entire length of the blade. The resulting gap between the aft edge of the boot and the forward edge of the fairing strip was filled with an epoxy filler (3M Corp. EC801) to smooth the transition to eliminate the breakup of the internal bleeder material, the material was changed from a bristled, plastic material to a ribbed, rubberized fabric.

APPENDIX C. HELICOPTER ICING SPRAY SYSTEM (HISS) DESCRIPTION

1. The Helicopter Icing Spray System (HISS) is installed in a modified CH-47C helicopter and consists of an internally mounted 1800-gallon water tank and an external spray boom assembly suspended 19 ft beneath the aircraft from a cross-tube through the cargo compartment. Hydraulic actuators rotate the cross-tube to raise and lower the boom assembly. Both the external boom assembly and water supply can be jettisoned in an emergency.

2. The spray boom consists of two 27 ft center sections, vertically separated by 5 ft, and two 17.6 ft outriggers attached to the upper center section. When lowered, the outriggers are swept aft 20° and angled down 10° giving a tip to tip boom width of 60 ft. The boom is assembled of concentric metal pipe; the inner pipe (1-1/2 in. diameter) acts as the water supply and leads to 30 manifolds spaced approximately 3 ft apart along the boom exterior; the outer pipe (4 in. diameter) contains bleed air from the aircraft engines and bleed air auxiliary power unit (APU) and is fitted with a total of 172 nozzle receptacles on the boom surface. These nozzle receptacles are spaced at one foot intervals along the top and bottom of the boom and are staggered to provide alternating upward and downward ejection ports every six inches.

3. A Solar T-62T-40C2 APU is installed in the HISS aircraft bolted to the trunnion assembly between fuselage station (FS) 160 and FS 200. For purposes of safety and noise reduction, the unit is enclosed in a stainless steel box with fiberglass sound proofing. Bleed air from the APU is ducted to a flow mixer which combines aircraft engine bleed air with APU bleed air. The combined APU and engine bleed air enters the boom through flexible tubing leading to the boom air intake pipes on either side of the cabin. Electrically-operated valves which are actuated from a single control panel are installed in the system to control both bleed air and water flow rates.

4. A calibrated air temperature probe and a Cambridge dew point hygrometer provide accurate ambient temperature and humidity measurement. A radar altimeter with aft-facing antenna is mounted on the CH-47 to allow positioning the test aircraft at a known standoff distance. The radar altimeter is wired to red and yellow station-keeping lights on the underside of the aircraft. These lights provide a visual indication to the test aircraft for maintaining the proper standoff distance.

5. Because of gross weight limitations, only 1425 gallons of water are carried. To facilitate photographic documentation during icing tests, a non-toxic, biodegradable chemical with coloration properties similar to sea marker dye is added to the water to impart a yellow color to the ice.

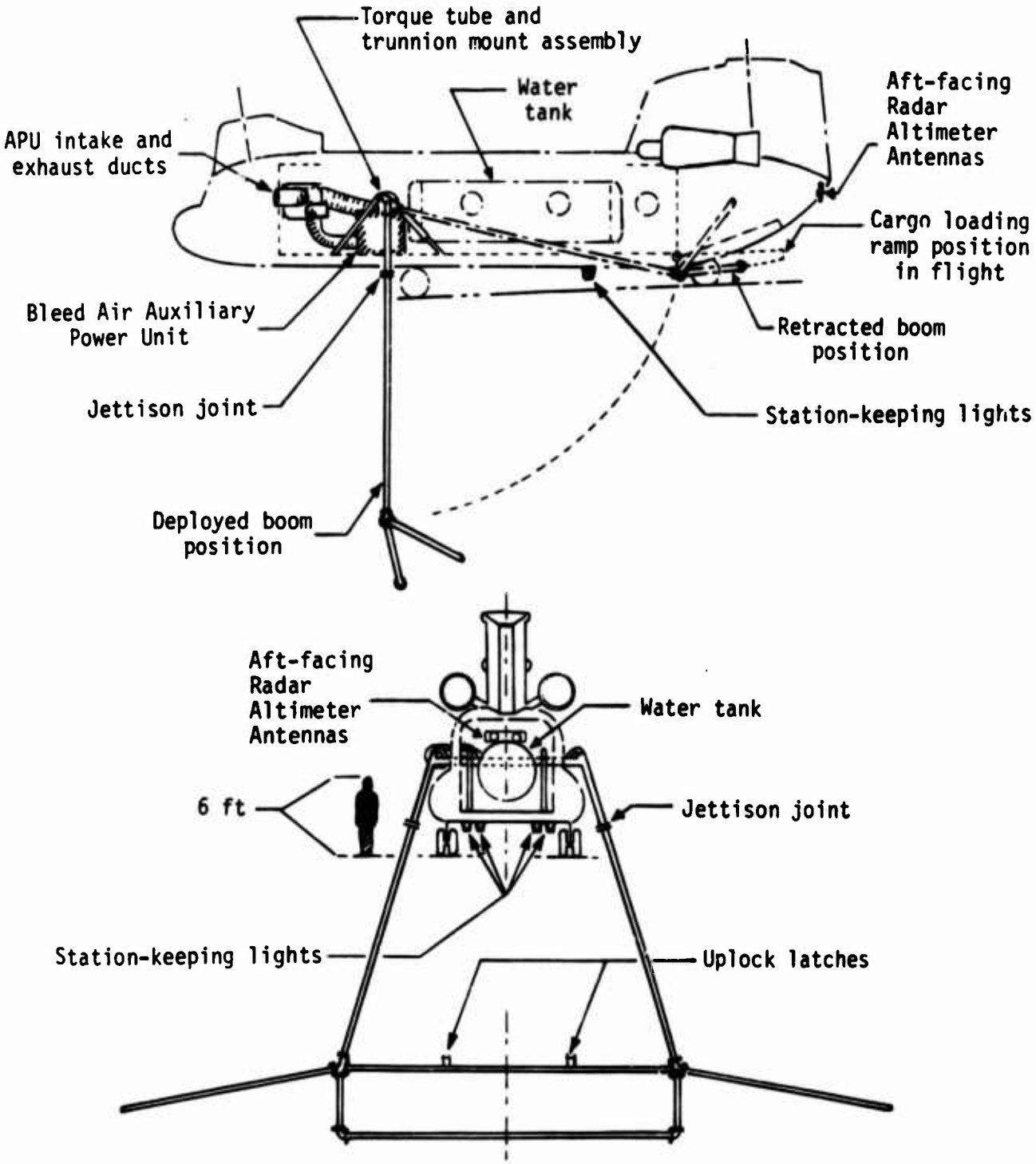

Figure 1. Helicopter Icing Spray System Side and Rear View Schematic

APPENDIX D. INSTRUMENTATION

INSTRUMENTATION

1. The test instrumentation was installed, calibrated, and maintained by the US Army Aviation Engineering Flight Activity (AEFA), with the exception of the load strain gages and slip ring assembly which were installed by Bell Helicopter Textron, Incorporated (BHTI). Digital and analog data were obtained from calibrated instrumentation and were recorded on magnetic tape and/or displayed in the cockpit. The digital instrumentation system consisted of various transducers, signal conditioning units, a ten-bit pulse code modulation (PCM) encoder, and an Ampex AR 700 tape recorder. Time correlation was accomplished with on-board recorded and displayed Inter-Range Instrumentation Group B time. Various specialized test indicators displayed data to the crew continuously during the flight. The instrument panel, in Phase 4 configuration, is shown in photo 1. The instrumentation rack is shown in photo 2. For Phase 4 testing, an instrumentation boom with a swiveling pitot-static tube was mounted on and extended 94 inches forward from the nose of the aircraft (photo 3). The boom provided airspeed, altitude, angle of attack, and sideslip information. Instrument boom airspeed calibration is presented in figure A. Also a T53-L-13B engine torquemeter system was calibrated at the Corpus Christi Army Depot. The calibration is shown in figure B.

2. To document ice forms and sheds, two video recording systems were installed. A NAC, Incorporated high speed video camera was mounted on the cabin roof and the output recorded by a NAC, incorporated high speed video recorder. Additionally, a Teledyne video camera was mounted on top of the rotor hub and focused on one blade as shown in photo 4. Its output was displayed in the aircraft on a Japan Victor Corporation 5-inch color monitor and recorded on a Teac 3/4-inch airborne video recorder (photo 5). A FOR-A video timer provided a visual time code for the hub mounted camera.

3. In addition to standard ship's instruments, the following parameters were displayed in the cockpit and hand recorded:

Pilot's Panel

Airspeed (ship's)* (Boom-Phase 4)
Altitude (ship's)* (Boom-Phase 4)
Fuel Flow*
Fuel Used*
Engine Torque*
Engine inlet screen differential pressure
Rosemount outside air temperature

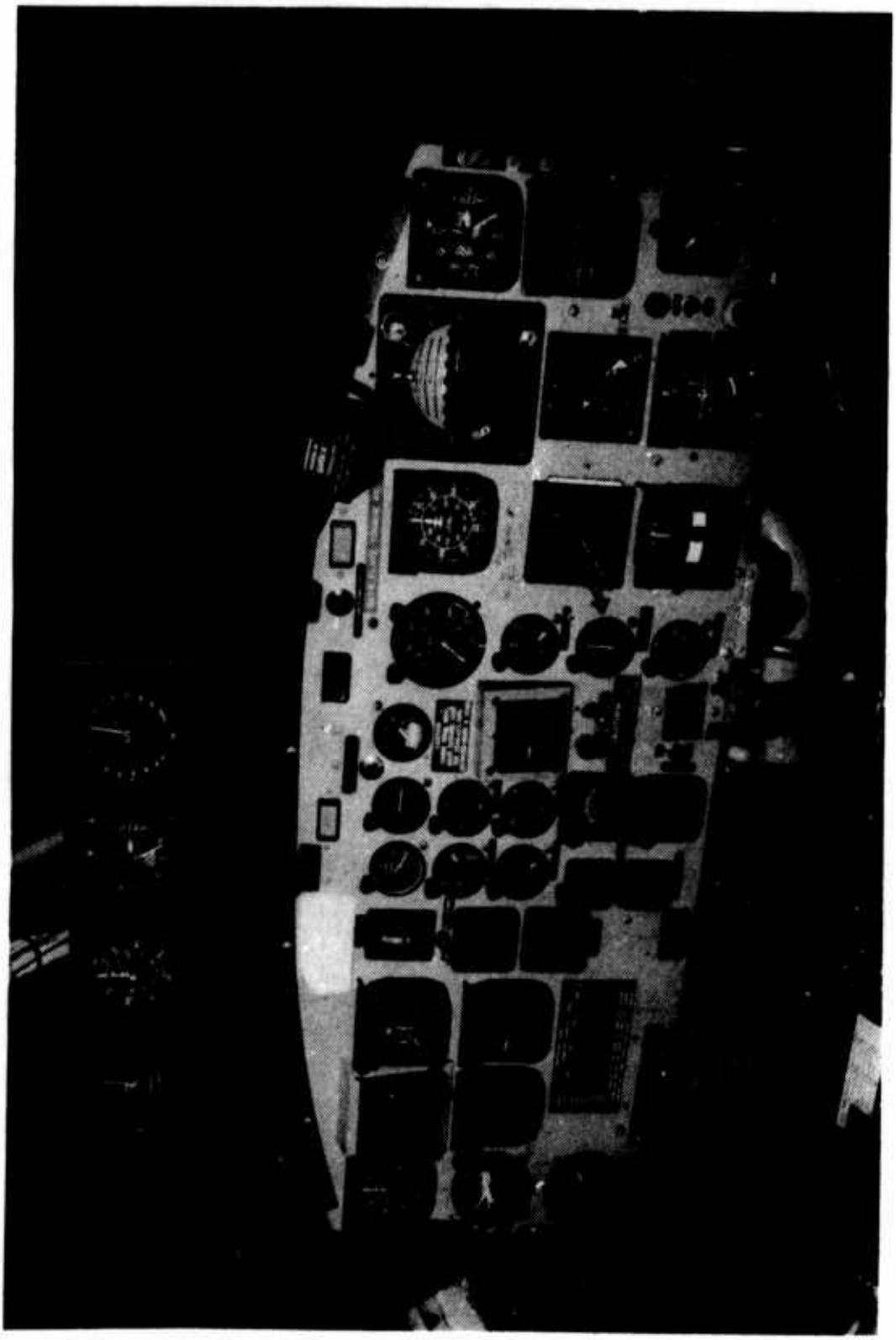

Photo 1. Instrument Panel

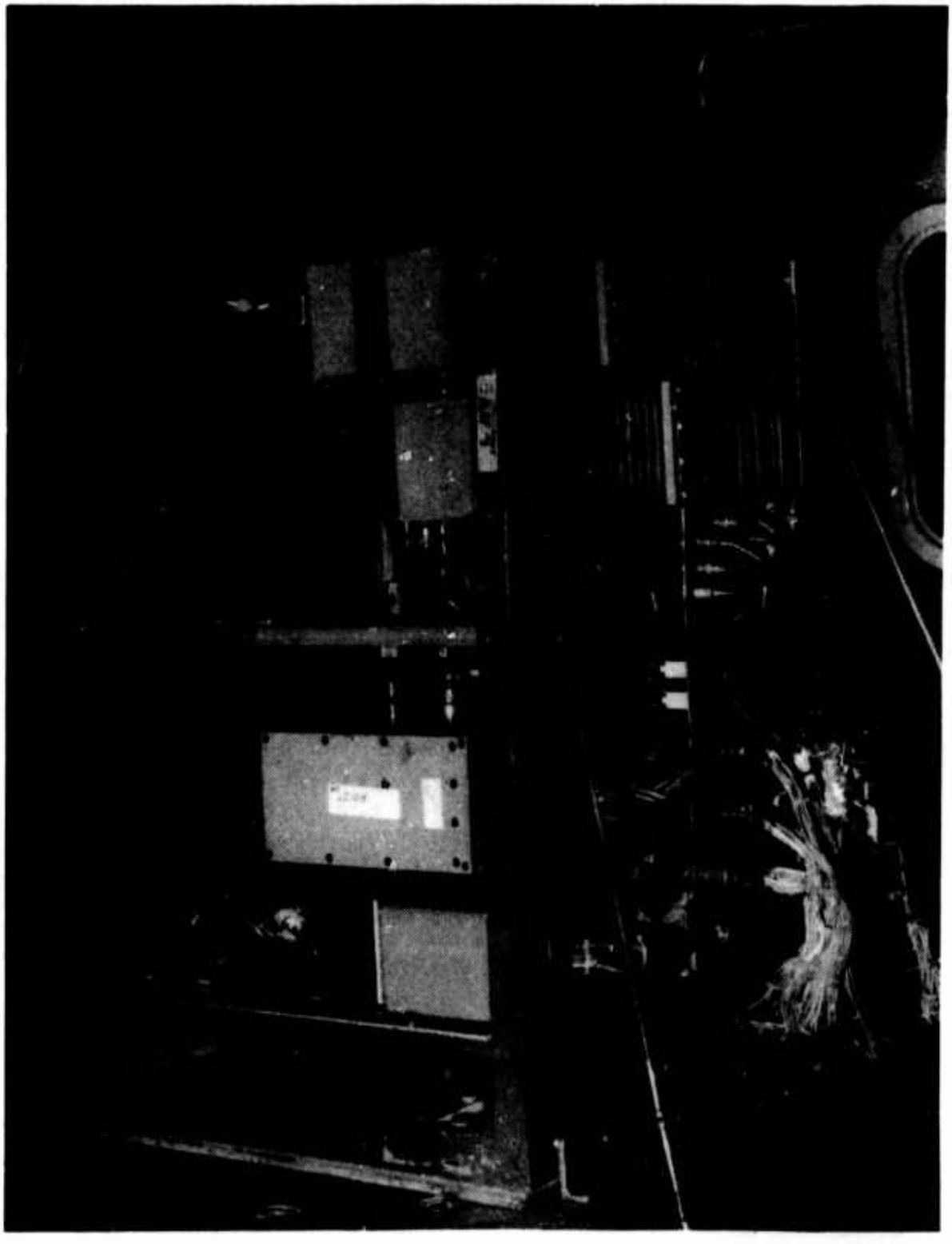

Photo 2. Instrumentation Rack

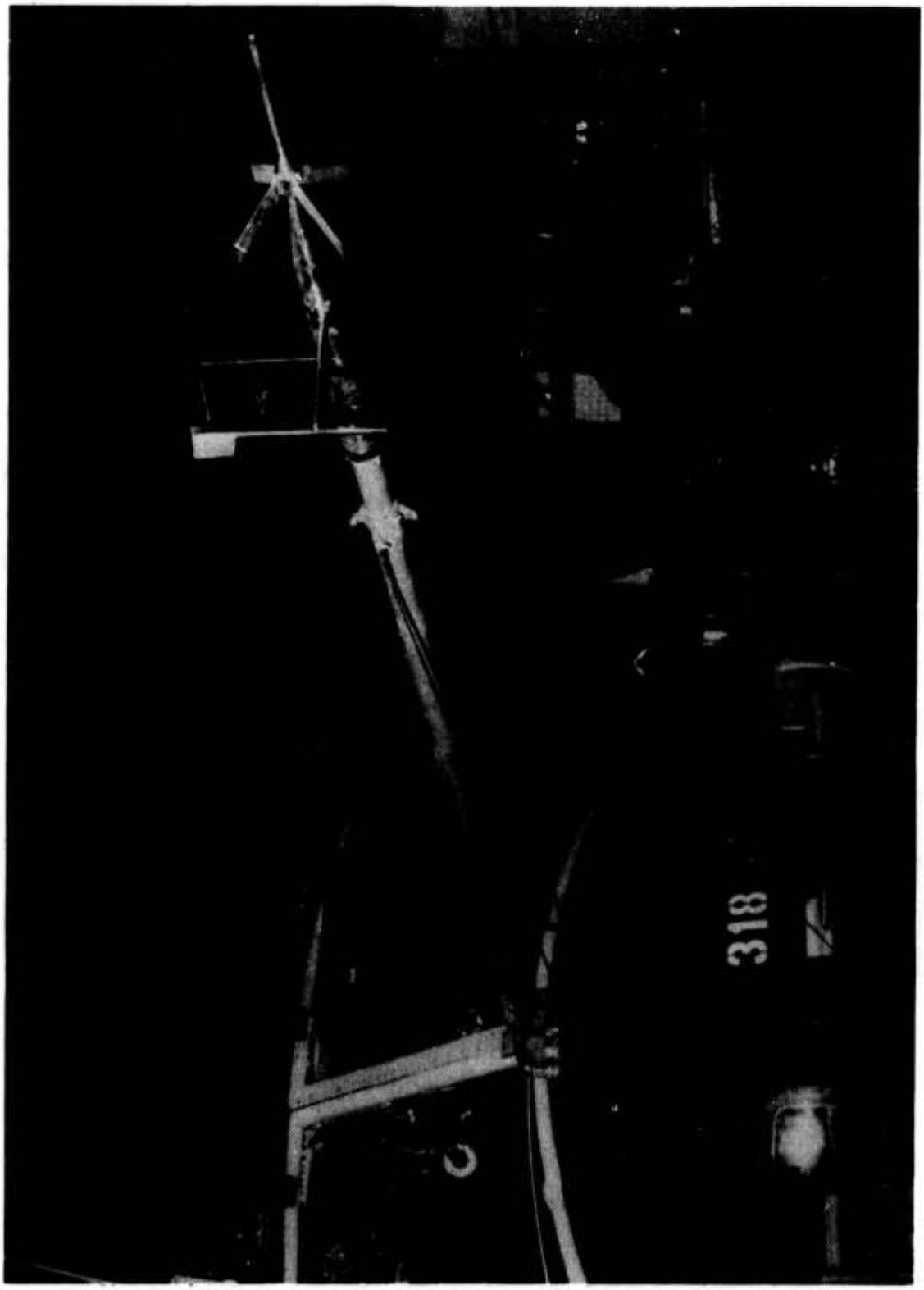

Photo 3. Airspeed Boom

FIGURE A
AIRSPEED CALIBRATION
UH-1H USA S/N 70-16316
BOOM SYSTEM POSITION ERROR

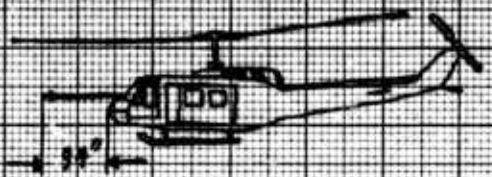

NOTE: TRAILING BOMB METHOD

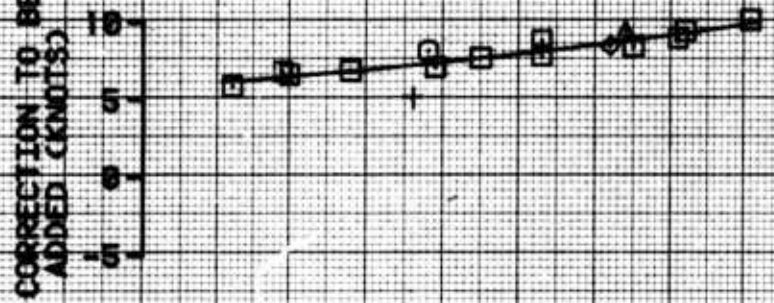

NOT FOR HANDBOOK USE

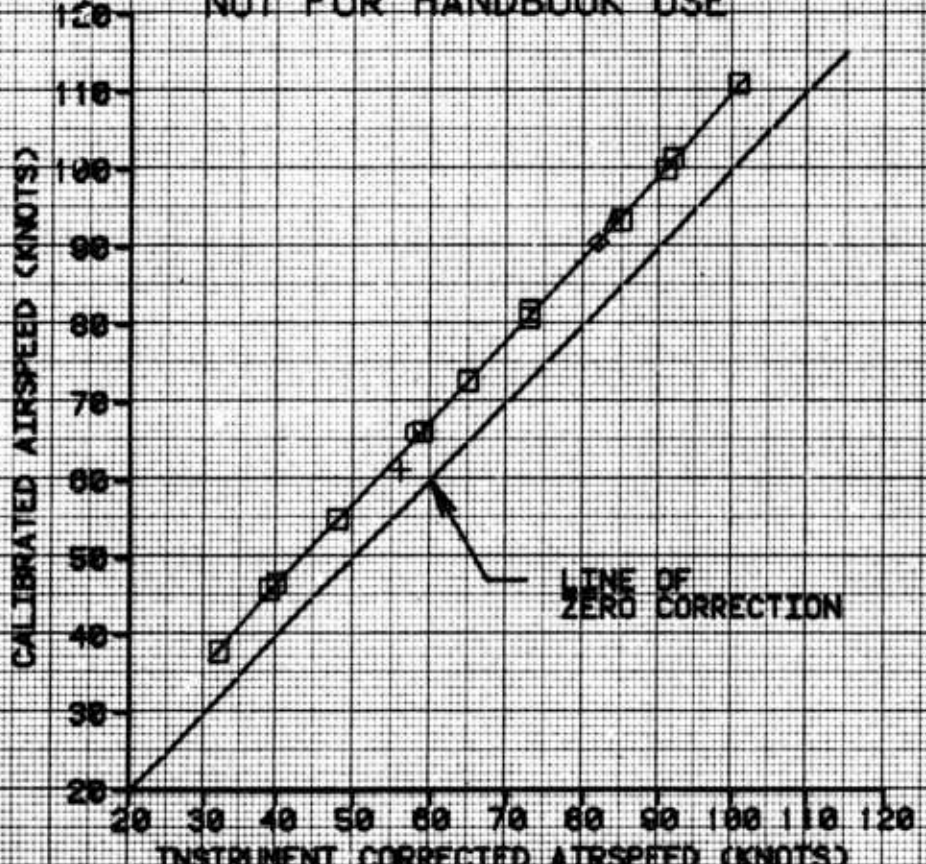

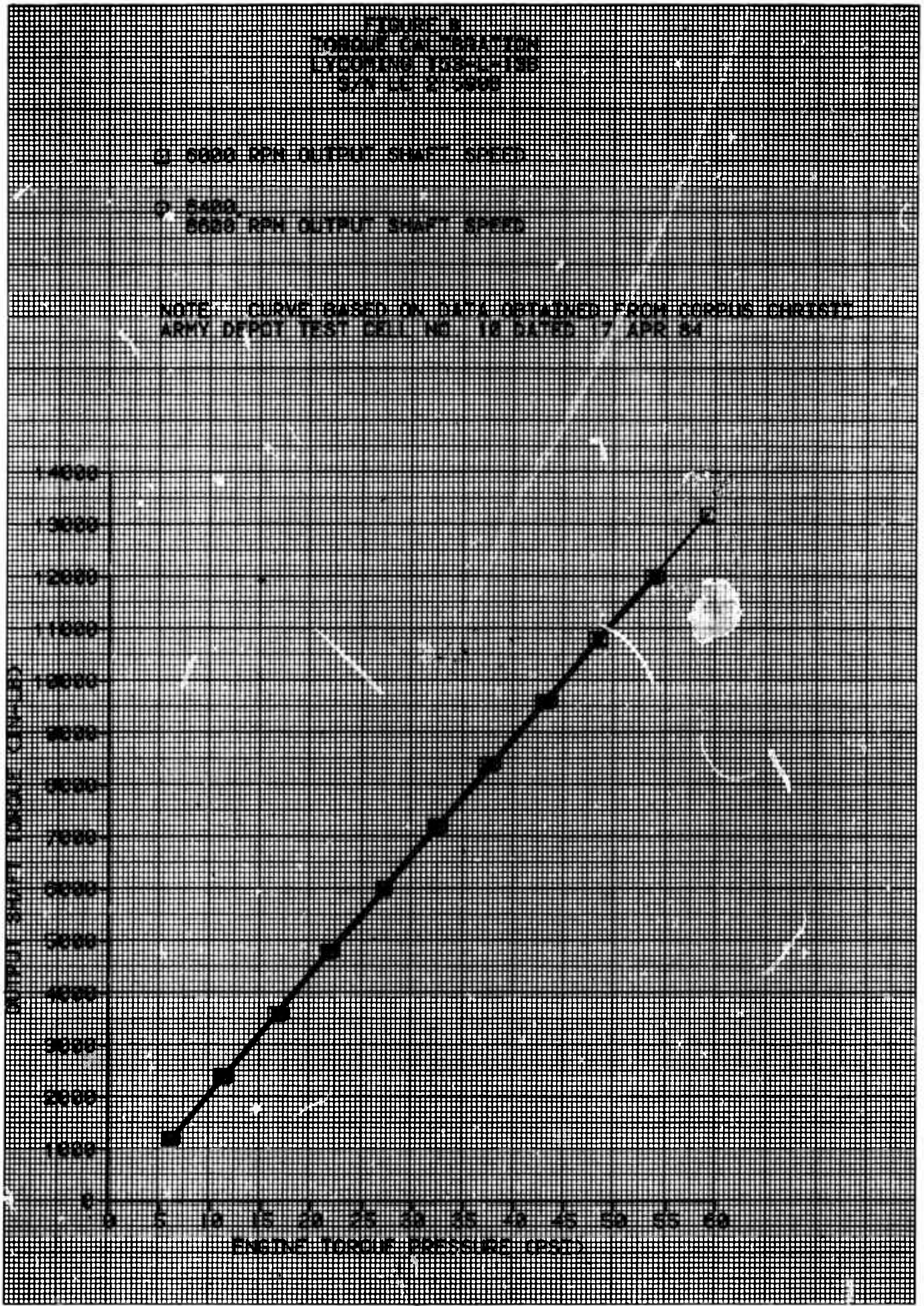
TORQUE &
TORQUE CALIBRATION
LYCOMING T53-L-13B
S/N LE 2-5208
@ 6600 RPM OUTPUT SHAFT SPEED
@ 6400
6600 RPM OUTPUT SHAFT SPEED
NOTE: CURVE BASED ON DATA OBTAINED FROM CORPUS CHRISTI
ARMY DEPOT TEST CELL NO. 18 DATED 17 APR 54
SHAFT HORSEPOWER
14000
13000
12000
11000
10000
9000
8000
7000
6000
5000
4000
3000
2000
1000
0
0
5
10
15
20
25
30
35
40
45
50
55
60
ENGINE TORQUE PRESSURE (PSI)

Photo 4. Hub Mounted Camera

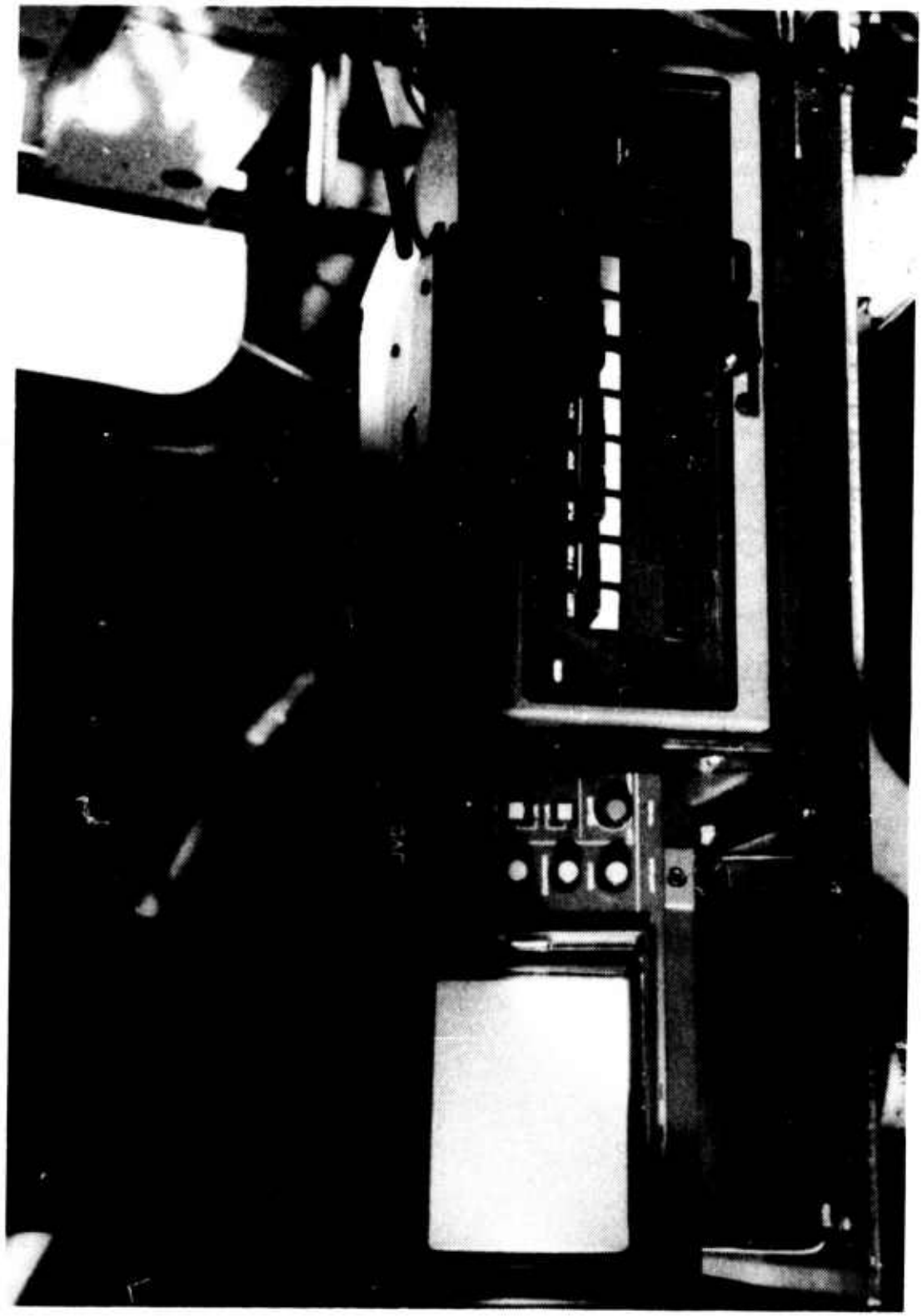

Photo 5. Video Monitor and Recorder

Rosemount liquid water content (LWC)
Leigh MK 12 liquid water content (LWC)
Leigh IRU-5 Integrating Rate Unit (IRU)
Tether cable tension*
Angle of attack (Phase III)*
Angle of sideslip (Phase III)*

Engineer's Panel

Main rotor speed *
Ejector control valve regulated pressure
Vacuum/Pressure of the deicer boot
Engine bleed air temperature at engine deck
Engine bleed air temperature at the ejector control valve
Engine bleed air temperature at the regulator-reliever/shut-off valve

*Calibrated

3. The following parameters were recorded on magnetic tape.

PCM Parameters

Control positions
  Longitudinal
  Lateral
  Directional
  Collective
Engine torque
Fuel flow
Fuel used
Airspeed (ship's)
  (boom-Phase III)
Altitude (ship's)
  (boom-Phase 4)
Main rotor speed
Aircraft attitudes
  Pitch
  Roll
  Yaw
Aircraft rates
  Pitch
  Roll
  Yaw
Outside air temperature
Center of gravity normal acceleration
Tether cable tension
Pilot's seat vibration

Vertical
Longitudinal
Lateral
Aircraft center of gravity vibration
Vertical
Longitudinal
Lateral
Sideslip angle
Rosemount Liquid Water Content
Leigh MK 12 Liquid Water Content
#1 Flight control actuator axial load
#2 Flight control actuator axial load
#3 Flight control actuator axial load
Main rotor mast torque
Main rotor mast bending perpendicular
Main rotor blade beam and chord bending at the following stations
Station 35
Station 84
Station 150
Station 234

4. The following frequency modulated parameters were recorded and telemetered to a ground station for real-time safety of flight monitoring.

Main rotor pitch link axial force
Main rotor mast parallel bending
Main rotor blade beam bending at station 192
Main rotor blade chord bending at station 192
Hub beam bending at station 5.5
Hub chord bending at station 5.5

CLOUD SAMPLING EQUIPMENT

5. Icing conditions were measured in both the natural and artificial environments, by an AEFA JU-21A fixed-wing aircraft, US Army S/N 66-18008. This aircraft was equipped with the following equipment: a Particle Measuring System (PMS), forward scattering spectrometer probe (model FSSP-100), a PMS optical array cloud droplet spectrometer probe (model OAP-200X), Rosemount OAT sensor and display, Cambridge model 137 chilled mirror dew point hygrometer and display, Leigh Mk 10 ice detector unit with digital display, Cloud Technology ice detector unit, and a Small Intelligent Icing Data System (SIIDS).

6. The FSSP-100 sizes particles by measuring the amount of light scattered into the collecting optics aperture during particle

interaction through a focused helium-neon high order, multimode laser beam. The signal pulses are alternating current coupled to a pulse height analyzer which compares their maximum amplitude with a reference voltage derived from a separate measurement of the direct current light signal illuminating the particles. The output of the pulse height analyzer is encoded to give the particle size in binary code. The probe is set up to size particles from 2 to 47 microns having velocities between 20 and 125 m/sec (39 to 243 knots).

7. The OAP-200X sizes using a linear array of photodiodes to sense the shadowing of array elements by particles passing through its field of view. Particles are illuminated by a helium-neon laser and imaged as shadowgraphs on the photodiode array. If the shadowing of each photodiode element is dark enough a flip-flop element is set. The particle size is determined by the number of elements set by a particle's passage, the size of each array element, and the magnification of the optical system. This probe contains 24 active photodiode elements capable of sizing into 15 size channels with a magnification set for a size range of 20 to 300 microns.

8. The SIIDS is a compact data acquisition system designed and programmed specifically for icing studies. It consists of four main components: a microprocessor, Techtran data cassette recorder, Axiom printer, and an operator control panel. The SIIDS has three operational modes: (1) data acquisition, in which averaged raw data are recorded on cassette tape and averaged engineering units are displayed on the printer, (2) a playback mode in which raw averaged data read from the cassette are converted to average engineering units which are displayed on the printer, (3) monitor mode used to set the calendar clock and alter programmed constants. During data acquisition, the operator may select an averaging period of 1/2, 1, 2, 5, or 10 seconds.

9. The following parameters are displayed on the SIIDS printer in engineering units.

a. calendar: year, month, day, hour, minute and second

b. pressure altitude (feet)

c. airspeed (knots)

d. outside air temperature (°C)

e. dew point (°C)

f. total liquid water content observed by the FSSP (g/m^3)

g. total liquid water content observed by both the FSSP and OAP (g/m^3)

h. median volumetric diameter (μm)

i. amount of liquid water content observed for each channel (total 30) of both probes (g/m^3)

APPENDIX E. TEST TECHNIQUES AND DATA ANALYSIS METHODS

PHASE I STRUCTURAL LOADS SURVEY

General

1. Reference 14, appendix A was used as a guide for evaluation purposes. Critical loads parameters indicated in appendix C were telemetered to a ground station for real-time safety of flight monitoring by a National Aeronautics and Space Administration structures engineer for phase 1A and an U.S. Army Aviation Engineering Flight Activity flight test engineer for phase 1B.

Phase 1A

2. Initial testing was conducted with the aircraft ballasted to 9500 pounds gross weight and tethered to a "deadman" anchor. Rotor system loads associated with the three Pneumatic Boot Deicing System (PBDS) configurations (deflated, inflated, and vented) were monitored via telemetry and analyzed during starting and acceleration to engine idle, normal operating speed, and maximum governing speed. Since no problems were encountered, power was increased in increments of 5 psi of engine torque to allowable limits at rotor speeds of 294 and 324 rpm. Dynamic system-engine compatibility was evaluated at each of the two rotor speeds at three power settings corresponding to minimum, mid-range, and maximum. This evaluation was accomplished by manually cycling the collective and directional controls at the critical frequency of the dynamic system.

3. After analysis of the ground test loads survey data, inflight testing was accomplished. The critical loads parameters were monitored and analyzed during hover, low-speed, level flight, climbs and descents, and autorotational entries. Inflight dynamic system-engine compatibility was also evaluated.

Phase 1B

4. After discussion with an U.S. Army Aviation Systems Command structures engineer, it was decided that the changes to the deicer boot should not cause any major change in loads, so only a limited flight loads survey was conducted. This consisted of ground runs with boots deflated, inflated and vented, free hover, forward and sideward accelerations and decelerations and forward flight. Critical load parameters were monitored real-time via telemetry

PHASE 2 ARTIFICIAL ICE TESTING

5. Phase 2 testing was conducted using the Helicopter Icing Spray System (HISS) described in appendix C. Standoff distance for the test aircraft was approximately 150 feet, measured by radar altimeters at the rear of the HISS. Colored lights on the bottom of the HISS and comments from the HISS and chase aircraft crews were used to advise the test aircraft on proper position in the spray cloud.

6. The test procedure involved first immersing the aircraft in the spray cloud for a time interval estimated necessary to accrete a 0.25 inch ice thickness at the main rotor blade midspan point. The aircraft then exited the cloud and the PBDS was activated. The cycle was recorded by aircraft- and chase-mounted video equipment and by still cameras from the HISS and chase aircraft. The spray cloud was reentered for an immersion time necessary to reach either a predetermined aircraft operating limit or 15 minutes, whichever occurred first. The applicable aircraft limits for this test were either an increase of 5 psi engine torque, an increase in inlet differential pressure of 10 inches of water, or onset of a moderate vibration level resulting from an asymmetric shed. When the aircraft exited the cloud, a PBDS activation cycle was performed and the results documented as described above. The aircraft reentered the cloud for multiple activations in the cloud. The time between cycles was reduced until the chase aircraft reported no ice shed. Several cycles at this immersion time were performed. The aircraft then exited the cloud for photographs and another activation cycle.

PHASE 2 NATURAL ICING TESTING

7. The techniques for natural icing were the same as for artificial icing tests. The U-21 chase/scout aircraft was sent to locate satisfactory natural conditions which were relayed to the test aircraft. All out-of-cloud PBDS activation cycles were documented by aircraft mounted video and still cameras in the U-21 chase aircraft.

PHASE 3 ARTIFICIAL RAIN EROSION TESTS

8. Artificial rain erosion tests were conducted behind the HISS with the spray system modified to produce much larger drop sizes than used for icing conditions. Drop sizes were measured on the ground with an oil-filled sample dish and inflight with gelatin slides and on the windshields with a steel ruler. Flight times were limited to approximately one hour by HISS water capacity.

PHASE 4 PERFORMANCE AND HANDLING QUALITIES

Weight and Balance

9. The aircraft empty weight (including full oil and trapped fuel) and longitudinal center of gravity (cg) location were determined with a portable electronic weighing kit.

10. A manometer-type external sight gauge was calibrated and used to determine fuel volume. Fuel specific gravity was measured with a hydrometer. The fuel loading for each test flight was determined both prior to engine start and following engine shutdown. Fuel used in flight was recorded manually from a test fuel used system and compared with the pre and post flight sight gauge readings. Fuel cg versus fuel volume contained in the fuel cell (209.0 gallon capacity) had been previously determined. This calibration was used to calculate aircraft cg for each test point. Aircraft engine start gross weight and cg were also controlled by ballast installed in the aircraft.

PERFORMANCE

Hover Performance

11. Hover performance was obtained by the tethered hover technique. Additional free-flight hover data were accumulated to verify the tethered hover data. All hover tests were conducted in winds of less than 3 knots. Tethered hover consists of restraining the helicopter to the ground by a cable in series with a load cell. An increase in cable tension, measured by the load cell, is equivalent to an increase in gross weight. Free flight hover tests consisted of stabilizing the helicopter at a desired height using a 5 ft length of rope tied to one skid as a height reference. All hovering data were reduced to nondimensional parameters of C_P and C_T using equations 1 and 2, respectively.

a. Coefficient of power (C_P):

$$C_P = \frac{SHP\ (550)}{\rho A(\omega R)^3} \qquad (1)$$

b. Coefficient of Thrust (C_T):

$$C_T = \frac{GW + CABLE\ TENSION}{\rho A(\omega R)^2} \qquad (2)$$

where:

SHP = Engine output shaft horsepower
550 = Conversion factor (ft-lb/sec/SHP)
ρ = Air density (slug/ft^3)
A = Main rotor disc area (ft^2) = 1809.6
Ω = Main rotor angular velocity (radians/sec = 33.93 at 324 RPM)
R = Main rotor radius (ft) = 24.0
GW = Gross weight (lb)

Level Flight Performance

12. Conventional level flight performance test techniques were used to conduct this evaluation. To achieve a constant C_T throughout each test, a constant referred gross weight (the ratio of gross weight to pressure ratio, W/δ) and referred rotor speed (the ratio of rotor speed to square root of temperature ratio, $N_R/\sqrt{\theta}$) were maintained. A constant W/δ was maintained by increasing pressure altitude as the aircraft gross weight decreased due to fuel burnoff. Rotor speed was varied to maintain a constant $N_R/\sqrt{\theta}$ as the ambient temperature varied. All tests were conducted in non-turbulent conditions to preclude atmospheric disturbances influencing the results.

13. The results of the level flight tests were converted to nondimensional form and plotted as C_P versus C_T at constant advance ratio (μ). This plot defined the level flight performance for all gross weights, density altitudes, and airspeeds throughout the C_T range tested.

14. The level flight performance data were generalized by the following nondimensional coefficients:

a. Coefficient of thrust (C_T):

$$C_T = \frac{\text{Thrust}}{\rho A(\Omega R)^2} \tag{3}$$

b. Advance ratio (μ):

$$\mu = \frac{(1.68781)V_T}{\Omega R} \tag{4}$$

c. Advancing blade tip Mach number (M_{tip}):

$$M_{tip} = \frac{(1.68781)V_T + (\Omega R)}{a} \quad (5)$$

Where:

Thrust = Gross weight (lb) during free flight in which there is no acceleration component in the vertical direction.
1.68781 = Conversion factor (ft/sec/knot)
V_T = True airspeed (knot) = (calibrated airspeed/$\sqrt{\sigma}$)
σ = Density ratio = $\rho/\rho_o = \delta/\theta$
ρ_o = air density at sea level standard day (slug/ft^3) = 0.002376892
$\delta = [1-(6.875586 \times 10^{-6}) H_P]^{5.255863}$
H_P = Pressure altitude (ft)
$\theta = (T + 273.15)/288.15$
T = ambient air temperature (°C)
a = Speed of sound (ft/sec) = $1116.45\sqrt{\theta}$

For normal operating rotor speed of 324 rpm the following constants were used:

A = 1809.6 ft^2
ΩR = 814.30 ft/sec
$A(\Omega R)^2 = 1.199891830 \times 10^9$ ft^4/sec^2
$A(\Omega R)^3 = 9.770728966 \times 10^{11}$ ft^5/sec^3

Shaft Horsepower Required

15. The engine output shaft torque was determined from the engine manufacturer's torque system. The relationship of measured torque pressure (PSI) to engine output shaft torque (ft-lb) was determined from the engine test cell calibration shown in figure 1, appendix C. The output shp was determined from the engine output shaft torque and rotational speed by the equation below.

$$SHP = \frac{2\pi \times N_P \times Q}{33{,}000} \quad (6)$$

where:

N_p = Engine output shaft rotational speed (rpm)
Q = Engine output shaft torque (ft-lb)
33,000 = Conversion factor (ft-lb/min/SHP)

Airspeed Calibration

16. The boom pitot-static system was calibrated by using the trailing bomb method to determine the airspeed position error, which is presented in figure 2, appendix C. Calibrated airspeed (V_{cal}) was obtained by correcting the boom indicated airspeed (V_i) using instrument (ΔV_{ic}) correction.

$$V_{cal} = V_{i_{bomb}} + \Delta V_{ic_{bomb}} \quad (7)$$

The airspeed position error (correction to be added) was determined by:

$$\Delta V_{pc_{boom}} = V_{cal} - (V_{i_{boom}} + \Delta V_{ic_{boom}}) \quad (8)$$

HANDLING QUALITIES

17. Handling qualities data were collected and evaluated using standard test methods as described in reference 8, appendix A.

18. The Handling Qualities Rating Scale presented in figure 1 was used to augment pilot comments relative to handling qualities and workload.

VIBRATION

19. The Vibration Rating Scale presented in figure 2 was used to augment pilot comments relative to vibration.

DEFINITIONS

Unsatisfactory Characteristics

20. An unsatisfactory characteristic is defined as a feature of the equipment that could compromise safety, result in damage to the equipment or injury to personnel if operation is continued, or jeoparidze the satisfactory completion of an assigned mission.

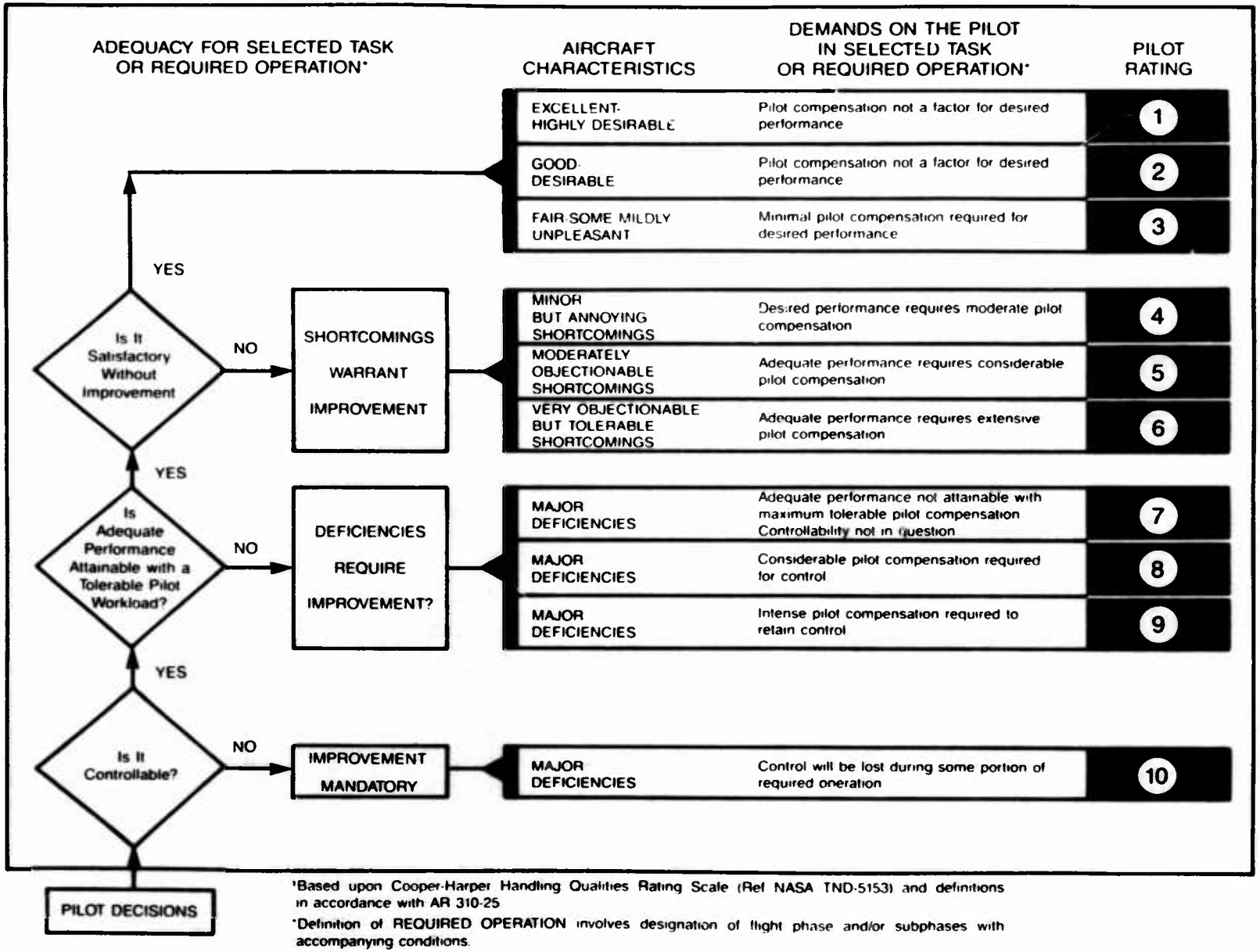

Figure 1. Handling Qualities Rating Scale

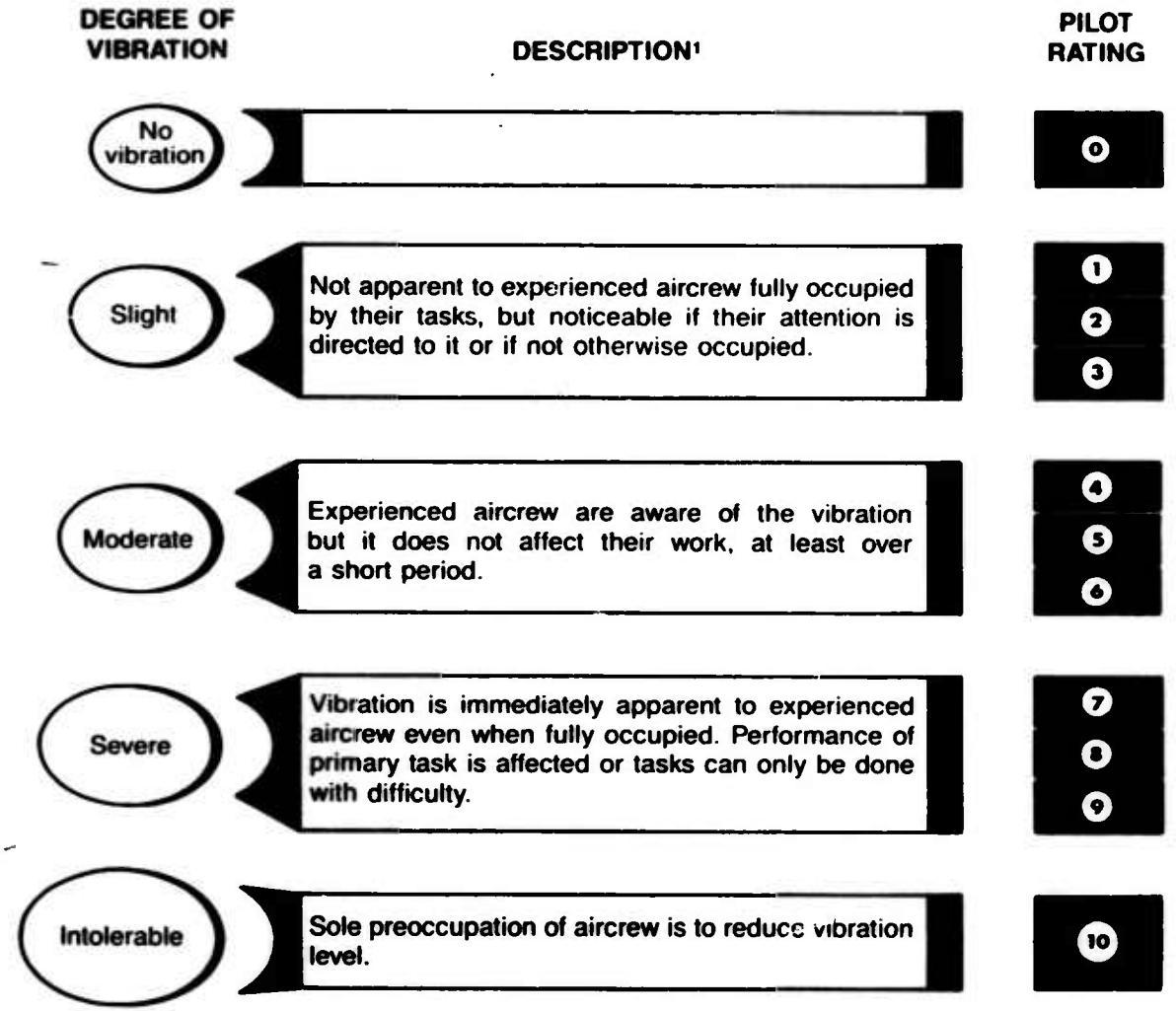

[1]Based on the Subjective Vibration Assessment Scale developed by the Aeroplane and Armament Experimental Establishment, Boscombe Down, England.

Figure 2. Vibration Rating Scale

Undesirable Characteristics

21. An undesirable characteristic is defined as a feature of the equipment that reduces efficiency, results in increased workload, or provides an unnecessary annoyance. It generally should not cause an immediate breakdown, jeopardize safety, or materially reduce the usability of the material or end product.

APPENDIX F. TEST DATA

FIGURE 1

PBDS ACTIVATION CYCLE

JUH-1H USA S/N 70-16318

AVG GROSS WEIGHT (LB)	AVG CG LOCATION LONG (FS)	AVG CG LOCATION LAT (BL)	TRIM DENSITY ALTITUDE (FEET)	AVG OAT (DEG C)	TRIM ROTOR SPEED (RPM)	TRIM CALIBRATED AIRSPEED (KNOTS)	FLIGHT CONDITION
9060	137.4(MID)	.5 RT	1315	6.0	322	0	GROUND RUN

NOTE: GROUND RUN, FLAT PI

SOLID LINE — SHORT DASH — LONG DASH

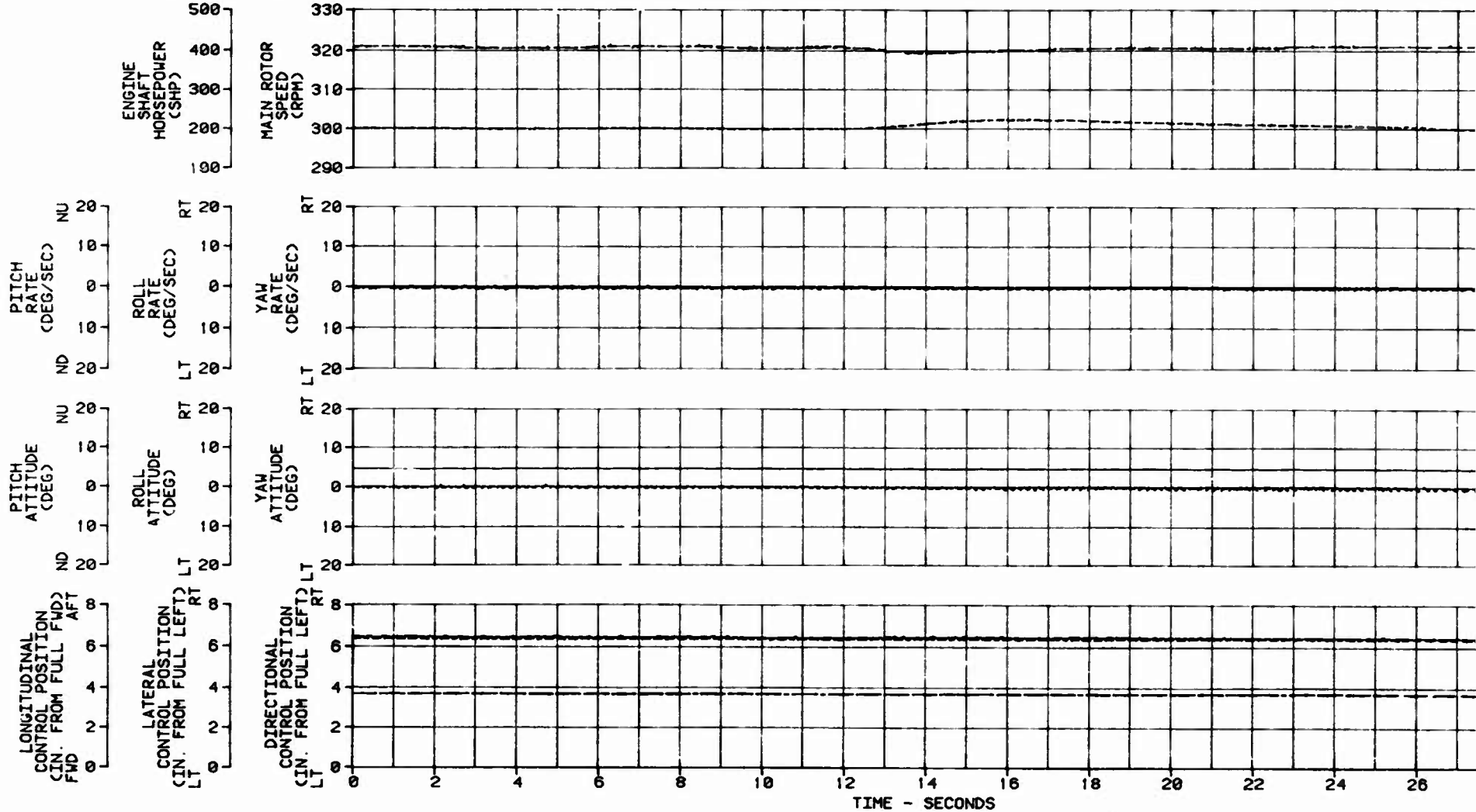

FIGURE 2

PBDS ACTIVATION CYCLE

JUH-1H USA S/N 70-16318

SHORT DASH / LONG DASH	AVG GROSS WEIGHT (LB)	AVG CG LOCATION LONG (FS)	AVG CG LOCATION LAT (BL)	TRIM DENSITY ALTITUDE (FEET)	AVG OAT (DEG C)	TRIM ROTOR SPEED (RPM)	TRIM CALIBRATED AIRSPEED (KNOTS)	FLIGHT CONDITION
	7430	136.2(MID)	0.5 RT	6920	11.0	321	80	LEVEL

NOTES: 1. DRY AIR TESTING
2. PILOT'S SEAT LATERAL ACCELEROMETER INOPERATIVE

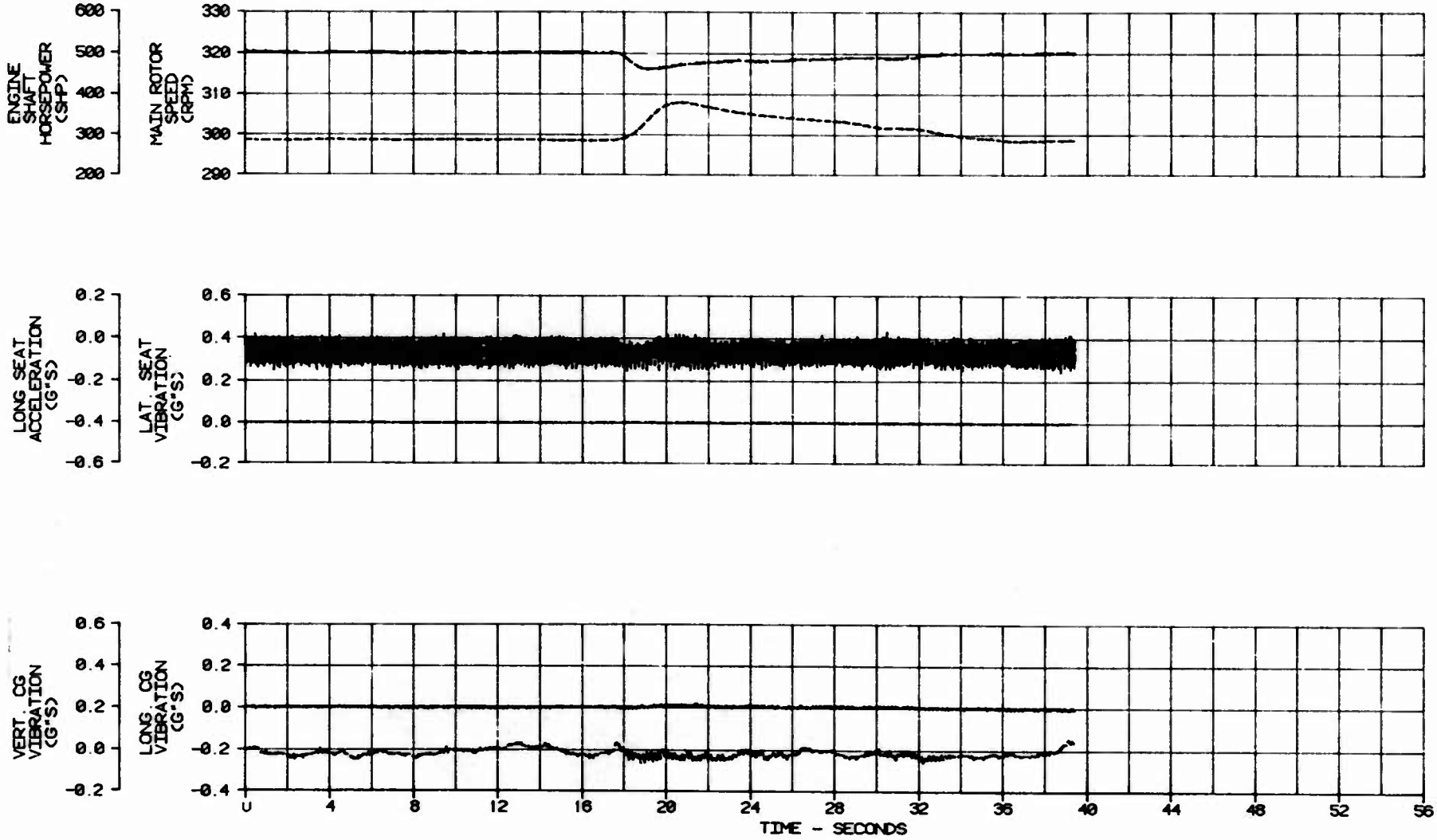

FIGURE 3

PBDS ACTIVATION CYCLE

JUH-1H USA S/N 70-16318

SOLID LINE	SHORT DASH	LONG DASH	AVG GROSS WEIGHT (LB)	AVG CG LOCATION LONG (FS)	AVG CG LOCATION LAT (BL)	TRIM DENSITY ALTITUDE (FEET)	AVG OAT (DEG C)	TRIM ROTOR SPEED (RPM)	TRIM CALIBRATED AIRSPEED (KNOTS)	FLIGHT CONDITION
			7560	135.1(FWD)	0.5 LT	1510	-13.0	314	79	LEVEL

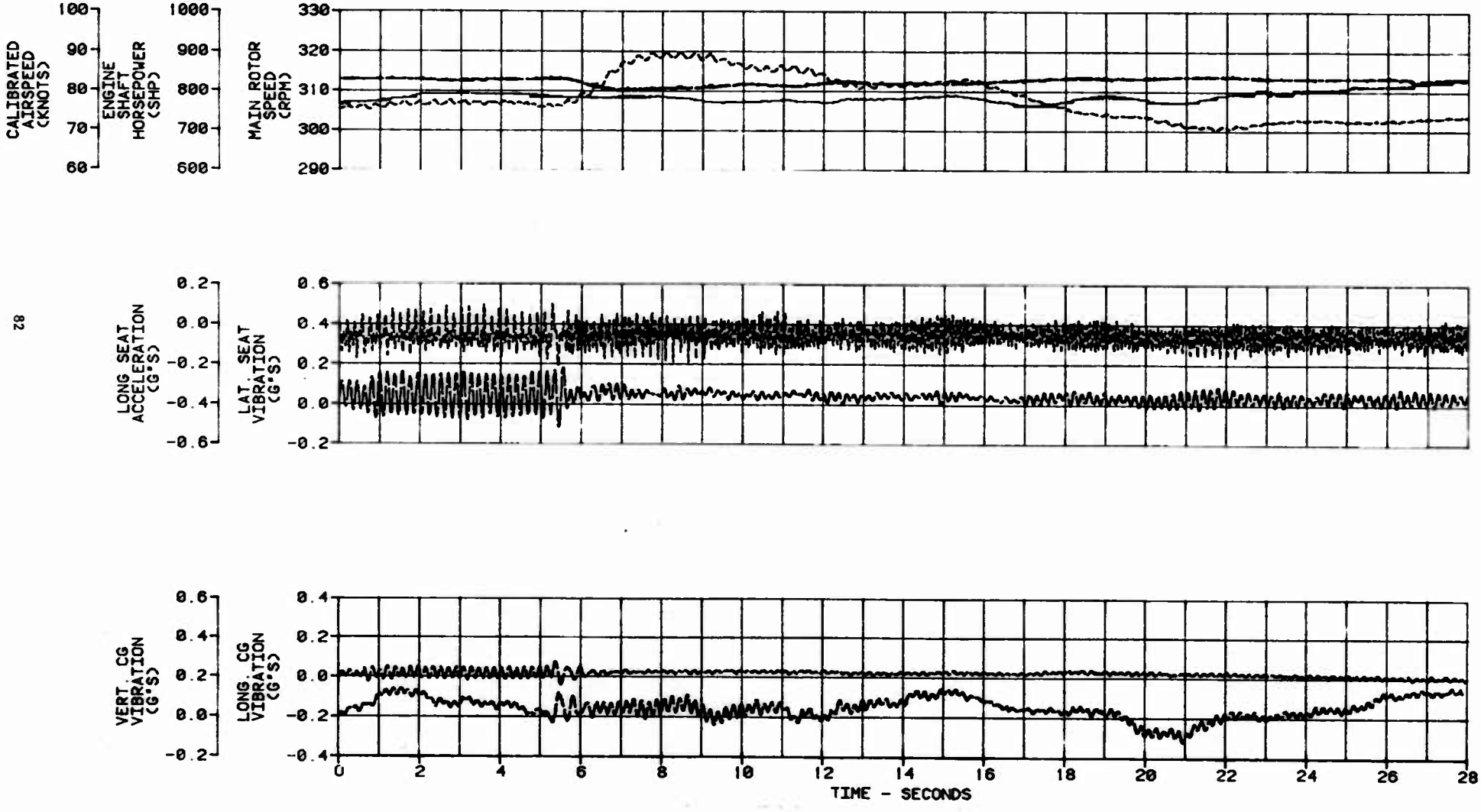

FIGURE 4
NONDIMENSIONAL HOVERING PERFORMANCE
JUH-1H USA S/N 70-15318

SYM	AVG OAT (°C)	AVG DENSITY (SLUGS/FT³)	CONFIGURATION
⊙	25.0	4180	SYSTEM DEFLATED
⊡	6.5	1450	CLEAN BLADES

NOTES:
1. TETHERED HOVER METHOD
2. SKID HEIGHT = 5 FT
3. WINDS LESS THAN 3 KNOTS

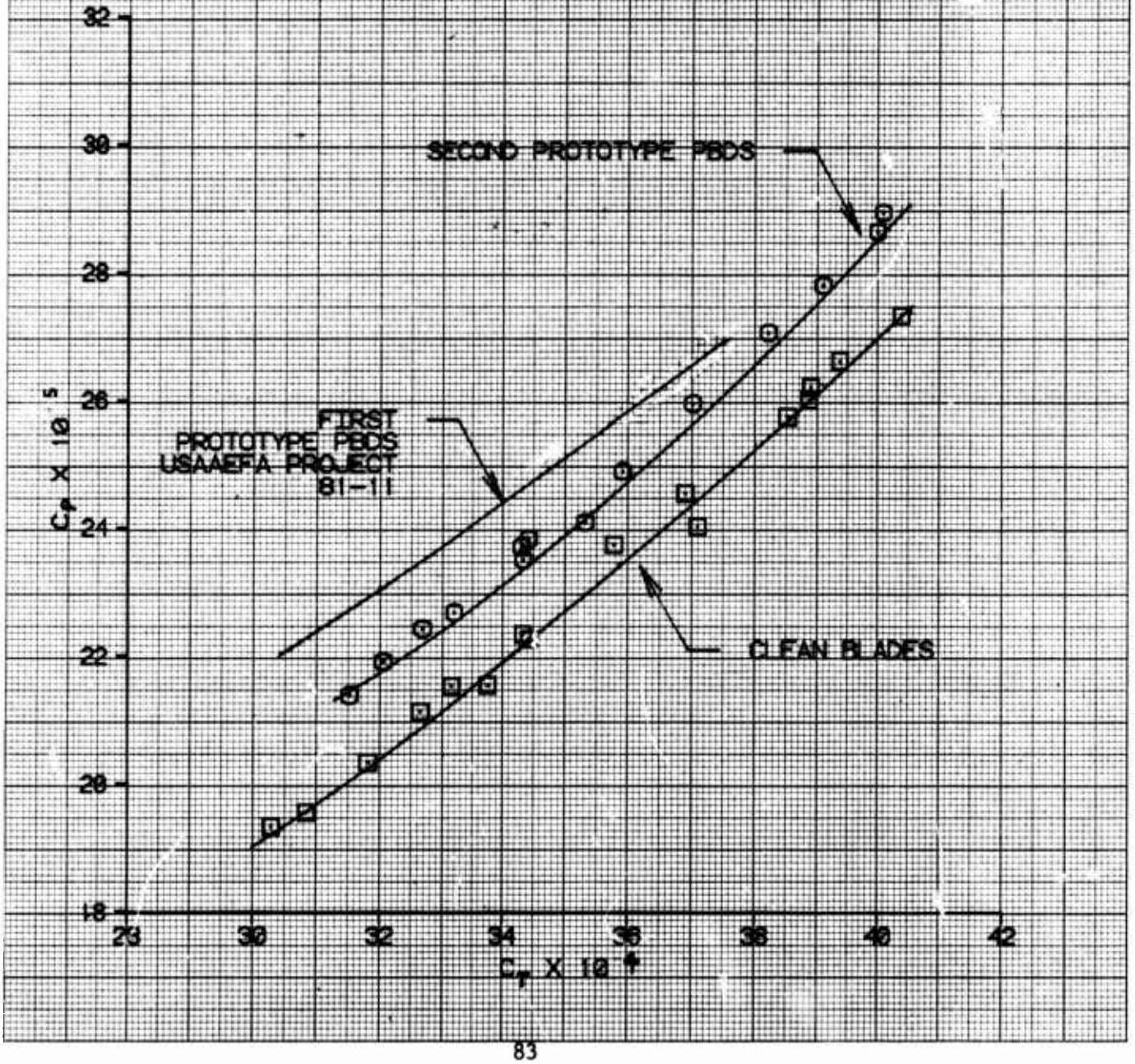

FIGURE 5

NONDIMENSIONAL LEVEL FLIGHT PERFORMANCE

UH-1H USA S/N 70-16318

PNEUMATIC BOOT DEICING SYSTEM

NOTES:
1. PODS DEFLATED
2. ZERO SIDESLIP
3. REFERRED ROTOR SPEED = 328 RPM
4. AVG LONG. CG LOCATION FS 134.1 (MID)
5. AVG LAT. CG LOCATION BL 0.5 (RT)
6. CURVES DERIVED FROM FIGS. -

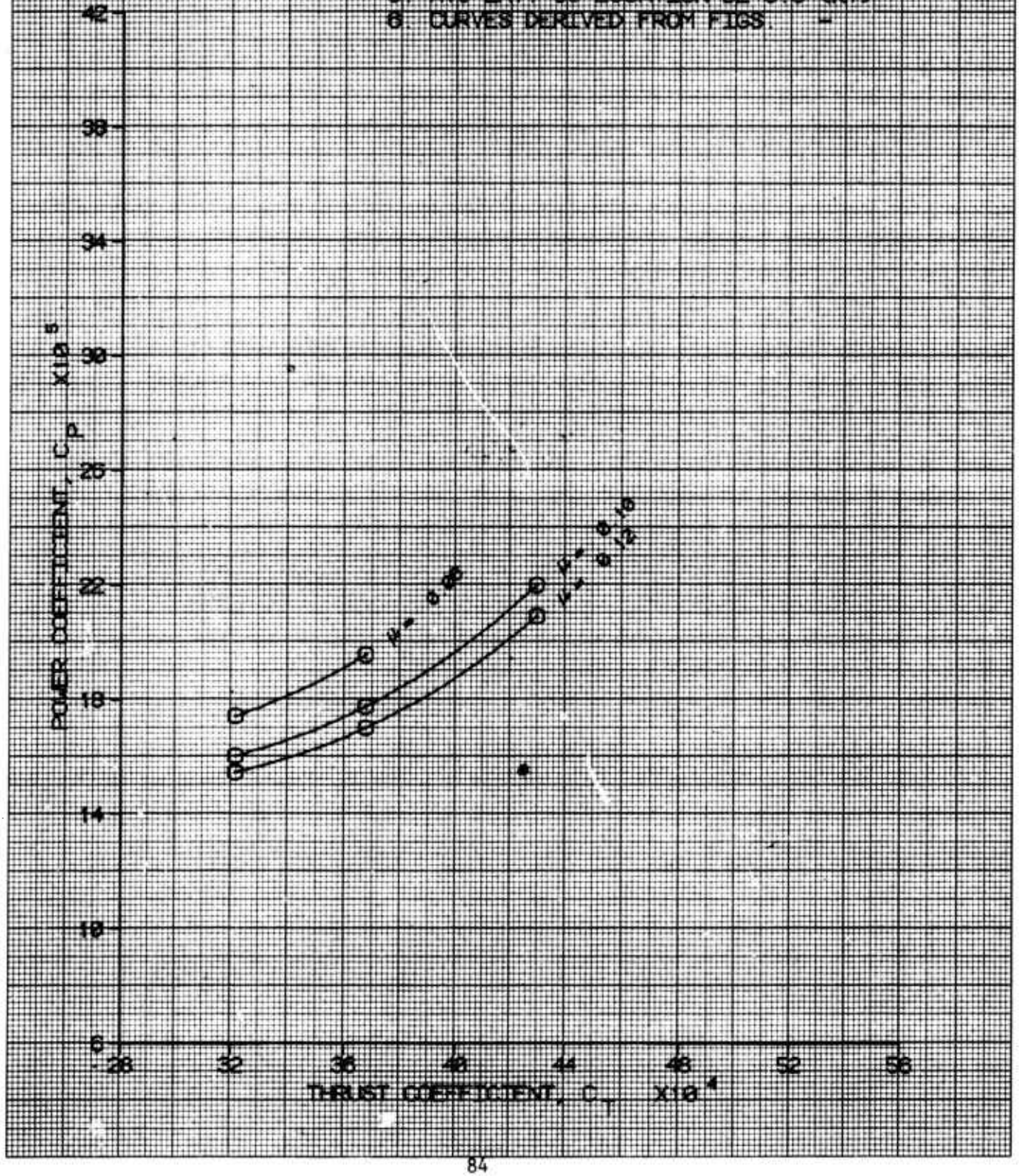

FIGURE 6

NONDIMENSIONAL LEVEL FLIGHT PERFORMANCE

JUH-1H USA S/N 70-16318

PNEUMATIC BOOT DEICING SYSTEM

NOTES:
1. BOOTS DEFLATED
2. ZERO SIDESLIP
3. REFERRED ROTOR SPEED = 328 RPM
4. AVG LONG CG LOCATION FS 194.1 (MID)
5. AVG LAT CG LOCATION BL 0.5 (RT)
6. CURVES DERIVED FROM FIGS. -

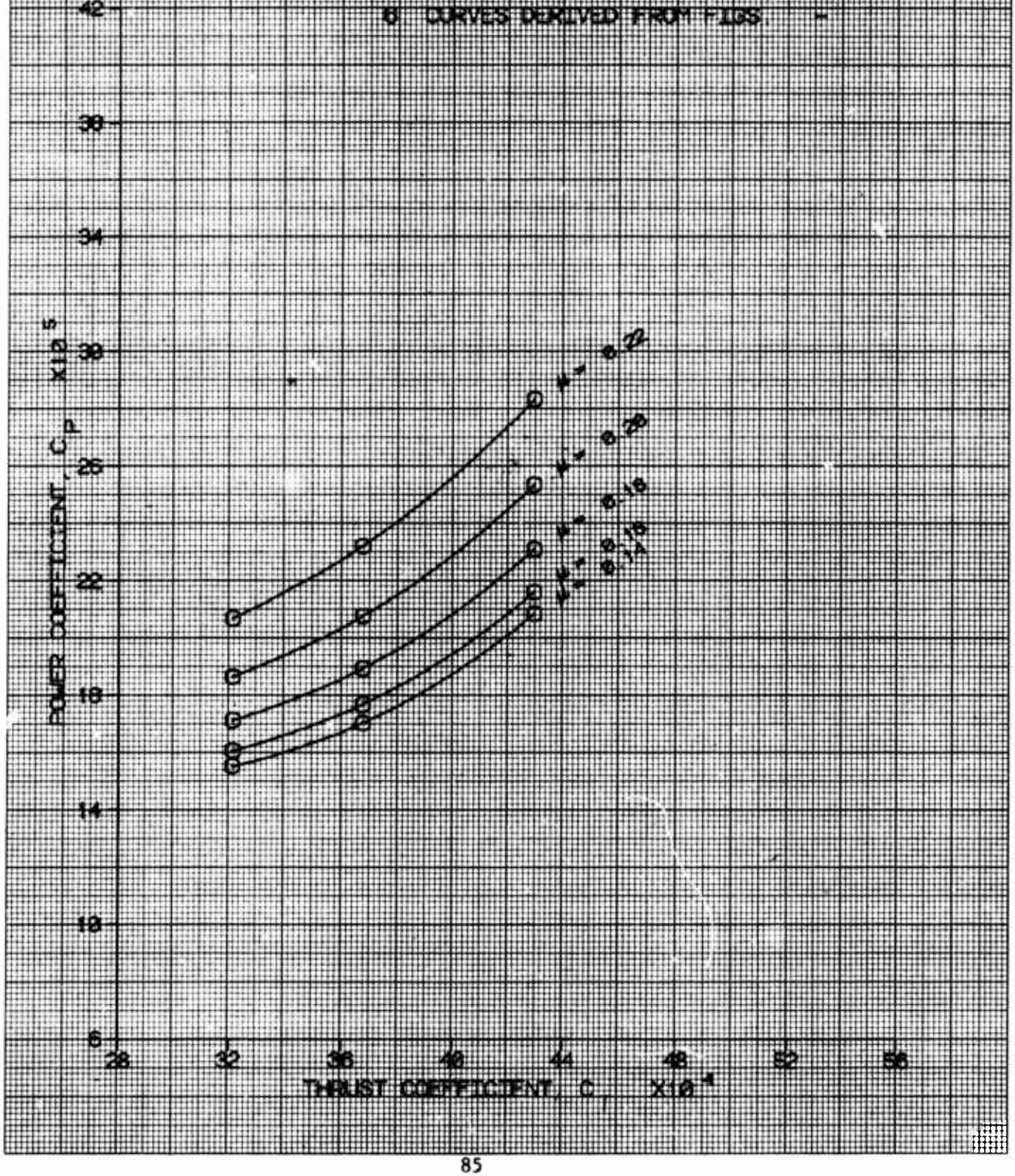

FIGURE 7
LEVEL FLIGHT PERFORMANCE
JO-1 (U.S.A. S/N 72-6018
PNEUMATIC BOOT DEICING SYSTEM

AVG GROSS WEIGHT (LBS)	C.G. LONG (FSD)	AVG LOCATION LAT (BL)	AVG DENSITY ALTITUDE (FEET)	AVG O.A.T. (DEG C)	AVG REF ROTOR SPEED (RPM)	AVG C_T	CONFIGURATION
7710	136.5	9.9	5970	22.5	320.7	0.000214	PBDS DEFLATED

NOTES 1. AVG ROTOR SPEED = 325 RPM
2. ZERO SIDESLIP

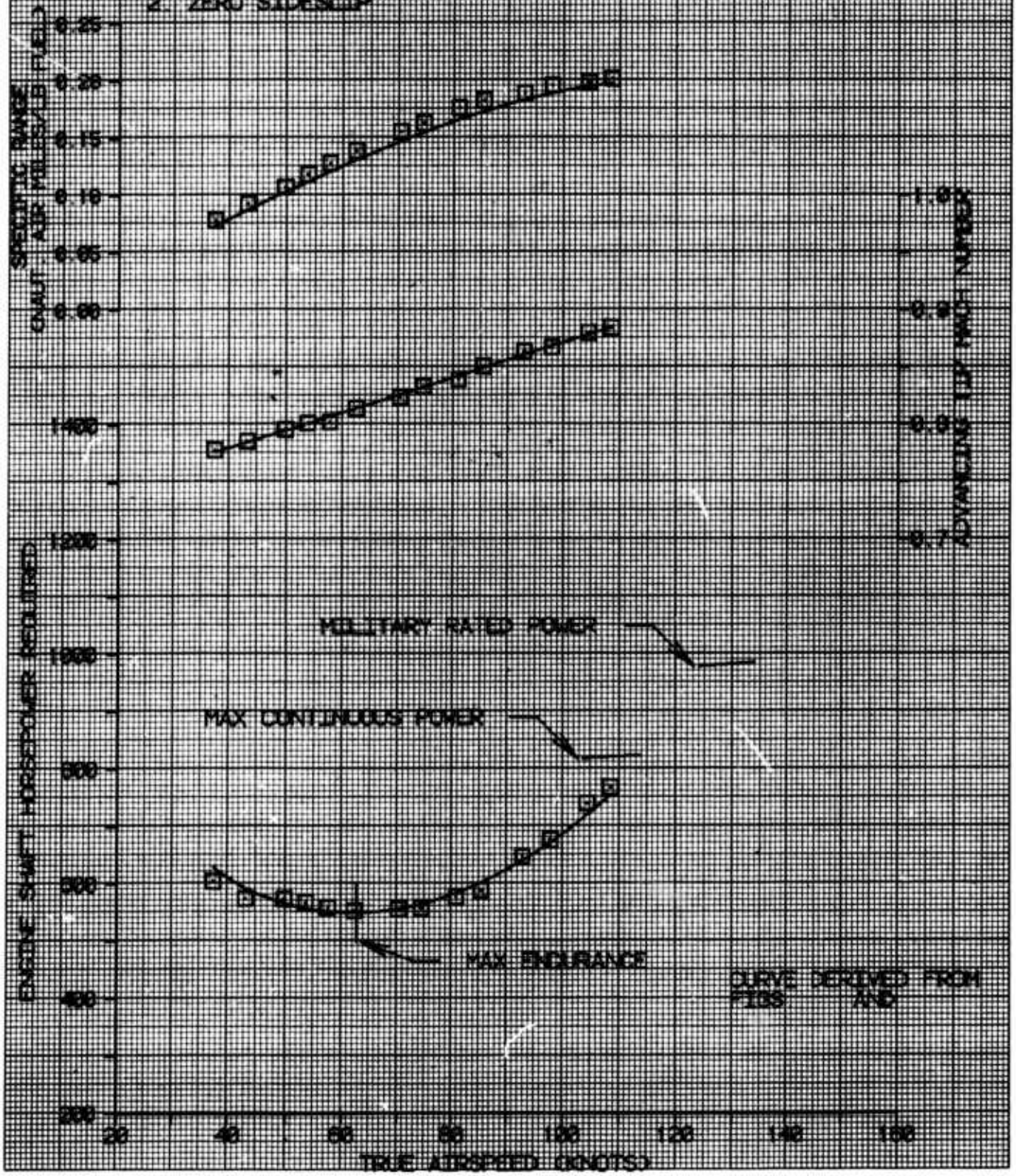

CURVE DERIVED FROM FTDS A/C

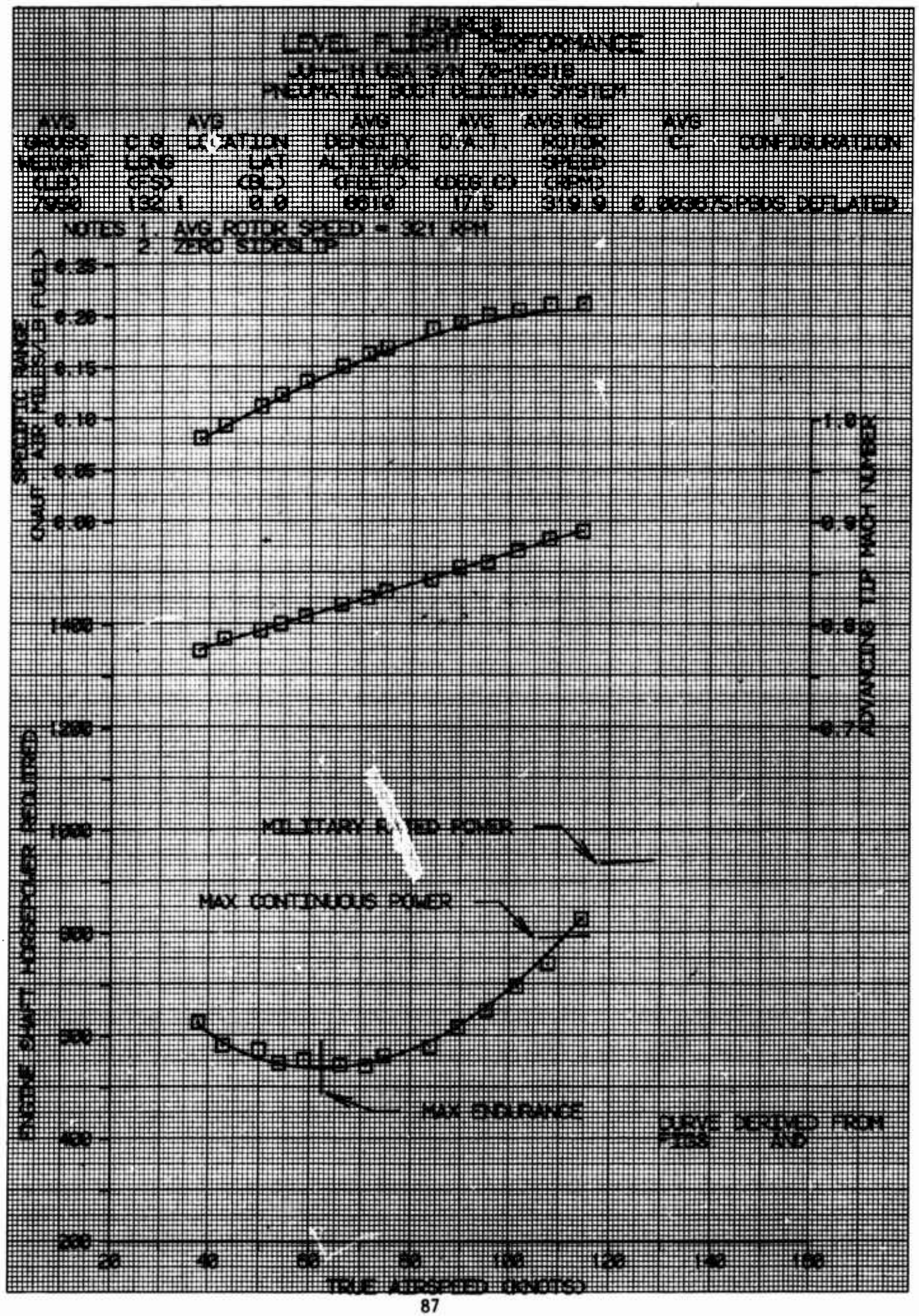
LEVEL FLIGHT PERFORMANCE
PNEUMATIC BOOT DEICING SYSTEM
AVG GROSS WT (LBS) 7,950
C.G. LONG (FS) 132.1
AVG LATERAL (BL) 0.0
AVG DENSITY ALTITUDE (FEET) 6610
AVG OAT (DEG C) 17.5
AVG REF ROTOR SPEED (RPM) 319.9
AVG CONFIGURATION
NOTES 1. AVG ROTOR SPEED = 321 RPM
2. ZERO SIDESLIP
QUAL. ENGINEERING FLIGHT TEST INSTRUMENTATION
MILITARY RATED POWER
MAX CONTINUOUS POWER
MAX ENDURANCE
CURVE DERIVED FROM
TRUE AIRSPEED (KNOTS)

FIGURE 9
LEVEL FLIGHT PERFORMANCE
UH-1H USA S/N 72-16318
PNEUMATIC BOOT DEICING SYSTEM

AVG GROSS WEIGHT (LB)	C.G. LOCATION LONG (FS)	C.G. LOCATION LAT (BL)	AVG DENSITY ALTITUDE (FEET)	O.A.T. (DEG C)	AVG REF ROTOR SPEED (RPM)	AVG C_T	CONFIGURATION
8280	133.6	0.0	11410	10.8	319.7	0.004296	BOOTS DEFLATED

NOTES 1. AVG ROTOR SPEED = 317 RPM
2. ZERO SIDESLIP

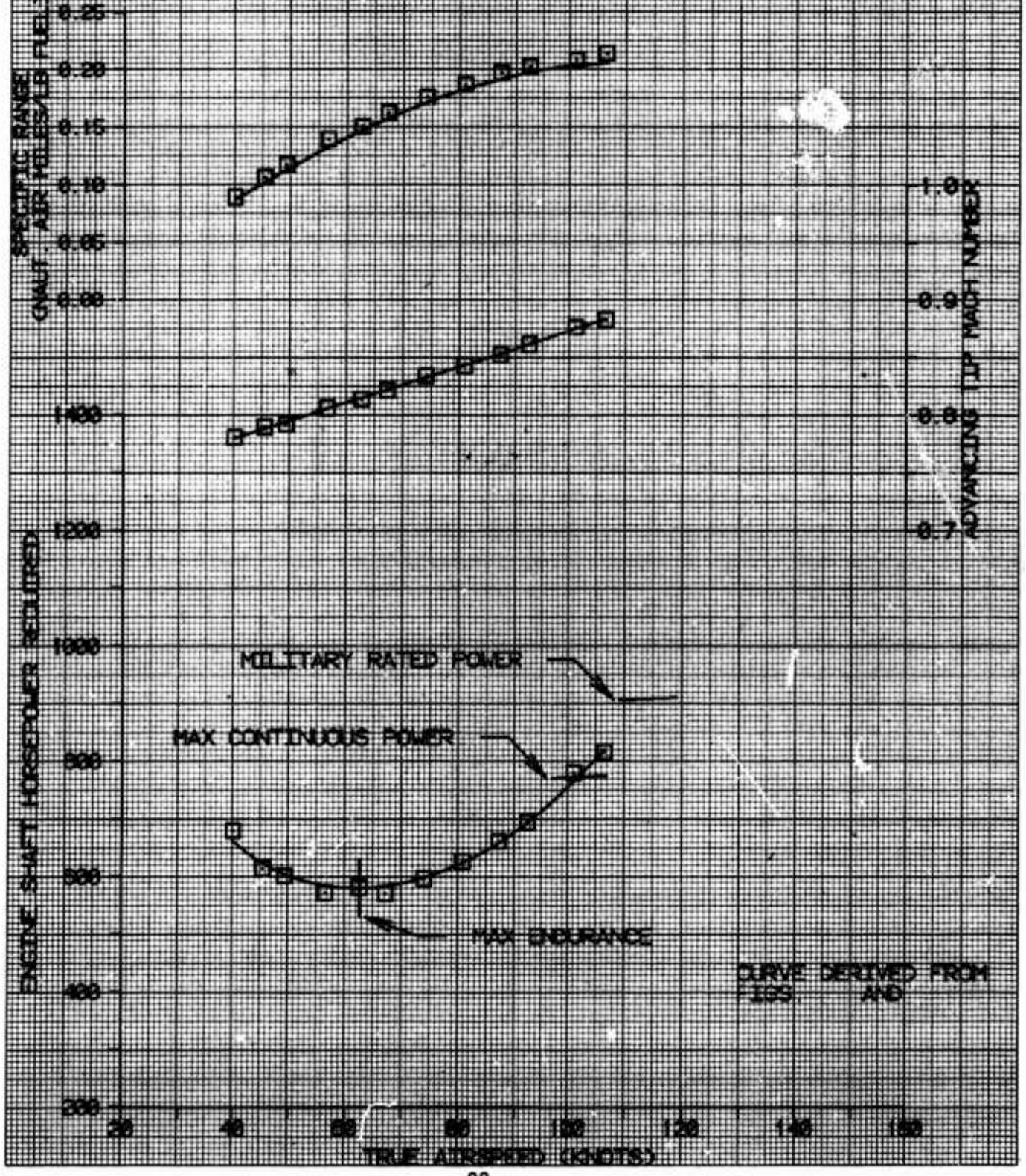

FIGURE 10

NONDIMENSIONAL LEVEL FLIGHT PERFORMANCE

JUH-1H PNEUMATIC DEICING SYSTEM USA S/N 70-16318

NOTES:
1. CLEAN BLADES
2. ZERO SIDESLIP
3. REFERRED ROTOR SPEED = 320 RPM
4. AVG LONG. CG LOCATION FS 133.0 (FWD)
5. AVG LAT. CG LOCATION BL 0.5 (RT)
6. CURVES DERIVED FROM FIGS. --

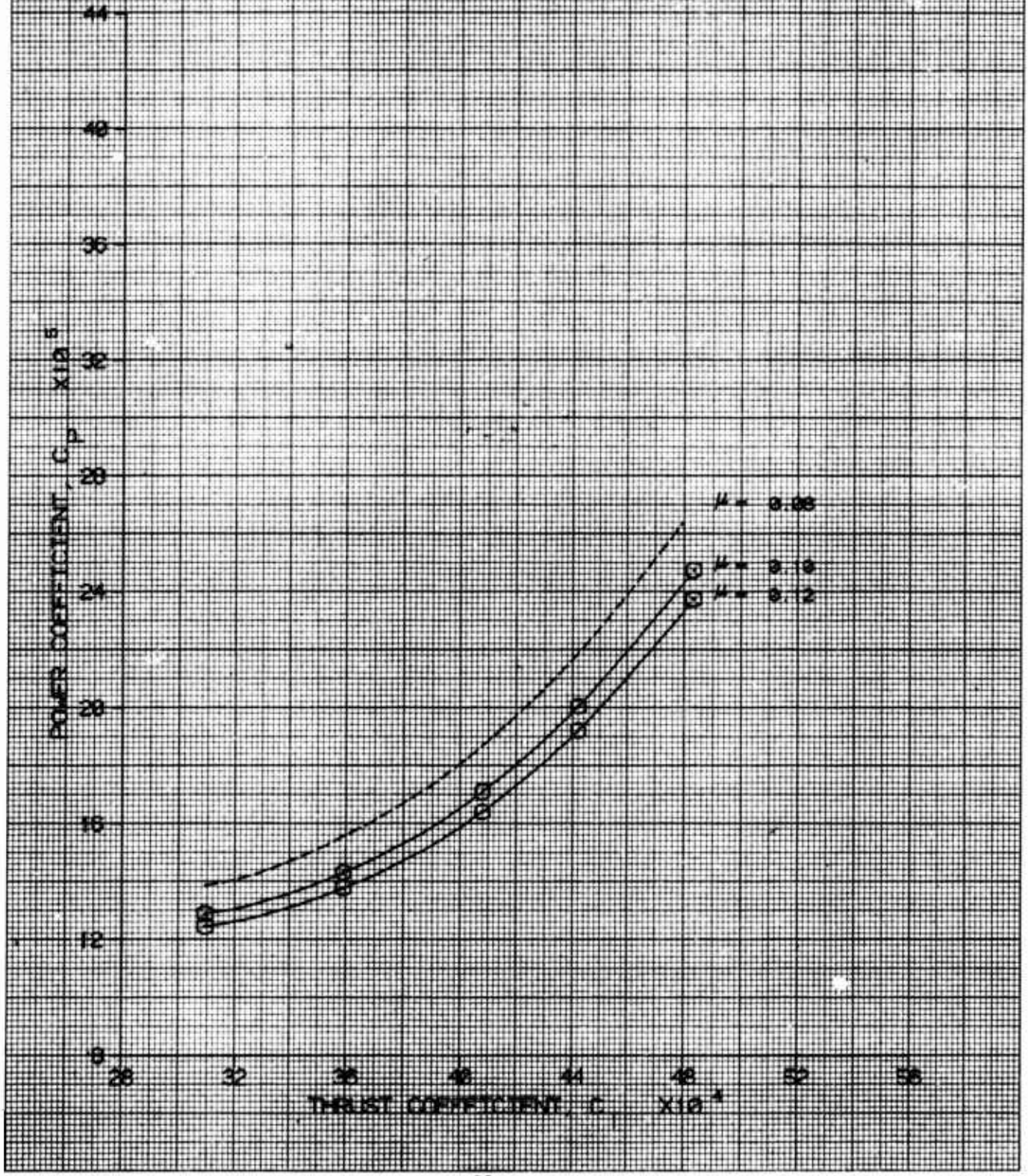

FIGURE 11

NONDIMENSIONAL LEVEL FLIGHT PERFORMANCE

UH-1H PNEUMATIC DEICING SYSTEM USA S/N 70-16318

NOTES:
1. CLEAN BLADES
2. ZERO SIDESLIP
3. REFERRED ROTOR SPEED = 328 RPM
4. AVG LONG. CG LOCATION FS 193.0 (FWD)
5. AVG LAT. CG LOCATION BL 0.5 (RT)
6. CURVES DERIVED FROM FIGS. --

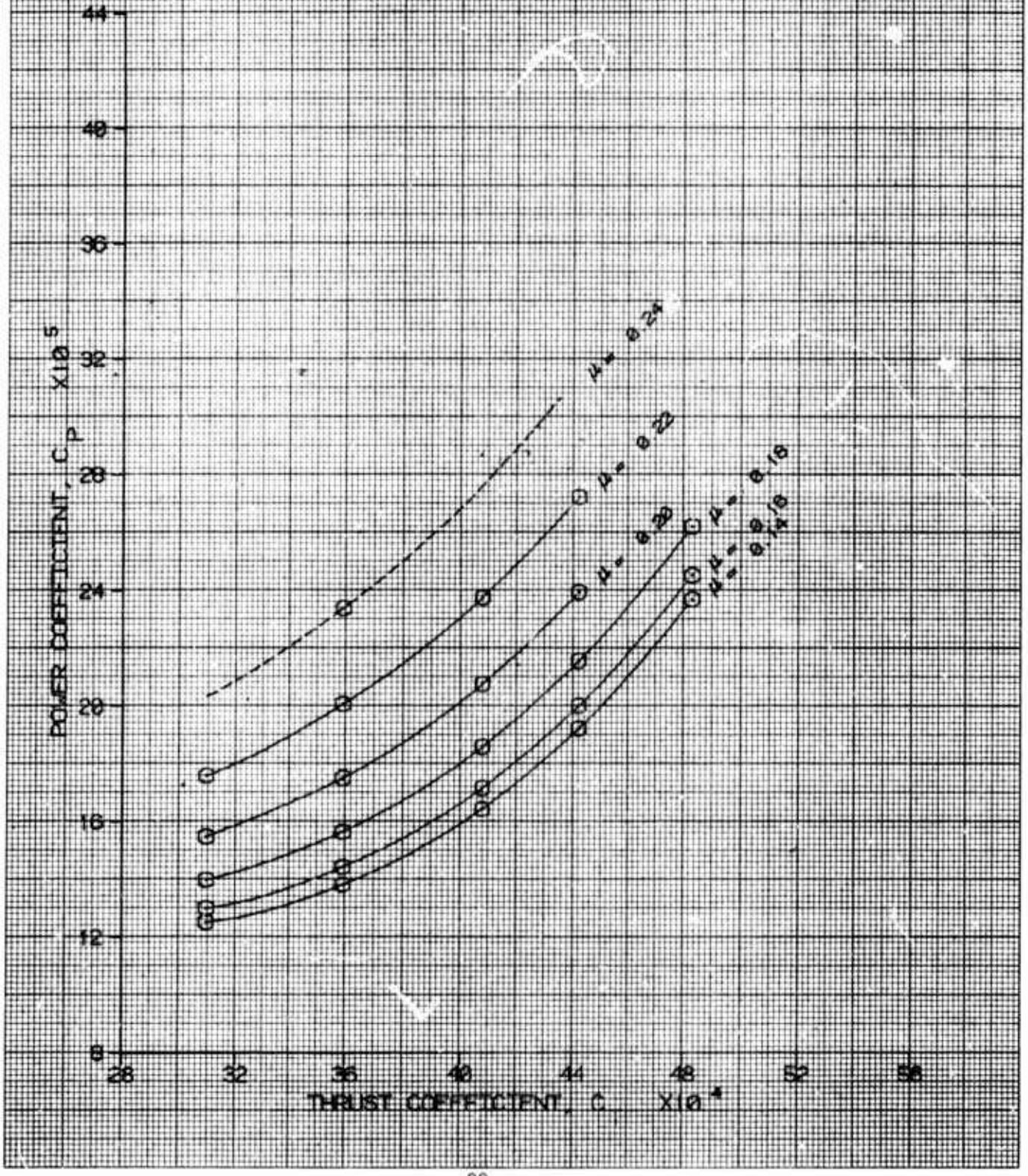

FIGURE 12

LEVEL FLIGHT PERFORMANCE

UH-1H PNEUMATIC DEICING SYSTEM USA S/N 70-16318

AVG GROSS WEIGHT (LB)	C.G. LOCATION LONG (FS)	LAT (BL)	AVG DENSITY ALTITUDE (FEET)	O.A.T. (DEG C)	AVG REF ROTOR SPEED (RPM)	AVG C_T	CONFIGURATION
7380	134.6(MID)	0.0	5860	17.0	322.4	0.003092	CLEAN

NOTES 1. AVG ROTOR SPEED = 324 RPM
2. CLEAN BLADES
3. ZERO SIDESLIP

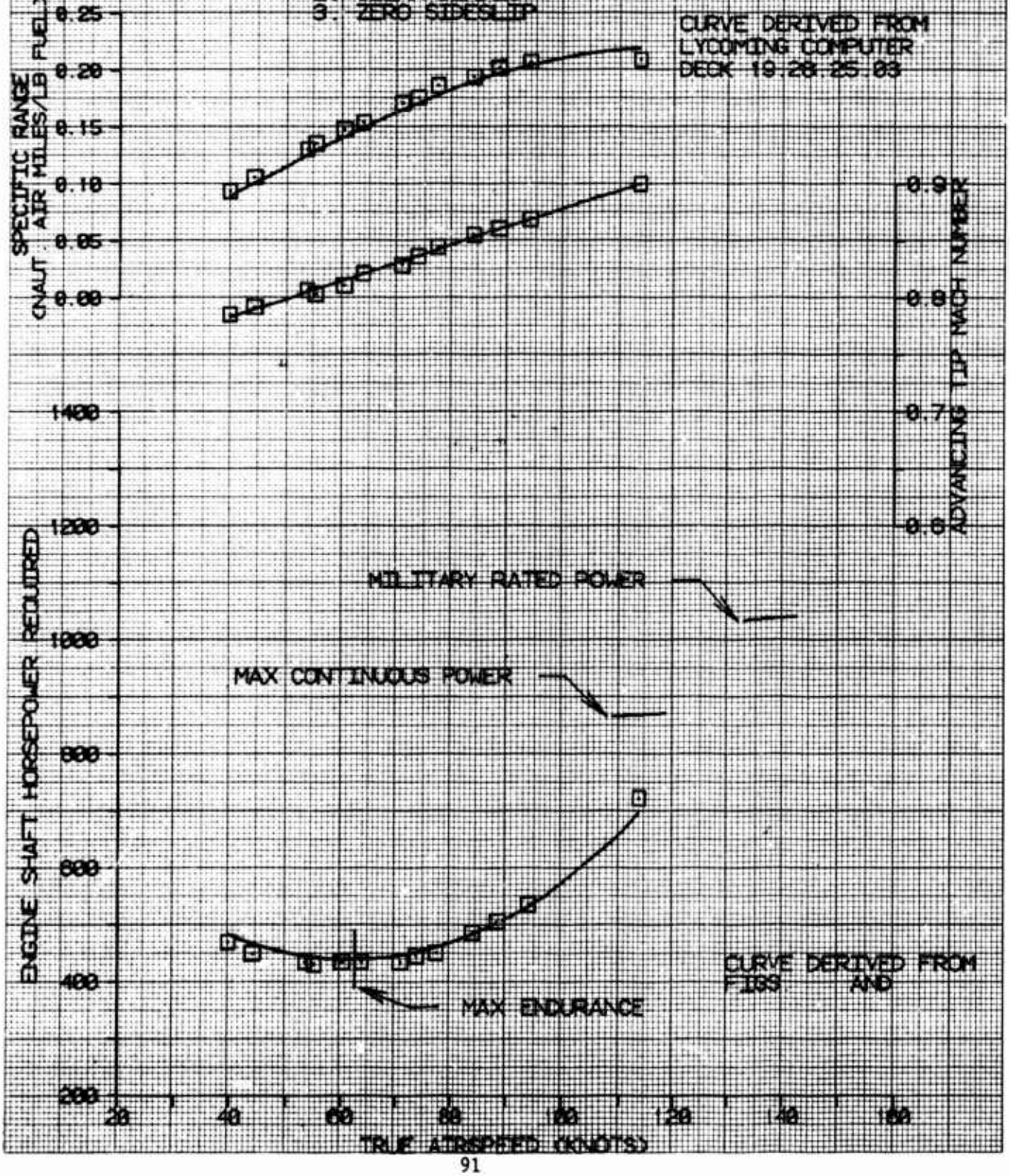

FIGURE 13
LEVEL FLIGHT PERFORMANCE

UH-1H PNEUMATIC DEICING SYSTEM USA S/N 70-16318

AVG GROSS WEIGHT (LB)	C.G. LOCATION LONG (FS)	LAT (BL)	AVG DENSITY ALTITUDE (FEET)	O.A.T. (DEG C)	AVG REF ROTOR SPEED (RPM)	AVG C_T	CONFIGURATION
8010	132.5(FWD)	0.0	7180	10.5	321.6	0.003592	CLEAN

NOTES 1. AVG ROTOR SPEED = 319 RPM
2. CLEAN BLADES
3. ZERO SIDESLIP

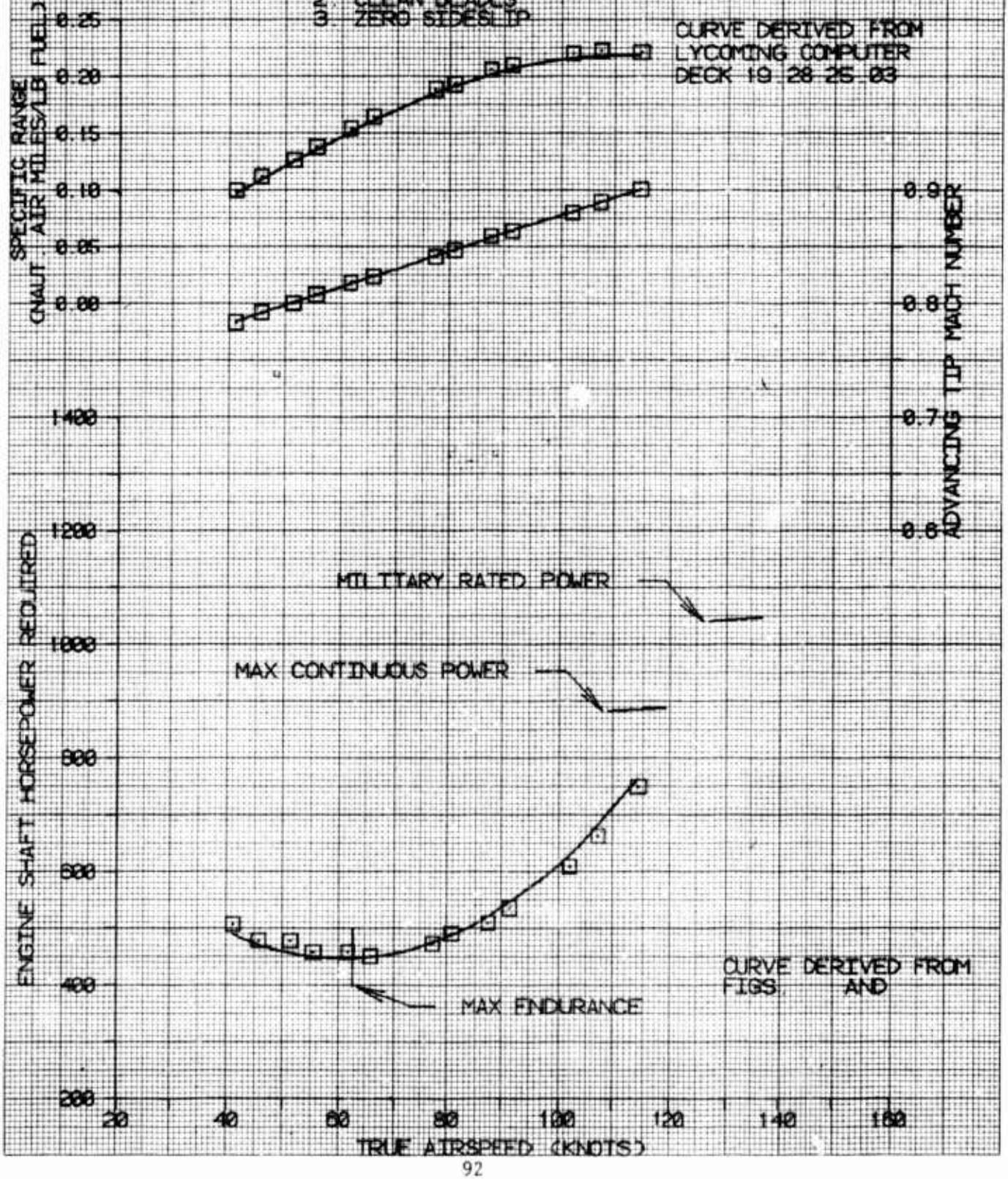

FIGURE 14

LEVEL FLIGHT PERFORMANCE

UH-1H PNEUMATIC DEICING SYSTEM USA S/N 70-16318

AVG GROSS WEIGHT (LB)	C.G. LOCATION LONG (FS)	LAT (BL)	AVG DENSITY ALTITUDE (FEET)	O.A.T. (DEG C)	AVG REF ROTOR SPEED (RPM)	C_T	CONFIGURATION
7910	132.8(FWD)	0.0	10790	4.0	321.0	0.0040878	CLEAN

NOTES 1. AVG ROTOR SPEED = 3.5 RPM
2. CLEAN BLADES
3. ZERO SIDESLIP

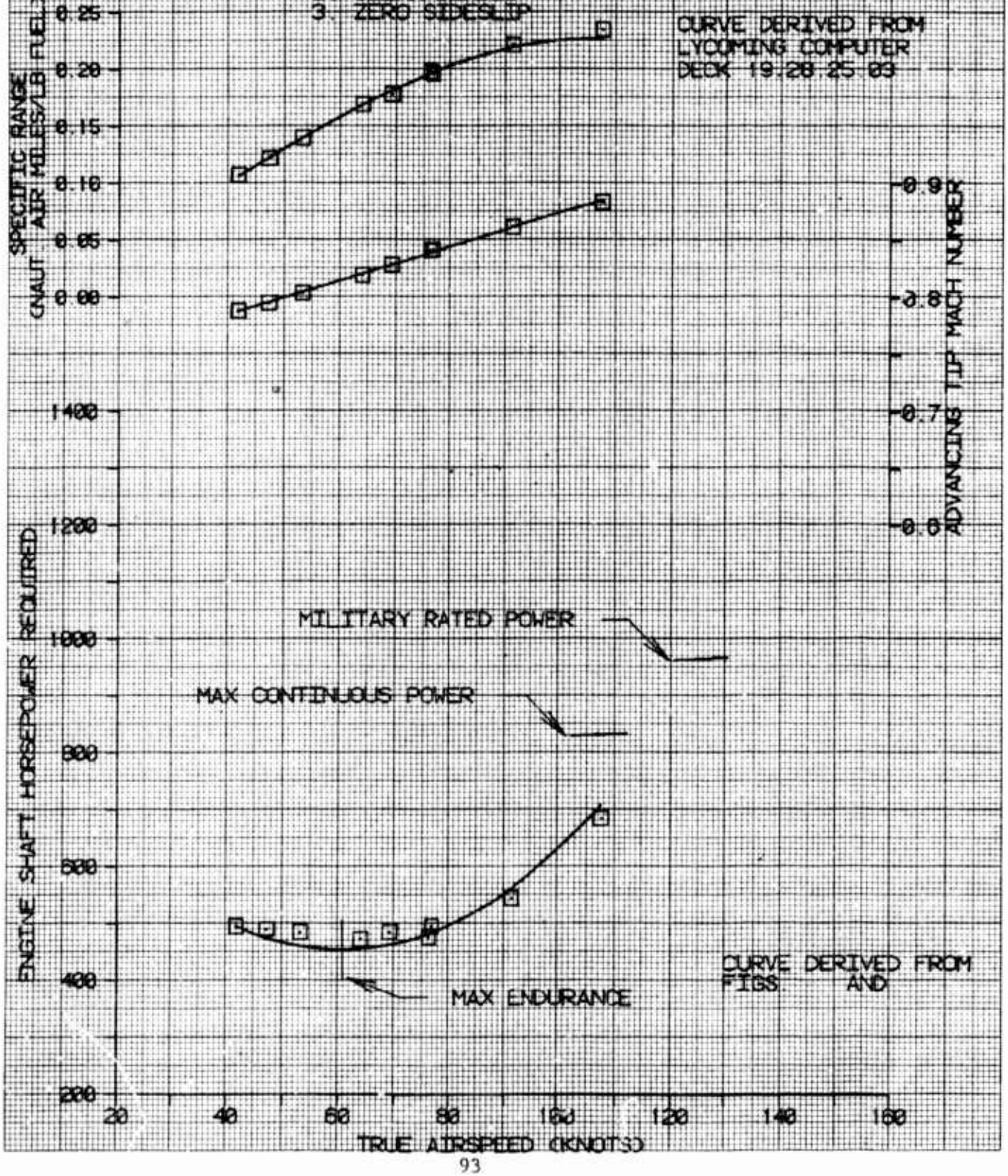

FIGURE 15

LEVEL FLIGHT PERFORMANCE

JUH-1H PNEUMATIC DEICING SYSTEM USA S/N 70-16318

AVG GROSS WEIGHT (LB)	C.G. LONG (FS)	AVG LOCATION LAT (BL)	AVG DENSITY ALTITUDE (FEET)	AVG O.A.T. (DEG C)	AVG REF. ROTOR SPEED (RPM)	AVG C_T	CONFIGURATION
8360	132.6(FWD)	0.0	11170	1.5	320.3	0.004421	CLEAN

NOTES 1. AVG ROTOR SPEED = 313 RPM
2. CLEAN BLADES
3. ZERO SIDESLIP

CURVE DERIVED FROM LYCOMING COMPUTER DECK 19.20.25.03

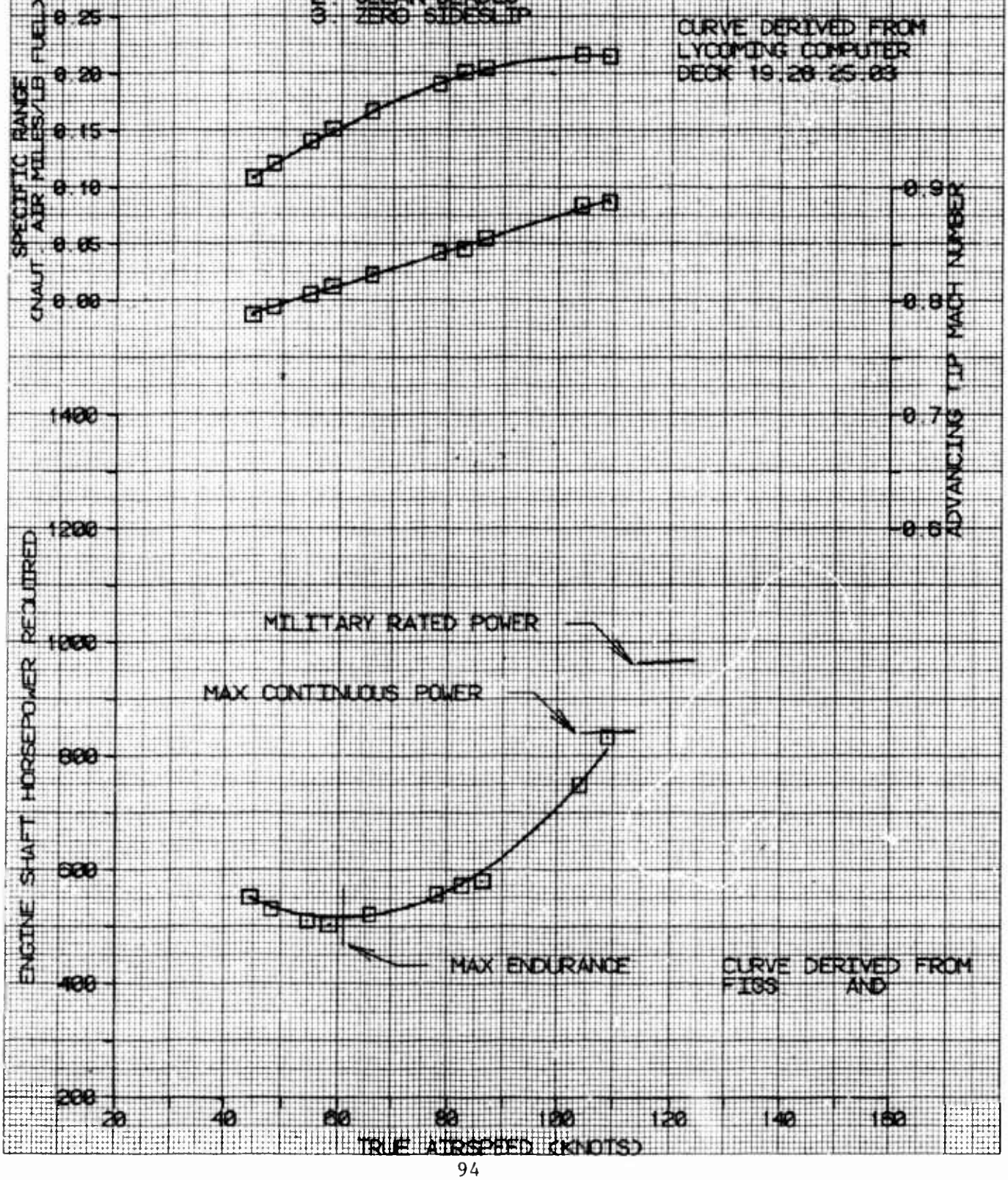

CURVE DERIVED FROM FIGS AND

FIGURE 16

LEVEL FLIGHT PERFORMANCE

JUH-1H PNEUMATIC DEICING SYSTEM USA S/N 70-16318

AVG GROSS WEIGHT (LB)	C.G. LOCATION LONG (FS)	LAT (BL)	AVG DENSITY ALTITUDE (FEET)	AVG O.A.T (DEG.C)	AVG REF ROTOR SPEED (RPM)	AVG C_T	CONFIGURATION
8980	132.6(FWD)	0.0	11730	1.5	320.4	0.004832	CLEAN

NOTES 1. AVG ROTOR SPEED = 313 RPM
2. CLEAN BLADES
3. ZERO SIDESLIP

CURVE DERIVED FROM LYCOMING COMPUTER DECK 10.28.26.03

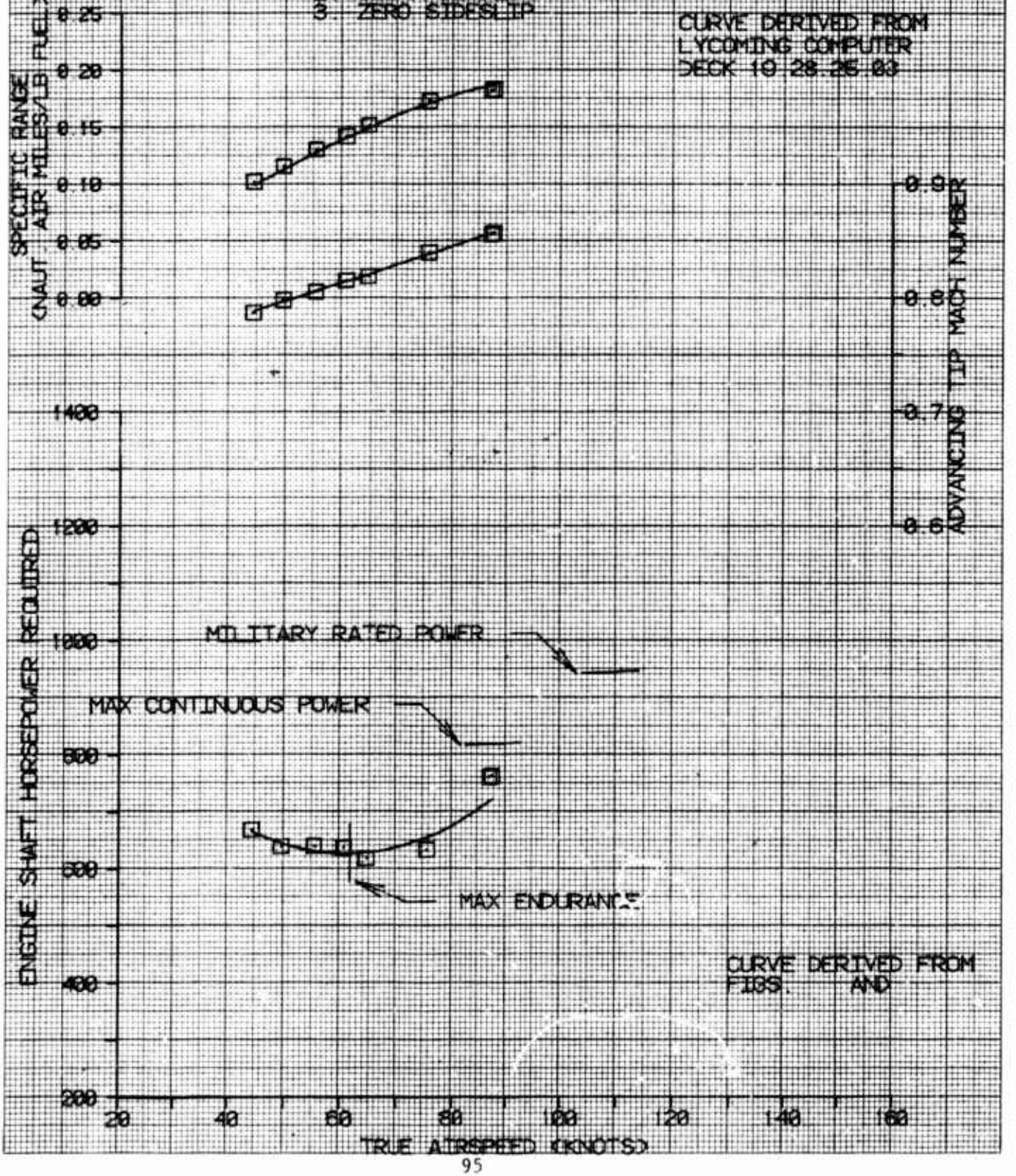

CURVE DERIVED FROM FIGS. AND

FIGURE 17
CONTROL POSITIONS IN TRIMMED FORWARD FLIGHT
JUH-1H USA S/N 70-16318

AVG GROSS WEIGHT (LB)	AVG CG LOCATION LONG (FS)	LAT (BL)	AVG DENSITY ALTITUDE (FT)	AVG OAT (DEG C)	AVG ROTOR SPEED (RPM)	FLIGHT CONDITION
7500	138.5(MID)	0.5 LT	6400	28.0	317	LEVEL

NOTES: 1. PBDS DEFLATED
2. ZERO SIDESLIP

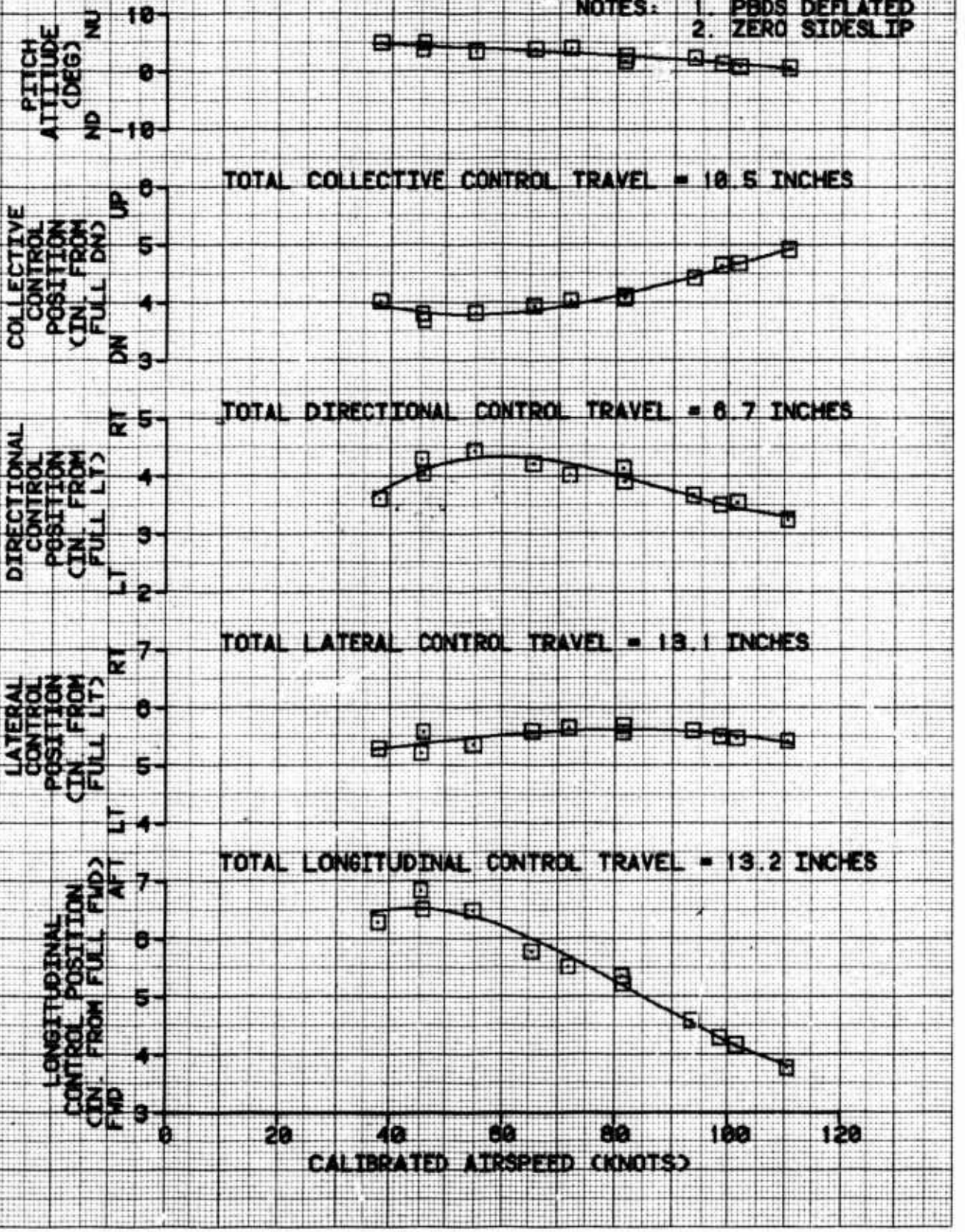

FIGURE 18
MANEUVERING STABILITY
JUH-1H USA S/N 70-16318

AVG GROSS WEIGHT (LB)	AVG CG LOCATION LONG (FS)	AVG CG LOCATION LAT (BL)	AVG DENSITY ALTITUDE (FT)	AVG OAT (DEG C)	AVG ROTOR SPEED (RPM)	AVG CALIBRATED AIRSPEED (KCAS)
7000	138.1 (MID)	0.5 RT	8700	19.0	321	81

NOTE: PBDS DEFLATED

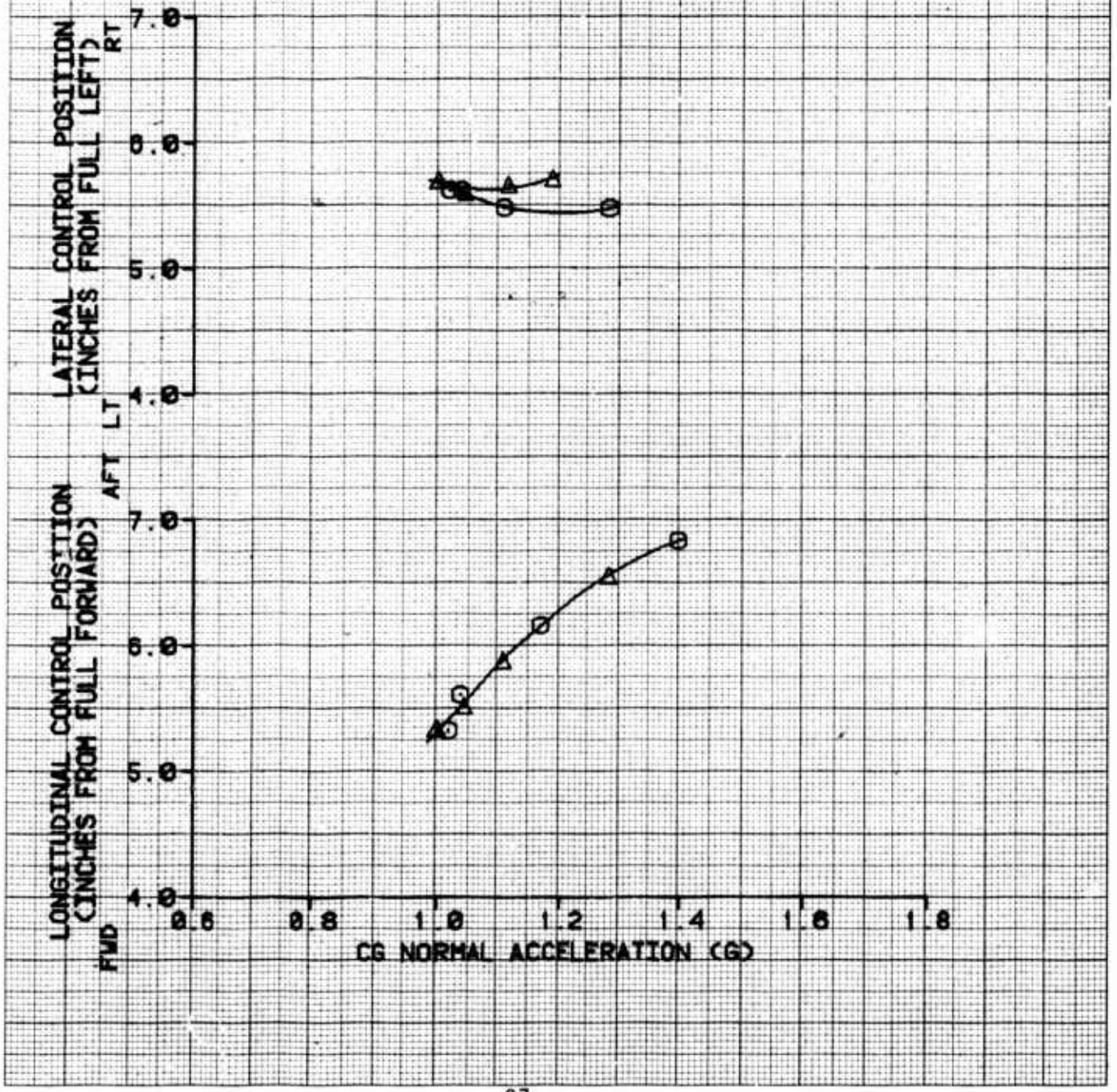

FIGURE 19
LONGITUDINAL CONTROLLABILITY
UH-1H USA S/N 70-16318

AVG GROSS WEIGHT (LB)	AVG CG LOCATION LONG (FS)	LAT (BL)	AVG DENSITY ALTITUDE (FT)	AVG OAT (DEG C)	AVG ROTOR SPEED (RPM)	TRIM CALIBRATED AIRSPEED (KCAS)	TRIM FLIGHT CONDITION
7700	136.6 (MID)	0.5 RT	8400	21.0	321	82	LEVEL

NOTE: PBOS DEFLATED

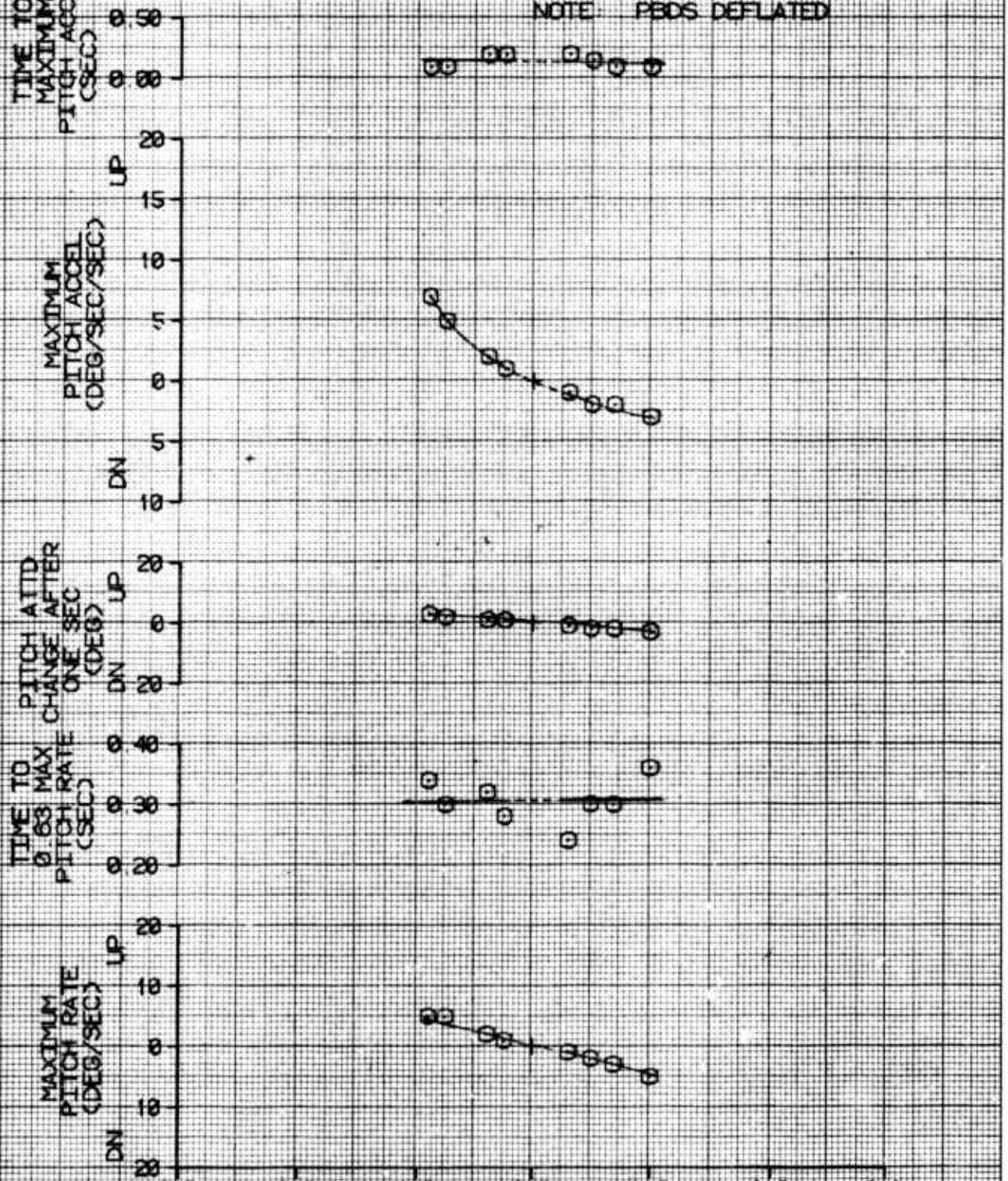

FIGURE 20
LATERAL CONTROLLABILITY
UH-1H USA S/N 70-16318

AVG GROSS WEIGHT (LB)	AVG CG LOCATION LONG (FS)	LAT (BL)	AVG DENSITY ALTITUDE (FT)	AVG OAT (DEG C)	AVG ROTOR SPEED (RPM)	TRIM CALIBRATED AIRSPEED (KCAS)	TRIM FLIGHT CONDITION
7650	136.6 (MID)	0.5 RT	6550	21.0	321	61	LEVEL

NOTE: PBOS DEFLATED

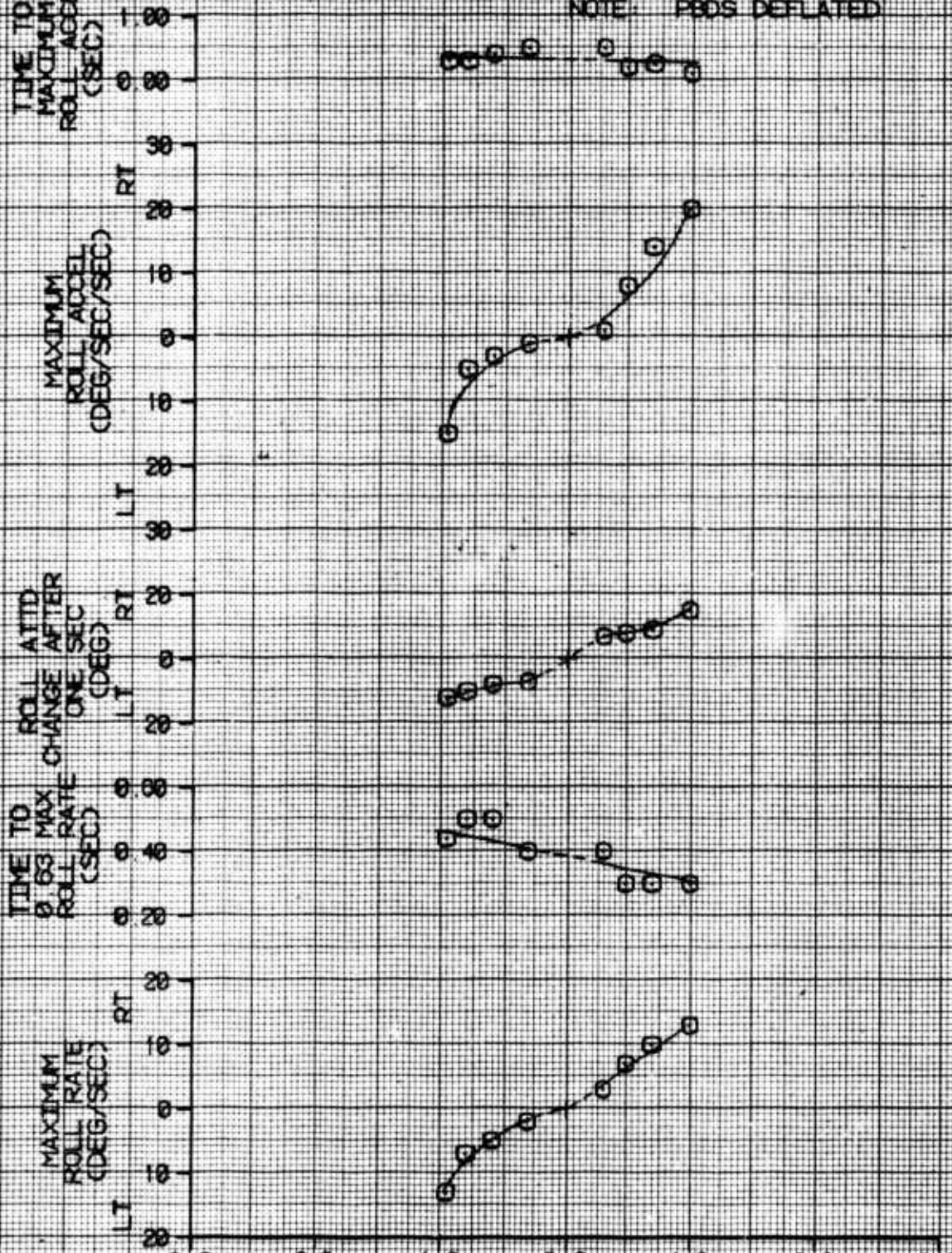

FIGURE 21
LOW SPEED FORWARD AND REARWARD FLIGHT
JUH-1H USA S/N 70-16318

SYM	AVG GROSS WEIGHT (LB)	AVG CG LOCATION LONG (FS)	AVG CG LOCATION LAT (BL)	AVG DENSITY ALTITUDE (FT)	AVG OAT (DEG C)	AVG ROTOR SPEED (RPM)	SKID HEIGHT (FT)
□	7715	137.5(MID)	0.5 RT	120	-4.0	321	10
○	7380	136.1(MID)	0.5 RT	180	-3.0	321	10

NOTES: 1. I DENOTES MAXIMUM CONTROL EXCURSION DURING ATTEMPTED STABILIZED POINT
2. PBDS DEFLATED

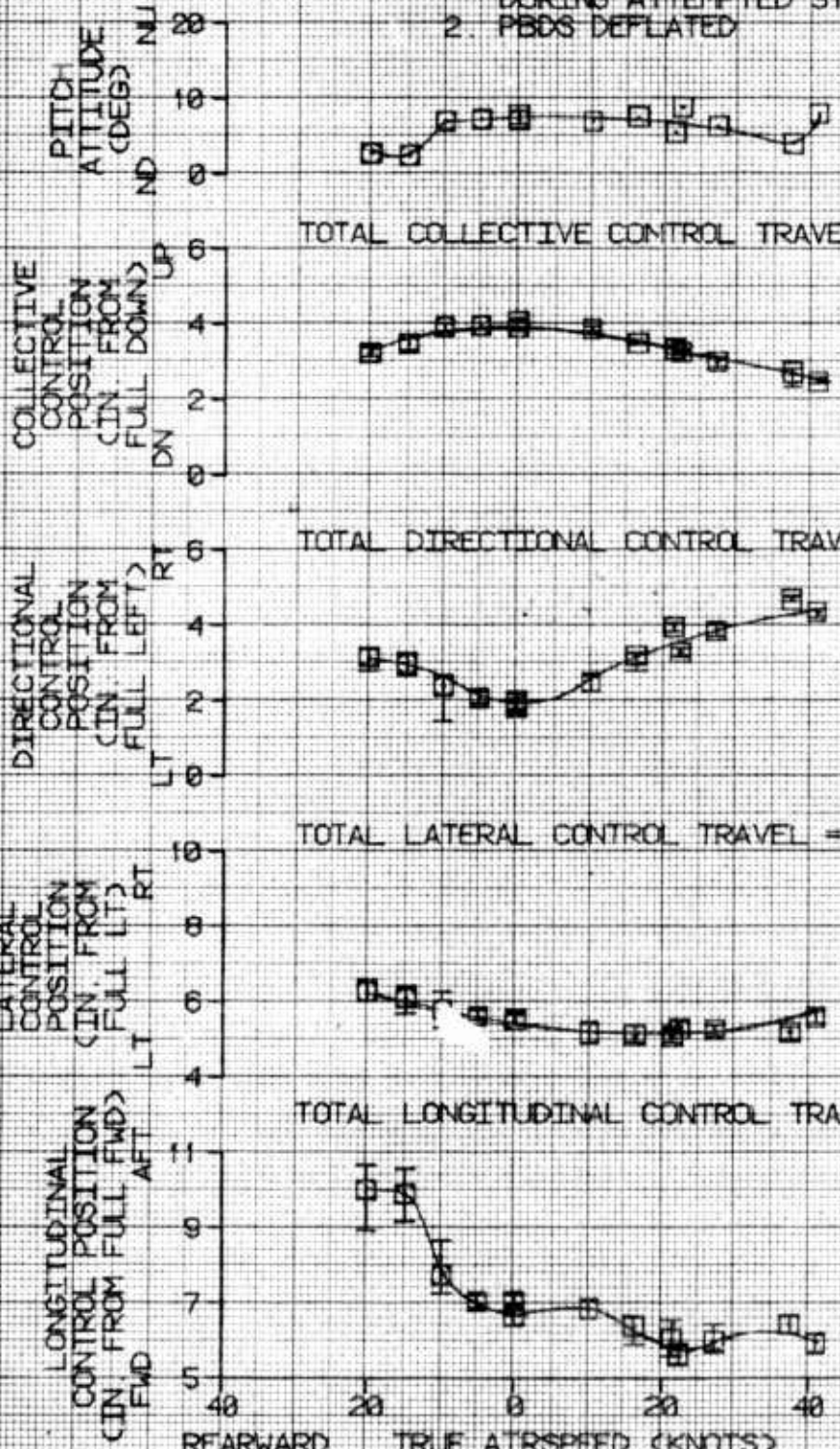

FIGURE 22
LOW SPEED SIDEWARD FLIGHT
UH-1H USA S/N 70-16318

SYM	AVG GROSS WEIGHT (LB)	AVG CG LOCATION LONG (FS)	LAT (BL)	AVG DENSITY ALTITUDE (FT)	AVG OAT (DEG C)	AVG ROTOR SPEED (RPM)	SKID HEIGHT (FT)
□	7485	136.3(MID)	0.5 LT	120	-4.0	321	10
○	7290	135.8(MID)	0.5 RT	220	-3.0	321	10

NOTES: 1. I DENOTES MAXIMUM CONTROL EXCURSION DURING ATTEMPTED STABILIZED POINT
2. PBDS DEFLATED

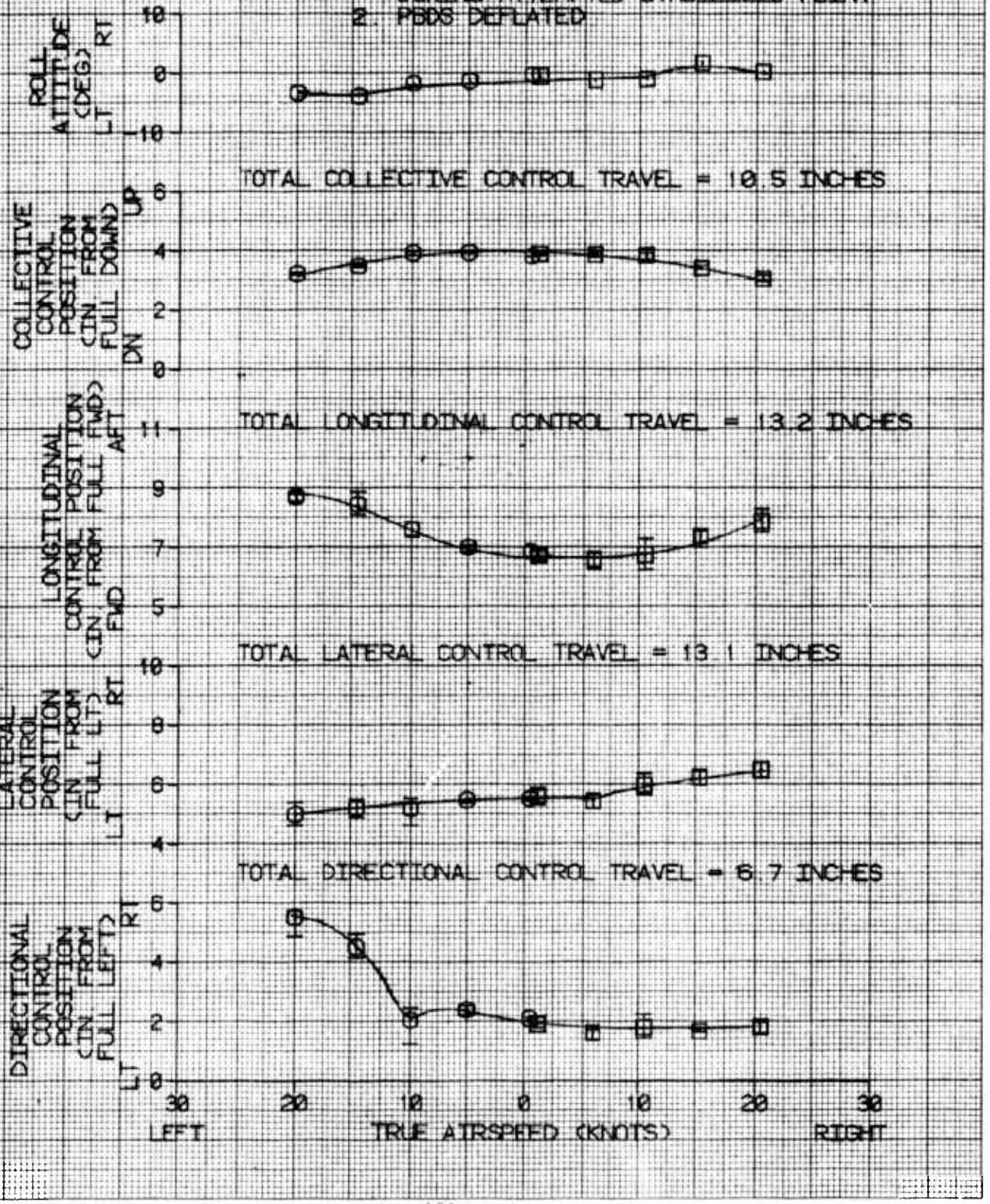

FIGURE 23
LOW SPEED FORWARD AND REARWARD FLIGHT
UH-1H USA S/N 70-16318

SYM	AVG GROSS WEIGHT (LB)	AVG CG LOCATION LONG (FS)	AVG CG LOCATION LAT (BL)	AVG DENSITY ALTITUDE (FT)	AVG OAT (DEG C)	AVG ROTOR SPEED (RPM)	SKID HEIGHT (FT)
□	7175	135.3(MID)	0.5 RT	430	-1.0	320	10
○	7040	135.0(MID)	0.5 RT	475	-1.0	320	10

NOTES: 1. I DENOTES MAXIMUM CONTROL EXCURSION DURING ATTEMPTED STABILIZED POINT
2. PBOS VENTED

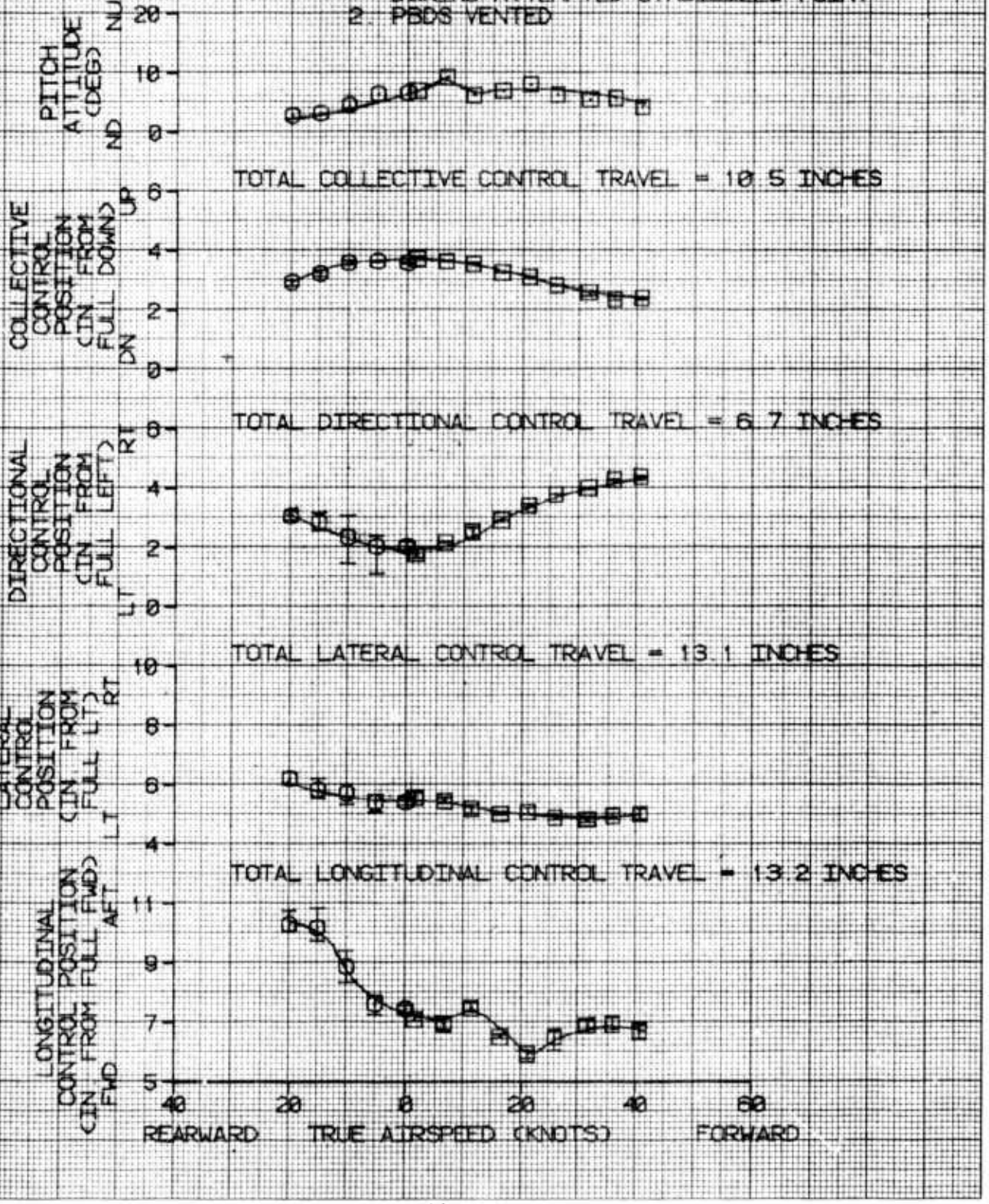

FIGURE 24
LOW SPEED SIDEWARD FLIGHT
UH-1H USA S/N 70-16318

SYM	AVG GROSS WEIGHT (LB)	AVG CG LOCATION LONG (FS)	LAT (BL)	AVG DENSITY ALTITUDE (FT)	AVG C.T. (DEG C)	AVG ROTOR SPEED (RPM)	SKID HEIGHT (FT)
◇	7130	135.3(MID)	0.5 RT	430	-1.0	320	10
○	7085	135.0(MID)	0.5 RT	475	-1.0	320	10

NOTES: 1. I DENOTES MAXIMUM CONTROL EXCURSION DURING ATTEMPTED STABILIZED POINT
2. PBOS VENTED

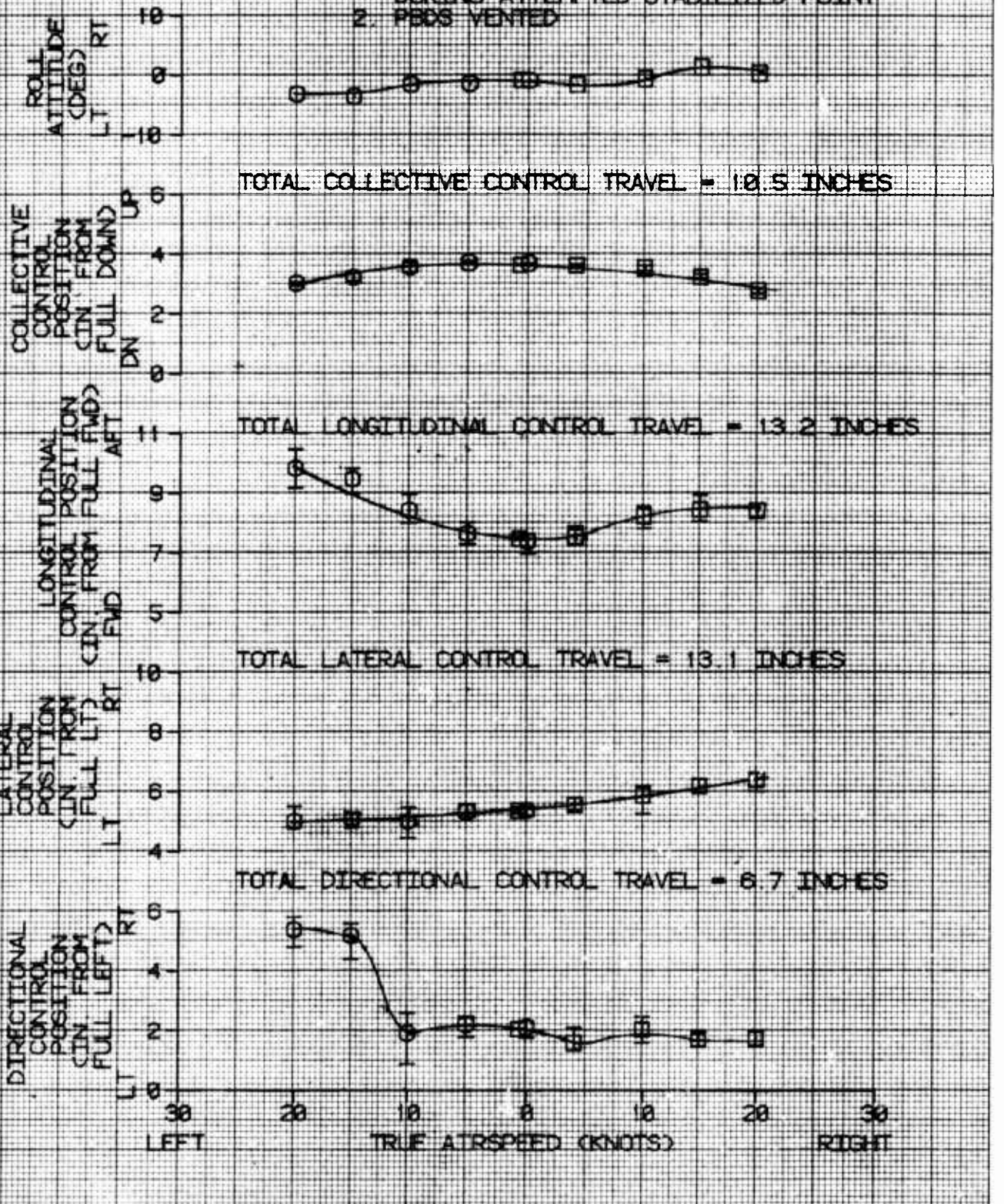

Table 1. Monitored Flight Loads (Second Generation)

Flight Condition	Main Rotor Beam Bend. Moment (Blade Station 192) (1000 in.-lb)						Main Rotor Blade Chord Bend. Moment (Blade Station 192) (1000 in.-lb)						Main Rotor Pitch Link Axial Load (lb)					
	Boot Condition				System Vented		Boot Condition				System Vented		Boot Condition				System Vented	
	Normal		Cycled				Normal		Cycled				Normal		Cycled			
	Stdy	Osc[1]	Stdy	Osc[1]	Stdy	Osc[1]	Stdy	Osc[2]	Stdy	Osc[2]	Stdy	Osc[2]	Stdy	Osc[3]	Stdy	Osc[3]	Stdy	Osc[3]
Ground Runs 294 RPM																		
7 psi Torque	-4.9	0.3	-4.9	0.3	---	---	-9.2	2.4	-9.2	2.4	---	---	115	200	115	200	---	---
13 psi Torque	-5.2	0.2	-5.2	0.3	---	---	-8.7	2.5	-8.7	2.5	---	---	115	250	115	300	---	---
17 psi Torque	-3.6	2.1	-3.6	2.2	---	---	-4.4	3.7	-4.4	3.7	---	---	115	400	115	400	---	---
22 psi Torque	-4.1	2.2	-3.1	2.2	---	---	6.8	3.3	8.1	3.0	---	---	115	400	115	430	---	---
26 psi Torque	-4.1	1.9	-4.1	2.0	---	---	-6.7	3.0	-6.7	3.7	---	---	115	400	115	450	---	---
31 psi Torque	-4.6	1.6	-4.1	2.2	---	---	6.9	5.0	6.8	5.0	---	---	115	400	115	500	---	---
34 psi Torque	-4.4	1.6	-4.1	2.2	---	---	7.9	5.0	8.1	8.7	---	---	115	550	165	600	---	---
Ground Runs 324 RPM																		
10 psi Torque	-2.0	0.9	-2.0	0.9	---	---	0.7	3.0	0.7	3.0	---	---	115	200	115	200	---	---
13 psi Torque	-2.5	1.6	-2.5	1.1	---	---	1.9	2.5	1.9	2.5	---	---	115	300	115	260	---	---
18 psi Torque	-3.6	2.2	-2.8	1.9	---	---	1.9	2.5	1.9	2.5	---	---	115	230	115	400	---	---
26 psi Torque	-3.9	1.9	-3.6	2.4	---	---	1.9	3.7	3.2	4.2	---	---	115	400	115	400	---	---
30 psi Torque	-4.1	1.9	-3.9	2.2	---	---	-9.2	4.0	-8.0	5.0	---	---	115	400	115	400	---	---
34 psi Torque	-4.1	1.9	-4.1	2.2	---	---	4.4	5.0	4.4	8.7	---	---	115	500	115	500	---	---
Ground Runs Engine-Dynamic System Compatibility Rapid Throttle Reductions																		
10 psi Torque	-1.9	1.6	---	---	---	---	5.1	2.5	---	---	---	---	115	170	---	---	---	---
	-1.7	1.1	---	---	---	---	0.6	2.5	---	---	---	---	115	270	---	---	---	---
22 psi Torque	-3.6	2.2	---	---	---	---	-22.9	3.7	---	---	---	---	165	450	---	---	---	---
	-1.9	1.9	---	---	---	---	4.4	2.5	---	---	---	---	115	200	---	---	---	---
33 psi Torque	-4.4	2.2	---	---	---	---	4.4	7.4	---	---	---	---	215	500	---	---	---	---
	-2.0	1.6	---	---	---	---	4.4	2.5	---	---	---	---	115	200	---	---	---	---
Ground Runs Rapid Collective Reduction																		
	-4.7	1.6	---	---	---	---	4.4	5.0	---	---	---	---	165	500	---	---	---	---
	-1.7	1.1	---	---	---	---	-C.6	3.7	---	---	---	---	115	250	---	---	---	---

NOTES:

[1]Steady state oscillatory endurance limit = N/A, maneuvering oscillatory endurance limit = N/A.
[2]Steady state oscillatory endurance limit = ±23,900 in-lb, maneuvering oscillatory endurance limit = ± 50,300 in.lb.
[3]Steady state oscillatory endurance limit = ±750 lb, maneuvering oscillatory endurance limit = ± 1750 lb.

Table 2. Monitored Flight Loads

Flight Condition	Main Rotor Beam Bend. Moment (Blade Station 5.5) (1000 in.-lb)						Main Rotor Hub Chord Bend. Moment (Blade Station 5.5) (1000 in.-lb)						Main Rotor Mast Parallel Bend (Blade Station 23) (1000 in.-lb)					
	Boot Condition				System		Boot Condition				System		Boot Condition				System	
	Normal		Cycled		Vented		Normal		Cycled		Vented		Normal		Cycled		Vented	
	Stdy	Osc[1]	Stdy	Osc[1]	Stdy	Osc[1]	Stdy	Osc[2]	Stdy	Osc[2]	Stdy	Osc[2]	Stdy	Osc[3]	Stdy	Osc[3]	Stdy	Osc[3]
Ground Runs 294 RPM																		
7 psi Torque	N/A[4]	N/A	N/A	N/A	N/A	N/A	N/A	N/A	N/A	N/A	N/A	N/A	-4.0	4.0	-4.0	4.0	N/A	N/A
13 psi Torque	-117.8	16.2	-114.4	14.5	---	---	N/A	N/A	N/A	N/A	N/A	N/A	-2.0	4.0	-4.0	4.0	---	---
17 psi Torque	-36.6	17.4	-59.8	17.4	---	---	-71.0	3.5	-69.3	5.2	---	---	0.0	7.0	-2.0	6.0	---	---
22 psi Torque	-30.8	17.4	-25.0	20.3	---	---	-67.6	5.2	-65.8	7.6	---	---	0.0	5.0	-2.0	4.4	---	---
26 psi Torque	-7.6	23.2	-1.8	23.2	---	---	-65.9	10.4	-64.1	10.4	---	---	2.0	5.0	-3.0	6.0	---	---
31 psi Torque	15.6	17.4	21.4	23.2	---	---	-63.4	10.4	-47.2	10.4	---	---	2.0	5.0	-2.0	5.0	---	---
34 psi Torque	33.0	23.2	38.8	23.2	---	---	-60.7	12.1	-53.8	17.3	---	---	2.0	5.2	-3.0	8.0	---	---
Ground Runs 324 RPM																		
10 psi Torque	N/A	N/A	N/A	N/A	---	---	-72.8	1.0	-72.8	1.0	---	---	-4.0	4.0	-4.0	4.0	---	---
13 psi Torque	-142.2	15.6	-112.0	14.5	---	---	-77.8	1.0	-71.7	1.8	---	---	-2.0	4.5	-3.6	5.0	---	---
18 psi Torque	-106.2	17.4	-100.9	23.2	---	---	-71.0	1.4	-69.3	3.5	---	---	-2.0	4.0	-2.0	6.0	---	---
26 psi Torque	-71.4	18.6	-65.6	17.4	---	---	-69.3	4.1	-66.9	6.4	---	---	0.0	8.0	-2.4	6.0	---	---
30 psi Torque	-68.5	14.5	-63.8	20.3	---	---	-67.6	8.6	-63.4	8.6	---	---	0.0	6.0	-4.0	4.4	---	---
34 psi Torque	-16.3	23.2	-7.6	23.2	---	---	-64.1	11.0	-57.2	14.5	---	---	0.0	5.4	-6.0	6.0	---	---
Ground Runs Engine-Dynamic System Compatibility Rapid Throttle Reductions																		
10 psi Torque	-115.0	14.5	---	---	---	---	-73.8	1.0	---	---	---	---	-1.0	3.2	---	---	---	---
	-187.4	17.4	---	---	---	---	-73.4	1.0	---	---	---	---	-4.0	6.0	---	---	---	---
22 psi Torque	-68.5	20.3	---	---	---	---	-69.3	6.9	---	---	---	---	-1.0	6.4	---	---	---	---
	-135.2	8.7	---	---	---	---	-74.5	0.3	---	---	---	---	-2.0	4.6	---	---	---	---
33 psi Torque	-6.9	23.2	---	---	---	---	-60.7	13.8	---	---	---	---	0.0	5.0	---	---	---	---
	-120.7	11.6	---	---	---	---	-73.8	0.7	---	---	---	---	0.0	4.0	---	---	---	---
Ground Runs Rapid Collective Reduction																		
	2.3	14.5	---	---	---	---	-60.7	8.6	---	---	---	---	0.0	5.0	---	---	---	---
	-149.7	0.0	---	---	---	---	-72.7	1.7	---	---	---	---	-4.0	6.0	---	---	---	---

NOTES:

[1]Steady state oscillatory endurance limit = ±200,600 in-lb, maneuvering oscillatory limit = ±237,300 in-lb.
[2]Steady state oscillatory endurance limit = N/A, maneuvering oscillatory limit = N/A
[3]Steady state oscillatory endurance limit = ±37,500 in.-lb, maneuvering oscillatory limit = ±494,000 in-lb.
[4]N/A = Not available

Table 3. Monitored Flight Loads

Flight Condition	Main Rotor Beam Bend. Moment (Blade Station 192) (1000 in.-lb)						Main Rotor Hub Chord Bend. Moment (Blade Station 192) (1000 in.-lb)						Main Rotor Blade Pitch Link Axial Load (lb)					
	Boot Condition				System		Boot Condition				System		Boot Condition				System	
	Normal		Cycled		Vented		Normal		Cycled		Vented		Normal		Cycled		Vented	
	Stdy	Osc[1]	Stdy	Osc[1]	Stdy	Osc[1]	Stdy	Osc[2]	Stdy	Osc[2]	Stdy	Osc[2]	Stdy	Osc[3]	Stdy	Osc[3]	Stdy	Osc[3]
Ground Runs																		
Engine-Dynamic System Compatibility																		
294 RPM																		
7.5 psi Torque																		
Pedal Pulse	-1.7	1.1	N/A[4]	N/A	-2.2	1.1	1.9	4.9	N/A	N/A	-10.5	5.7	115	---	N/A	N/A		415
Collective Pulse	-1.5		---	---	0.7		-22.9	5.0	---	---	3.2	3.7	215	---				315
21 psi Torque																		
Pedal Pulse	-4.1	2.2	---	---	-3.9	1.9	-8.0	6.2	---	---	1.9	7.4	315	---				415
Collective Pulse	-2.5		---	---	-2.2		5.6	7.4	---	---	4.4	7.4	415	---				315
31 psi Torque																		
Pedal Pulse	-4.7	1.4	---	---	-4.1	1.6	6.9	7.4	---	---	-5.5	12.4	465	---				435
Collective Pulse	-3.0		---	---	-2.9		6.9	5.0	---	---	6.8	6.2	415	---				415
Ground Runs																		
324 RPM																		
10 psi Torque																		
Pedal Pulse	-1.7	1.1	---	---	-1.9	1.1	0.6	6.2	---	---	-1.8	7.4	215	---				315
Collective Pulse	-1.4		---	---	-1.4		-11.7	3.7	---	---	1.9	5.7	215	---				315
21.5 psi Torque																		
Pedal Pulse	-3.6	2.2	---	---	-3.6	2.2	3.2	7.4	---	---	10.5	12.4	415	---				515
Collective Pulse	-2.5		---	---	-2.5		-4.2	5.0	---	---	3.2	7.4	415	---				415
35 psi Torque																		
Pedal Pulse	-7.1	1.6	---	---	-4.7	1.6	-5.5	9.9	---	---	6.8	12.4	465	---				515
Collective Pulse	-3.0		---	---	-3.0		6.9	8.7	---	---	5.6	7.4	465	---				515
Free Hover																		
Pedal Pulse	-3.0	3.2	---	---	-3.6	3.2	-10.4	4.9	---	---	-10.5	9.9	115	---				165
Collective Pulse	-4.1		---	---	-2.5		-10.4	4.9	---	---	-10.5	12.4	115	---				115

NOTES:

[1]Steady state oscillatory endurance limit = N/A, maneuvering oscillatory endurance limit = N/A.
[2]Steady state oscillatory endurance limit = ±23,900 in-lb, maneuvering oscillatory endurance limit = ± 50,300 in.lb.
[3]Steady state oscillatory endurance limit = ±750 lb, maneuvering oscillatory endurance limit = ± 1750 lb.
[4]N/A = Not available.

Table 4. Monitored Flight Loads

Flight Condition	Main Rotor Hub Beam Bend. Moment (Blade Station 5.5) (1000 in.-lb)						Main Rotor Hub Chord Bend. Moment (Blade Station 5.5) (1000 in.-lb)						Main Rotor Mast Parallel Bend. (Blade Staion 23) (1000 in.-lb)					
	Boot Condition				System Vented		Boot Condition				System Vented		Boot Condition				System Vented	
	Normal		Cycled				Normal		Cycled				Normal		Cycled			
	Stdy	Osc[1]	Stdy	Osc[1]	Stdy	Osc[1]	Stdy	Osc[2]	Stdy	Osc[2]	Stdy	Osc[2]	Stdy	Osc[3]	Stdy	Osc[3]	Stdy	Osc[3]
Ground Runs Engine-Dynamic System Compatability 294 RPM																		
7.5 psi Torque Pedal Pulse	-146.8		N/A[4]	N/A	-146.8		-72.8	3.5	N/A	N/A	-72.8	3.5	-3.0	6.0	N/A	N/A	-3.0	6.0
Collective Pulse	-36.6		---	---	-83.0		-72.0	2.1	---	---	-72.0	1.7	-2.0	4.0			-2.0	4.0
21 psi Torque Pedal Pulse	-42.4		---	---	-25.0		-67.6	10.4	---	---	-65.8	12.1	1.0	6.0			0.0	4.0
Collective Pulse	27.2		---	---	15.6		-65.8	10.4	---	---	-67.6	10.4	1.0	6.0			0.0	4.0
31 psi Torque Pedal Pulse	-28.4		---	---	15.6		-60.7	17.3	---	---	-62.4	20.7	2.0	6.0			0.0	6.0
Collective Pulse	44.6		---	---	50.4		-60.7	15.5	---	---	-60.7	10.4	2.0	6.0			0.0	4.0
Ground Runs 324 RPM																		
10 psi Torque Pedal Pulse	-146.8		---	---	-146.8		-70.4	2.8	---	---	-71.7	3.5	6.0	4.0			-3.0	6.0
Collective Pulse	-123.6		---	---	-129.4		-71.0	1.7	---	---	-71.7	1.7	-3.0	6.0			-2.0	4.4
21.5 psi Torque Pedal Pulse	-65.6		---	---	-54.0		-67.6	12.1	---	---	-60.7	15.6	-2.0	6.0			0.0	6.0
Collective Pulse	-25.0		---	---	-25.0		-67.6	10.4	---	---	-67.6	8.6	-2.0	6.0			0.0	6.0
35 psi Torque Pedal Pulse	4.0		---	---	21.4		-60.7	24.2	---	---	-60.7	20.7	-2.0	6.0			0.0	6.0
Collective Pulse	41.7		---	---	44.6		-60.7	20.7	---	---	-60.7	17.3	-3.0	6.0			0.0	6.0
Free Hover Pedal Pulse	-25.0		---	---	-36.6		-64.1	10.4	---	---	-62.4	17.3	0.0	8.0			-2.0	10.0
Collective Pulse	-7.6		---	---	4.0		-64.1	10.4	---	---	-62.4	20.7	0.0	6.0			-2.0	6.0

NOTES:

[1]Steady state oscillatory endurance limit = ±200,600 in-lb, maneuvering oscillatory limit = ±237,300 in-lb.
[2]Steady state oscillatory endurance limit = N/A, maneuvering oscillatory limit = N/A.
[3]Steady state oscillatory endurance limit = ±37,500in.-lb, maneuvering oscillatory limit = ±494,000 in-lb.
[4]N/A = Not available

Table 5. Monitored Flight Loads

Flight Condition	Main Rotor Beam Bend. Moment (Blade Station 192) (1000 in.-lb)						Main Rotor Blade Chord Bend. Moment (Blade Station 192) (1000 in.-lb)						Main Rotor Blade Pitch Link Axial Load (lb)					
	Boot Condition				System		Boot Condition				System		Boot Condition				System	
	Normal		Cycled		Vented		Normal		Cycled		Vented		Normal		Cycled		Vented	
Low Speed Flight	Stdy	Osc[1]	Stdy	Osc[1]	Stdy	Osc[1]	Stdy	Osc[2]	Stdy	Osc[2]	Stdy	Osc[2]	Stdy	Osc[2]	Stdy	Osc[2]	Stdy	Osc[2]
0° Azmiuth																		
0 KTAS	-4.7	1.5	-4.4	1.6	-4.1	1.4	-13.0	5.0	-11.7	6.2	-0.6	7.4	165	600	165	800	115	600
5 KTAS	-4.7	1.6	-4.7	1.6	-4.7	1.1	-13.0	5.0	-13.0	5.7	-0.6	5.0	165	500	165	700	115	550
10 KTAS	-3.9	2.7	-3.6	3.0	-3.6	2.7	-0.6	11.2	-13.0	12.4	-12.9	9.9	165	550	165	700	115	700
15 KTAS	-3.6	3.2	-3.9	3.2	-3.6	2.7	-13.0	12.4	-13.0	14.9	-3.0	12.4	165	500	115	700	215	500
20 KTAS	-4.1	3.2	-3.6	2.5	-4.7	1.9	-1.8	12.4	-15.4	17.4	-3.0	17.4	165	500	115	700	215	500
25 KTAS	-4.1	2.7	-4.4	2.7	-4.6	2.2	-3.0	12.4	-15.4	13.6	-3.0	12.4	215	500	115	600	215	500
30 KTAS	-4.6	1.6	-4.6	1.9	-4.6	1.6	-3.0	14.9	-15.4	14.9	-5.5	12.4	165	400	115	600	215	700
35 KTAS	-4.6	1.6	-5.2	1.4	-5.2	1.1	-3.0	9.9	-3.0	12.4	-3.0	14.9	115	450	115	650	115	700
40 KTAS	-4.6	2.2	-4.6	1.8	-5.2	1.1	-3.0	12.4	-14.2	11.2	-4.3	7.4	115	500	115	600	215	650
90° Azimuth																		
0 KTAS	-4.9	1.1	-4.6	1.4	-5.2	2.1	-1.8	3.7	-0.6	5.0	-3.1	12.4	115	500	115	600	215	700
5 KTAS	-4.4	2.2	-3.6	2.2	-4.6	2.3	-1.8	5.0	-14.2	7.4	-3.1	9.9	165	500	115	500	115	600
10 KTAS	-4.1	2.2	-4.1	2.7	-4.1	3.2	-1.8	7.4	-1.8	7.4	-3.0	14.9	165	550	165	700	115	1000
15 KTAS	-3.6	3.2	-3.6	3.2	-4.1	3.2	-3.0	17.4	-12.9	17.4	-3.0	17.3	115	700	115	730	115	1200
20 KTAS	-3.6	3.2	-4.1	3.2	-4.6	2.8	-1.8	18.6	-12.9	19.8	-3.0	20.1	165	900	165	950	115	1050
180° Azimuth																		
0 KTAS	-4.9	1.1	-4.6	1.1	-4.6	1.6	-3.0	2.5	-14.2	3.7	-3.0	7.4	115	500	215	550	115	800
5 KTAS	-5.2	1.6	-4.1	3.2	-4.7	2.4	-14.2	4.9	4.4	7.4	-3.0	2.5	165	500	165	700	115	650
10 KTAS	-3.9	3.8	-3.6	4.3	-4.1	2.8	-8.0	9.9	-8.0	8.7	-3.0	14.4	165	650	163	750	115	1050
15 KTAS	N/A		N/A		-4.1	2.8	N/A		N/A		-3.0	22.3	N/A		N/A		115	1000
20 KTAS	-3.9	3.0	-3.6	3.2	-4.7	4.6	-0.6	9.9	1.9	11.2	-3.0	22.3						
270° Azimuth																		
0 KTAS	-4.6	1.1	-4.1	2.0	-4.6	1.5	-14.2	6.2	-14.2	7.4	-1.8	3.7	165	550	165	700	215	600
5 KTAS	-4.6	1.6	-4.1	1.9	-4.6	3.2	-12.9	6.2	-12.9	7.4	-3.0	5.0	165	600	165	700	115	650
10 KTAS	-3.6	2.2	-4.1	2.7	-4.1	2.4	-12.9	8.7	-12.9	13.6	-3.0	12.4	115	850	115	900	115	900
15 KTAS	-3.8	3.2	N/A		-4.1	4.4	-1.8	17.3	N/A		-4.4	18.6	-1300	300	N/A		215	1100
20 KTAS	-3.6	4.1	N/A		-4.7	3.5	-14.2	18.6	N/A		-3.0	17.3	165	1100	N/A		112	10[illegible]

NOTES:

[1]Steady state oscillatory endurance limit = N/A, maneuvering oscillatory endurance limit = N/A.
[2]Steady state oscillatory endurance limit = ±23,900 in-lb, maneuvering oscillatory endurance limit = ± 50,300 in.lb.
[3]Steady state oscillatory endurance limit = ±750 lb, maneuvering oscillatory endurance limit = ± 1750 lb.
[4]N/A = Not available.

Table 6. Monitored Flight Loads

Flight Condition	Main Rotor Beam Bend. Moment (Blade Station 5.5) (1000 in.-lb)						Main Rotor Hub Chord Bend. Moment (Blade Station 5.5) (1000 in.-lb)						Main Rotor Mast Parallel Bend (1000 in.-lb)					
	Boot Condition				System Vented		Boot Condition				System Vented		Boot Condition				System Vented	
	Normal		Cycled				Normal		Cycled				Normal		Cycled			
Low Speed Flight	Stdy	Osc[1]	Stdy	Osc[1]	Stdy	Osc[1]	Stdy	Osc[2]	Stdy	Osc[2]	Stdy	Osc[2]	Stdy	Osc[2]	Stdy	Osc[2]	Stdy	Osc[2]
0° Azimuth																		
0 KTAS	-45.3	17.4	-71.4	23.2	-48.2	17.4	-64.1	7.6	-60.6	10.4	-64.1	10.4	0.0	5.0	-2.2	5.4	-2.0	10.0
5 KTAS	-77.2	26.1	-71.4	29.0	-54.0	17.4	-64.1	12.1	-60.7	13.8	-60.7	6.9	0.0	9.0	-2.4	8.0	-2.0	6.0
10 KTAS	-42.4	29.0	-59.8	29.0	-48.2	34.8	-64.1	13.8	-60.7	20.7	-60.7	17.3	0.0	8.0	-3.0	10.0	-2.0	9.0
15 KTAS	-71.4	23.2	-65.6	40.6	-48.2	31.9	-60.7	17.3	-60.7	19.0	-60.7	17.3	0.0	8.0	-2.0	14.0	-6.0	9.0
20 KIAS	-74.3	40.6	-71.4	40.6	-54.0	46.4	-60.7	19.0	-60.7	23.5	-64.1	17.3	-1.0	12.0	-4.0	12.0	-4.0	12.0
25 KTAS	-71.4	40.6	-59.8	34.8	-48.2	43.5	-64.1	20.7	-60.7	24.2	-67.6	19.0	-2.0	12.0	-4.0	12.0	-2.0	12.0
30 KTAS	-71.4	46.4	-71.4	40.6	-54.0	55.0	-64.1	17.3	-60.7	20.7	-60.7	17.3	-2.0	8.0	-4.0	14.0	-4.0	14.0
35 KTAS	-71.4	46.4	-77.2	46.4	-42.4	52.2	-65.8	13.8	-60.7	20.7	-67.6	13.8	-2.0	8.0	-4.0	10.0	-4.0	10.6
40 KTAS	-77.2	52.2	-68.5	46.4	-54.0	46.4	-65.8	17.3	-60.7	17.3	-67.6	10.4	-2.0	12.0	-5.0	10.0	-4.0	12.0
90° Azimuth																		
0 KTAS	-77.2	17.4	-74.3	20.3	-54.0	31.9	-65.8	6.9	-60.7	13.8	-64.1	13.8	0.0	4.0	-2.0	4.0	-2.0	14.0
5 KTAS	-77.2	17.4	-71.4	23.2	-65.6	29.0	-65.8	8.6	-62.4	13.1	-60.7	15.5	0.0	6.0	-2.0	5.0	-2.0	4.0
10 KTAS	-77.2	23.2	-65.6	27.2	-54.0	46.4	-64.1	10.4	-60.7	17.3	-64.1	22.4	0.0	6.0	-2.0	8.0	-2.0	12.0
15 KTAS	-74.3	40.6	-59.8	40.6	-54.0	40.6	-60.7	25.9	-57.2	27.6	-60.7	20.7	0.0	7.0	-4.0	10.0	-4.0	6.0
20 KTAS	-74.3	58.0	-65.6	58.0	-54.0	63.8	-60.7	24.2	-60.7	29.3	-64.1	24.2	0.0	10.0	-4.0	10.0	-2.0	7.0
180° Azimuth																		
0 KTAS	-80.1	14.5	-74.3	20.3	-112.0	58.0	-46.9	5.2	-60.7	6.9	-67.5	24.8	0.0	5.0	-3.0	5.6	-4.0	8.0
5 KTAS	-80.1	17.4	-71.4	40.6	-54.0	34.8	-60.7	7.6	-58.9	13.8	-60.7	13.8	0.0	8.0	-2.0	10.0	-2.0	8.0
10 KTAS	-77.2	29.0	-77.2	46.4	-54.0	46.4	-60.7	17.3	-60.7	20.7	-64.1	13.8	0.0	10.0	-3.0	10.0	-2.0	8.0
15 KTAS	N/A		N/A		-59.8	29.0	N/A		N/A		-64.1	20.7	N/A		N/A		-4.0	16.0
20 KTAS	-77.2	29.0	-71.4	40.6	-54.0	69.6	-60.7	17.3	-60.7	20.7	-60.7	32.8	0.0	12.0	-4.0	12.0	-4.0	12.0
270° Azimuth																		
0 KTAS	-83.0	23.2	-65.6	34.8	-54.0	72.5	-64.1	10.4	-60.7	15.5	-133.1	31.7	0.0	4.0	-2.0	8.0	-2.0	18.0
5 KTAS	-83.0	23.2	-77.2	29.0	-59.8	23.2	-64.1	9.7	-60.7	13.8	-64.1	6.9	0.0	7.0	-2.0	8.0	-2.0	6.0
10 KTAS	-80.1	34.8	-74.3	34.8	-59.8	20.3	-64.1	15.5	-58.9	19.0	-64.1	5.2	0.0	12.0	-2.0	10.0	-2.0	5.0
15 KTAS	-77.2	46.4	N/A		-59.8	40.6	-60.7	22.4	N/A		-64.1	10.4	0.0	15.0	N/A		-2.0	10.0
20 KTAS	-83.0	40.6	N/A		43.5	-69.1	-60.7	25.9	N/A		-64.1	24.2	-0.4	17.4	N/A		4.0	17.0

NOTES:

[1]Steady state oscillatory endurance limit = ±200,600 in-lb, maneuvering oscillatory limit = ±237,300 in-lb.
[2]Steady state oscillatory endurance limit = N/A, maneuvering oscillatory limit = N/A.
[3]Steady state oscillatory endurance limit = ±37,500in.-lb, maneuvering oscillatory limit = ±494,000 in-lb.
[4]N/A = Not available

Table 7. Monitored Flight Loads

Flight Condition	Main Rotor Beam Bend. Moment (Blade Station 192) (1000 in.-lb)						Main Rotor Blade Chord Bend. Moment (Blade Station 192) (1000 in.-lb)						Main Rotor Pitch Link Axial Load (lb)					
	Boot Condition				System		Boot Condition				System		Boot Condition				System	
	Normal		Cycled		Vented		Normal		Cycled		Vented		Normal		Cycled		Vented	
	Stdy	Osc[1]	Stdy	Osc[1]	Stdy	Osc[1]	Stdy	Osc[2]	Stdy	Osc[2]	Stdy	Osc[2]	Stdy	Osc[3]	Stdy	Osc[3]	Stdy	Osc[3]
Stabilized Level Flight 324 RPM																		
50 KIAS	N/A[4]	N/A	N/A	N/A	-4.1	2.2	N/A	N/A	N/A	N/A	-3.0	7.4	N/A	N/A	N/A	N/A	215	500
60 KIAS	N/A	N/A	N/A	N/A	-4.1	2.2	N/A	N/A	N/A	N/A	-12.9	7.4	N/A	N/A	N/A	N/A	215	500
70 KIAS	N/A	N/A	N/A	N/A	-3.6	3.0	N/A	N/A	N/A	N/A	1.9	7.4	N/A	N/A	N/A	N/A	215	600
80 KIAS	-3.9	2.7	-3.0	3.8	-3.6	3.2	0.7	6.7	1.9	7.4	1.9	7.4	215	480	215	700	215	600
90 KIAS	-3.9	3.2	-3.0	4.3	-3.0	3.8	1.9	8.9	1.9	11.2	4.4	13.6	215	640	215	800	215	700
100 KIAS	-3.3	3.8	-2.5	5.1	-3.0	3.8	1.9	11.2	4.4	13.6	-9.2	9.9	215	800	215	850	215	700
Stabilized Level Flight 310 RPM																		
50 KIAS	-4.1	2.6	-3.6	2.7	-4.1	2.7	0.7	7.4	-.5	7.0	1.9	7.4	215	450	215	600	215	600
60 KIAS	-4.1	2.2	N/A	N/A	-3.8	2.7	1.9	7.4	N/A	N/A	1.9	6.9	215	450	N/A	N/A	215	600
70 KIAS	-4.1	2.3	-0.9	3.5	-3.0	4.3	1.9	7.0	1.9	9.9	3.1	12.4	215	600	165	700	215	600
80 KIAS	-3.8	2.7	-3.0	4.3	-3.0	3.8	1.9	7.4	1.9	12.4	3.2	9.9	165	550	165	700	215	600
90 KIAS	-3.6	3.8	-2.7	4.9	-2.7	4.6	1.9	9.9	3.2	12.4	3.2	12.4	215	600	215	680	165	750
100 KIAS	-3.0	3.9	-2.5	5.4	-3.0	4.3	3.1	7.4	3.2	18.1	1.9	11.1	215	700	215	800	165	600
Stabilized Level Flight 297 RPM																		
50 KIAS	-3.8	2.7	-3.8	3.2	-3.8	2.4	1.9	9.9	1.9	9.9	1.9	8.7	215	600	215	650	215	600
60 KIAS	-3.8	2.4	-3.6	3.2	-3.8	2.8	1.9	8.7	1.9	9.9	2.4	7.4	215	600	215	600	165	550
70 KIAS	-3.8	2.7	-3.6	3.8	-3.6	3.2	1.9	7.4	0.7	9.9	1.9	7.4	215	720	115	720	165	600
80 KIAS	-3.3	3.8	-2.5	5.4	-3.0	4.1	1.9	8.7	4.4	12.4	1.9	9.9	215	600	165	700	215	650
90 KIAS	-3.3	3.6	-2.5	5.7	-2.7	4.6	1.9	9.9	3.1	12.3	1.9	12.4	215	600	215	700	215	650
60 KIAS Climb@ 30.8 psi Torque	-3.8	1.6	N/A	N/A	N/A	N/A	-12	6.2	N/A	N/A	N/A	N/A	215	500	N/A	N/A	N/A	N/A
60 KIAS Climb@ 33.6 psi Torque	-3.0	2.2	N/A	N/A	N/A	N/A	-8	7.4	N/A	N/A	N/A	N/A	315	750	N/A	N/A	N/A	N/A
60 KIAS Climb@ 38.5 psi Torque	-2.8	1.7	N/A	N/A	N/A	N/A	6.8	7.4	N/A	N/A	N/A	N/A	415	800	N/A	N/A	N/A	N/A
90 KIAS Climb@ 27.8 psi Torque	-4.1	2.2	N/A	N/A	N/A	N/A	-0.6	9.9	N/A	N/A	N/A	N/A	165	650	N/A	N/A	N/A	N/A
90 KIAS Climb@ 35.2 psi Torque	-3.9	2.7	N/A	N/A	N/A	N/A	1.9	5.5	N/A	N/A	N/A	N/A	265	950	N/A	N/A	N/A	N/A
90 KIAS Climb@ 37.1 psi Torque	12.6	3.2	N/A	N/A	N/A	N/A	1.9	6.2	N/A	N/A	N/A	N/A	215	800	N/A	N/A	N/A	N/A

NOTES:

[1]Steady state oscillatory endurance limit = N/A, maneuvering oscillatory endurance limit = N/A.
[2]Steady state oscillatory endurance limit = ±23,900 in-lb, maneuvering oscillatory endurance limit = ± 50,300 in.lb.
[3]Steady state oscillatory endurance limit = ±750 lb, maneuvering oscillatory endurance limit = ± 1750 lb.
[4]N/A = Not available.

Table 8. Monitored Flight Loads

Flight Condition	Main Rotor Hub Beam Bend. Moment (Blade Station 5.5) (1000 in.-lb)						Main Rotor Hub Blade Chord Bend. Moment (Blade Station 5.5) 1000 in.-lb						Main Rotor Mast Parallel Bend. (Blade Station 23) (1000 in.-lb)					
	Boot Condition				System		Boot Condition				System		Boot Condition				System	
	Normal		Cycled		Vented		Normal		Cycled		Vented		Normal		Cycled		Vented	
	Stdy	Osc[1]	Stdy	Osc[1]	Stdy	Osc[1]	Stdy	Osc[2]	Stdy	Osc[2]	Stdy	Osc[2]	Stdy	Osc[3]	Stdy	Osc[3]	Stdy	Osc[3]
Stabilized Level Flight 324 RPM																		
50 KIAS	N/A[4]	N/A	N/A	N/A	-42.4	40.6	N/A	N/A	N/A	N/A	-64.1	17.3	N/A	N/A	N/A	N/A	-4.0	10.0
60 KIAS	N/A	N/A	N/A	N/A	-42.4	34.8	N/A	N/A	N/A	N/A	-64.1	13.6	N/A	N/A	N/A	N/A	-4.0	10.0
70 KIAS	N/A	N/A	N/A	N/A	-42.4	29.0	N/A	N/A	N/A	N/A	-60.7	17.3	N/A	N/A	N/A	N/A	-4.0	14.0
80 KIAS	-42.4	23.2	-94.6	37.7	-36.6	26.1	-62.4	17.3	-57.2	24.2	-60.7	20.7	-1.0	18.0	-2.0	19.0	-2.0	16.0
90 KIAS	-36.6	29.0	-30.8	40.6	-42.4	34.8	-60.7	19.7	-53.8	29.3	-53.8	27.6	-1.0	22.0	-4.0	23.0	-1.0	18.0
100 KIAS	-30.8	34.8	-30.8	52.2	-42.4	40.6	-57.2	25.9	-53.8	34.5	-57.2	20.7	1.0	23.0	-2.0	28.0	-1.0	20.0
Stabilied Level Flight 310 RPM																		
50 KIAS	-30.8	34.8	-25.0	40.6	-25.0	29.0	-64.1	12.1	-62.4	17.3	-64.1	13.8	-0.4	8.0	-4.0	8.6	-4.0	10.0
60 KIAS	-25.0	26.1	N/A	N/A	-25.0	29.0	-64.1	13.8	N/A	N/A	-62.4	17.3	0.0	10.0	N/A	N/A	-2.0	12.0
70 KIAS	-30.8	17.4	-25.0	58.0	-27.9	29.0	-60.1	12.1	-43.4	20.7	-53.8	31.1	0.0	14.0	-3.0	15.0	-1.0	19.0
80 KIAS	-25.0	29.0	-22.1	34.8	-25.0	40.6	-64.1	17.3	-57.2	27.6	-57.2	31.1	0.0	18.0	-1.0	19.0	0.0	21.0
90 KIAS	-38.8	34.8	-2.0	20.7	-30.8	29.0	-60.7	20.7	-55.5	28.6	-57.2	27.6	0.0	20.0	-1.0	22.0	0.0	20.0
100 KIAS	-25.0	34.8	-19.2	58.0	-25.0	40.6	-41.7	24.2	-50.3	38.0	-57.2	26.2	1.0	21.0	0.0	26.0	0.0	20.0
Stabilized Level Flight 297 RPM																		
50 KIAS	-19.2	23.2	-19.2	29.0	-13.4	29.0	-64.1	13.8	-62.4	29.7	-64.1	13.8	0.0	9.0	1.0	12.0	-2.0	8.0
60 KIAS	-13.4	29.0	-10.5	46.4	-7.6	34.8	-64.1	-60.7	20.7	-62.4	-62.4	17.3	0.0	10.0	-3.0	12.0	-1.0	12.0
70 KIAS	-16.3	29.0	-19.2	46.4	-13.4	32.2	-64.1	13.8	-60.7	20.7	-62.4	17.3	1.0	14.0	-2.0	14.0	-1.0	14.0
80 KIAS	-13.4	34.8	-10.5	46.4	-10.5	34.8	-60.7	20.7	-53.8	31.1	-60.7	22.5	2.0	18.2	0.0	20.0	0.0	16.0
90 KIAS	-10.5	40.6	7.6	52.2	-16.3	34.8	-60.7	20.7	-55.5	132.8	-57.2	29.3	1.0	20.0	0.0	24.0	0.0	19.0
60 KIAS Climb@ 30.8 psi Torque	-36.6	31.9	N/A	N/A	N/A	N/A	-60.7	15.5	N/A	N/A	N/A	N/A	2.0	14.0	N/A	N/A	N/A	N/A
60 KIAS Climb@ 33.5 psi Torque	-25.0	23.2	N/A	N/A	N/A	N/A	-50.3	17.3	N/A	N/A	N/A	N/A	6.0	16.0	N/A	N/A	N/A	N/A
60 KIAS Climb@ 38.5 psi Torque	-19.2	23.2	N/A	N/A	N/A	N/A	-50.3	23.5	N/A	N/A	N/A	N/A	8.0	16.0	N/A	N/A	N/A	N/A
90 KIAS Climb@ 27.8 psi Torque	-39.5	34.8	N/A	N/A	N/A	N/A	-62.4	20.7	N/A	N/A	N/A	N/A	10.0	20.0	N/A	N/A	N/A	N/A
90 KIAS Climb@ 35.2 psi Torque	-39.5	34.8	N/A	N/A	N/A	N/A	-53.8	17.3	N/A	N/A	N/A	N/A	2.0	22.0	N/A	N/A	N/A	N/A
90 KIAS Climb@ 37.1 psi Torque	-30.8	34.8	N/A	N/A	N/A	N/A	-53.8	24.2	N/A	N/A	N/A	N/A	4.0	21.0	N/A	N/A	N/A	N/A

NOTES:

[1]Steady state oscillatory endurance limit = ±200,600 in-lb, maneuvering oscillatory limit = ±237,300 in-lb.
[2]Steady state oscillatory endurance limit = N/A, maneuvering oscillatory limit = N/A.
[3]Steady state oscillatory endurance limit = ±37,500in.-lb, maneuvering oscillatory limit = ±494,000 in-lb.
[4]N/A = Not available

Table 9. Monitored Flight Loads

Flight Condition	Main Rotor Beam Bend. Moment (Blade Station 192) (1000 in.-lb)						Main Rotor Blade Chord Bend. Moment (Blade Station 192) (1000 in.-lb)						Main Rotor Pitch Link Load (lb)					
	Boot Condition				System Vented		Boot Condition				System Vented		Boot Condition				System Vented	
	Normal		Cycled				Normal		Cycled				Normal		Cycled			
	Stdy	Osc[1]	Stdy	Osc[1]	Stdy	Osc[1]	Stdy	Osc[2]	Stdy	Osc[2]	Stdy	Osc[2]	Stdy	Osc[2]	Stdy	Osc[2]	Stdy	Osc[2]
60 KIAS Descent@ 19.0 psi Torque	-4.9	0.5	-4.9	0.5	-4.9	0.5	-10.5	5.5	-10.4	7.4	-11.7	6.2	215	600	165	620	215	600
60 KIAS Descent@ 13.8 psi Torque	-4.9	0.5	-4.9	0.5	-4.9	0.6	-11.2	4.9	N/A[4]	N/A	-10.4	4.9	215	600	215	700	216	600
60 KIAS Descent@ 6.2 psi Torque	-4.9	0.4	-4.6	0.4	-4.9	0.3	-10.9	3.7	-10.4	5.4	-10.4	4.9	215	600	215	620	215	550
90 KIAS Descent@ 12.0 psi Torque	-9.9	2.1	-4.1	2.2	-4.9	0.5	-15.4	9.9	-3.0	11.2	-10.4	5.5	215	600	215	700	215	600
90 KIAS Descent@ 16.1 psi Torque	-4.1	1.9	-3.6	3.2	-4.9	0.4	-3.0	9.9	-15.4	7.4	- 2.9	7.4	215	550	215	600	215	650
90 KIAS Descent@ 13.8 psi Torque	-4.6	1.1	-4.5	1.3	-4.9	0.4	-15.4	11.2	-3.0	9.9	-10.4	4.9	215	550	215	500	215	600
20° Banked Turn to Left	-4.9	0.8	-4.2	1.9	-4.6	1.1	-5.5	7.4	-15.4	13.0	-5.5	9.9	215	620	215	800	215	700
35° Banked Turn to Left	-4.9	0.5	-4.9	1.6	-4.6	1.3	-19.2	7.4	-17.9	12.4	-4.3	12.4	215	700	215	800	215	750
20° Banked Turn to Right	-3.6	2.9	-3.0	3.9	-4.6	1.1	1.9	6.2	3.1	12.4	-4.3	9.9	215	600	215	700	215	700
35° Banked Turn to Right	-3.6	2.7	-3.0	3.8	-4.6	1.8	1.9	12.4	4.4	14.9	-3.0	12.4	215	800	215	850	215	800
	Normal		Throttle Chop		System Vented		Normal		Throttle Chop		System Vented		Normal		Throttle Chop		System Vented	
	Stdy	Osc[1]	Stdy	Osc[1]	Stdy	Osc[1]	Stdy	Osc[2]	Stdy	Osc[2]	Stdy	Osc[2]	Stdy	Osc[2]	Stdy	Osc[2]	Stdy	Osc[2]
70 KIAS Autorotation[5]	-4.1	1.9	-4.1	2.3	-4.6	1.1	-2.5	7.4	-4.2	7.4	-17.9	6.2	215	400	215	200	215	430
80 KIAS Autorotation	-4.6	1.4	-4.4	1.6	-4.7	1.1	-16.6	7.4	-17.9	7.4	-16.7	7.4	215	550	215	200	-290	500
90 KIAS Autorotation	-3.4	2.7	N/A	N/A	-4.7	1.1	-0.6	7.4	N/A	N/A	-5.5	7.4	215	500	N/A	N/A	165	660

NOTES:

[1]Steady state oscillatory endurance limit = N/A, maneuvering oscillatory endurance limit = N/A.
[2]Steady state oscillatory endurance limit = ±23,900 in-lb, maneuvering oscillatory endurance limit = ± 50,300 in.lb.
[3]Steady state oscillatory endurance limit = ±750 lb, maneuvering oscillatory endurance limit = ± 1750 lb.
[4]N/A = Not available.
[5]Boot not cycled during autorotation.

Table 10. Monitored Flight Loads

Flight Condition	Main Rotor Beam Bend. Moment (Blade Station 5.5) (1000 in.-lb)						Main Rotor Blade Chord Bend. Moment (Blade Station 5.5) (1000 in.-lb)						Main Rotor Mast Parallel Bend (Blade Station 23) (1000 in.-lb)					
	Boot Condition				System		Boot Condition				System		Boot Condition				System	
	Normal		Cycled		Vented		Normal		Cycled		Vented		Normal		Cycled		Vented	
	Stdy	Osc[1]	Stdy	Osc[1]	Stdy	Osc[1]	Stdy	Osc[2]	Stdy	Osc[2]	Stdy	Osc[2]	Stdy	Osc[3]	Stdy	Osc[3]	Stdy	Osc[3]
60 KIAS Descent@ 19.0 psi Torque	-51.1	29.0	-48.2	37.8	-88.8	23.2	-67.5	6.9	-60.7	13.8	-69.3	3.5	-2.0	11.1	-4.0	9.0	-4.0	9.0
60 KIAS Descent@ 13.8 psi Torque	-30.8	37.7	-42.4	29.0	-48.2	31.9	-67.5	6.9	-67.5	6.9	-67.5	6.9	-4.0	12.0	-6.0	10.0	-4.0	10.0
60 KIAS Descent@ 6.2 psi Torque	-48.2	37.7	-42.4	29.0	-48.2	34.8	-69.3	3.5	-67.6	5.2	-67.5	5.1	-4.0	10.0	-6.0	9.0	-4.0	10.0
90 KIAS Descent@ 21.0 psi Torque	-51.0	31.3	-25.0	34.8	-42.4	29.0	-64.1	12.1	-60.7	13.8	-65.8	10.3	0.0	18.0	-2.0	18.0	-4.0	14.4
90 KIAS Descent@ 16.1 psi Torque	-54.0	29.0	-74.3	34.8	-54.0	23.2	-65.8	6.9	-64.1	12.1	-67.5	6.2	-3.0	13.0	-5.0	11.4	-5.0	11.0
90 KIAS Descent@ 13.7 psi Torque	-54.0	34.8	-74.3	34.8	-85.9	26.1	-67.5	6.9	-66.5	9.7	-69.3	3.5	-4.0	12.0	-5.0	11.0	-6.0	8.0
20° Banked Turn to Left	-42.4	29.0	-25.0	40.6	-19.2	34.8	-58.9	20.7	-50.3	34.5	-55.5	31.1	2.0	20.0	-2.0	25.0	0.0	22.0
35° Banked Turn to Left	-25.0	29.0	-19.2	29.0	4.0	40.6	-60.7	22.4	-53.7	17.2	-53.8	32.8	0.0	22.0	2.0	26.0	2.0	23.0
20° Banked Turn to Right	-7.6	29.0	-18	34.8	-13.4	34.8	-60.7	20.7	-53.8	31.1	-53.8	31.1	0.0	20.0	-2.0	21.0	0.0	24.0
35° Banked Turn to Right	1.1	31.9	15.6	40.6	4.0	46.4	-58.9	24.2	-52.0	34.5	-53.8	37.9	0.0	24.0	2.0	26.0	4.0	30.0
	Normal		Throttle Chop		System Vented		Normal		Throttle Chop		System Vented		Normal		Throttle Chop		System Vented	
	Stdy	Osc[1]	Stdy	Osc[1]	Stdy	Osc[1]	Stdy	Osc[2]	Stdy	Osc[2]	Stdy	Osc[2]	Stdy	Osc[2]	Stdy	Osc[2]	Stdy	Osc[2]
70 KIAS Autorotation[5]	-42.4	26.1	-7.6	20.3	-19.2	29.0	-66.9	10.4	-69.3	3.5	-70.3	2.1	0.0	12.0	-2.0	6.0	-4.0	10.0
80 KIAS Autorotation	-42.4	34.8	-13.4	29.0	-42.4	29.0	-65.8	10.4	-69.3	4.1	-70.3	2.1	0.0	18.0	-3.0	6.0	-6.0	11.0
90 KIAS Autorotation	-42.4	29.0	N/A	N/A	-30.8	23.2	-62.4	17.3	N/A	N/A	-69.3	3.4	2.0	18.0	N/A	N/A	-4.0	12.0

NOTES:

[1]Steady state oscillatory endurance limit = ±200,600 in-lb, maneuvering oscillatory limit = ±237,300 in-lb.
[2]Steady state oscillatory endurance limit = N/A, maneuvering oscillatory limit = N/A.
[3]Steady state oscillatory endurance limit = ±37,500 in.-lb, maneuvering oscillatory limit = ±494,000 in-lb.
[4]N/A = Not available
[5]Boot not cycled during autorotation.

Table 11. Monitored Flight Loads (Third Generation)

Flight Condition	Main Rotor Beam Bend. Moment (Blade Station 192) (1000 in.-lb)						Main Rotor Blade Chord Bend. Moment (Blade Station 192) (1000 in.-lb)						Main Rotor Blade Pitch Link Axial Load (lb)					
	Boot Condition				System Vented		Boot Condition				System Vented		Boot Condition				System Vented	
	Normal		Cycled				Normal		Cycled				Normal		Cycled			
	Stdy	Osc[1]	Stdy	Osc[1]	Stdy	Osc[1]	Stdy	Osc[2]	Stdy	Osc[2]	Stdy	Osc[2]	Stdy	Osc[3]	Stdy	Osc[3]	Stdy	Osc[3]
Flat Pitch Ground Runs 310 RPM																		
12 psi Torque	-1.6	0.7	-0.9	0.5	-1.1	1.0	-7.0	3.7	6.6	4.5	-6.6	4.3	20	150	30	250	60	220
Flat Pitch Ground Runs 320 RPM																		
12.5 psi Torque	-1.1	0.8	-1.0	0.7	-1.1	1.1	-7.8	2.7	-7.8	2.7	-7.8	3.5	50	250	100	250	100	210
Free Hover 310 RPM	-2.8	1.9	-2.9	2.4	-2.8	2.2	-4.1	4.2	-4.1	6.2	-2.8	6.2	200	350	50	320	150	300
Free Hover 322 RPM	-2.9	2.2	-2.9	2.7	-2.9	2.7	-4.1	5.0	-1.6	6.2	-4.1	5.0	250	300	100	350	100	300
Stabilized Level Flight 310 RPM																		
50 KIAS	-2.6	2.7	-2.3	3.3	-2.3	3.0	-2.8	9.9	-0.9	11.7	-4.1	8.7	200	550	150	800	150	650
60 KIAS	-2.3	3.3	-1.8	3.8	-2.3	3.3	-0.3	7.4	0.9	9.9	-1.6	9.4	200	550	200	1000	200	700
70 KIAS	-2.0	3.3	-1.8	4.9			0.9	8.2	3.3	16.2			300	600	450	1300		
80 KIAS	-2.1	3.5	-1.8	4.9			-1.5	9.4	-0.3	12.4			350	720	400	1500		

NOTES:

[1]Steady state oscillator endurance limit = N/A, maneuvering oscillatory endurance limit = N/A.
[2]Steady state oscillator endurance limit = ±23,900 in-lb, maneuvering oscillatory endurance limit = ± 50,300 in.lb.
[3]Steady state oscillator endurance limit = ±750 lb, maneuvering oscillatory endurance limit = ± 1750 lb.

Table 12. Monitored Flight Loads

Flight Condition	Main Rotor Beam Bend. Moment (Station 192) (1000 in.-lb)						Main Rotor Blade Chord Bend. Moment (Station 5.5) (1000 in.-lb)						Main Rotor Mast Parallel Bend. (Station 5.5) (1000 in.-lb)					
	Boot Condition				System Vented		Boot Condition				System Vented		Boot Condition				System Vented	
	Normal		Cycled				Normal		Cycled				Normal		Cycled			
	Stdy	Osc[1]	Stdy	Osc[1]	Stdy	Osc[1]	Stdy	Osc[2]	Stdy	Osc[2]	Stdy	Osc[2]	Stdy	Osc[3]	Stdy	Osc[3]	Stdy	Osc[3]
Flat Pitch Ground Runs 310 RPM																		
12 psi Torque	-56.7	1.2	-56.1	1.2	-54.9	1.2	-25.8	3.7	-24.9	4.7	-23.7	4.7	0.3	6.0	0.9	6.6	-1.0	6.0
Flat Pitch Ground Runs 320 RPM																		
12.5 psi Torque	-56.1	0.5	-56.1	1.2	-56.1	0.5	-27.6	1.8	-26.7	3.7	-26.7	2.8	0.1	6.0	0.3	6.0	0.5	6.0
Free Hover 310 RPM	13.7	10.4	-38.6	23.2	14.4	17.5	-9.9	15.8	4.1	46.6	-0.6	32.6	-2.0	12.0	-2.1	17.1	-2.1	12.0
Free Hover 322 RPM	25.3	11.6	37.0	20.3	31.1	14.5	-9.9	18.6	-0.6	40.1	-0.6	37.3	-2.1	11.0	-2.1	13.1	-2.1	12.0
Stabilized Level Flight 310 RPM																		
50 KIAS	19.4	26.2	10.7	52.3	13.7	45.4	13.4	32.6	22.7	55.9	27.4	55.9	-0.5	15.0	-0.5	20.1	-0.5	18.1
60 KIAS	13.7	23.3	25.3	52.4	17.7	40.7	18.0	37.3	32.0	65.2	27.3	55.9	-0.5	17.1	-0.5	20.1	-0.5	18.1
70 KIAS	19.5	23.3	19.5	75.6			18.0	37.3	46.0	83.9			-0.9	18.1	-0.5	22.1		
80 KIAS	25.3	29.1	13.7	63.9			22.7	46.6	46.0	102.6			-0.5	18.1	-0.5	23.1		

NOTES:

[1]Steady state oscillatory endurance limit = ±200,600 in-lb, maneuvering oscillatory limit = ±237,300 in-lb.
[2]Steady state oscillatory endurance limit = N/A, maneuvering oscillatory limit = N/A.
[3]Steady state oscillatory endurance limit = ±37,500in.-lb, maneuvering oscillatory limit = ±494,000 in-lb.

APPENDIX G. PHOTOGRAPHS

Photograph	Photograph Number
Artificial Icing Environment	1
Deice Cycle	2
Deice Cycle	3
Deice Cycle	4
Deice Cycle	5
Ice Remaining after Single Deice Cycle	6
Ice Remaining after Successive Deice Cycle	7
Self Shedding of Noninflatable Section	8
Debonding of Noninflatable Section	9
Debonding of Hose and Flap Assembly	10
Rupture of Inflatable Section	11
Pneumatic Hose and Damper Control Tube	12
Abrasion of Damper Control Tube	13
Lumps in Inflatable Section	14
Depression Created by Missing Manifold Material	15
Cuts to Remove Manifold Material	16
Repaired Cuts	17
Impact Damage to Inflatable Section	18
Water Pockets Under Deicer	19
Damage to Tail Rotor Blade	20

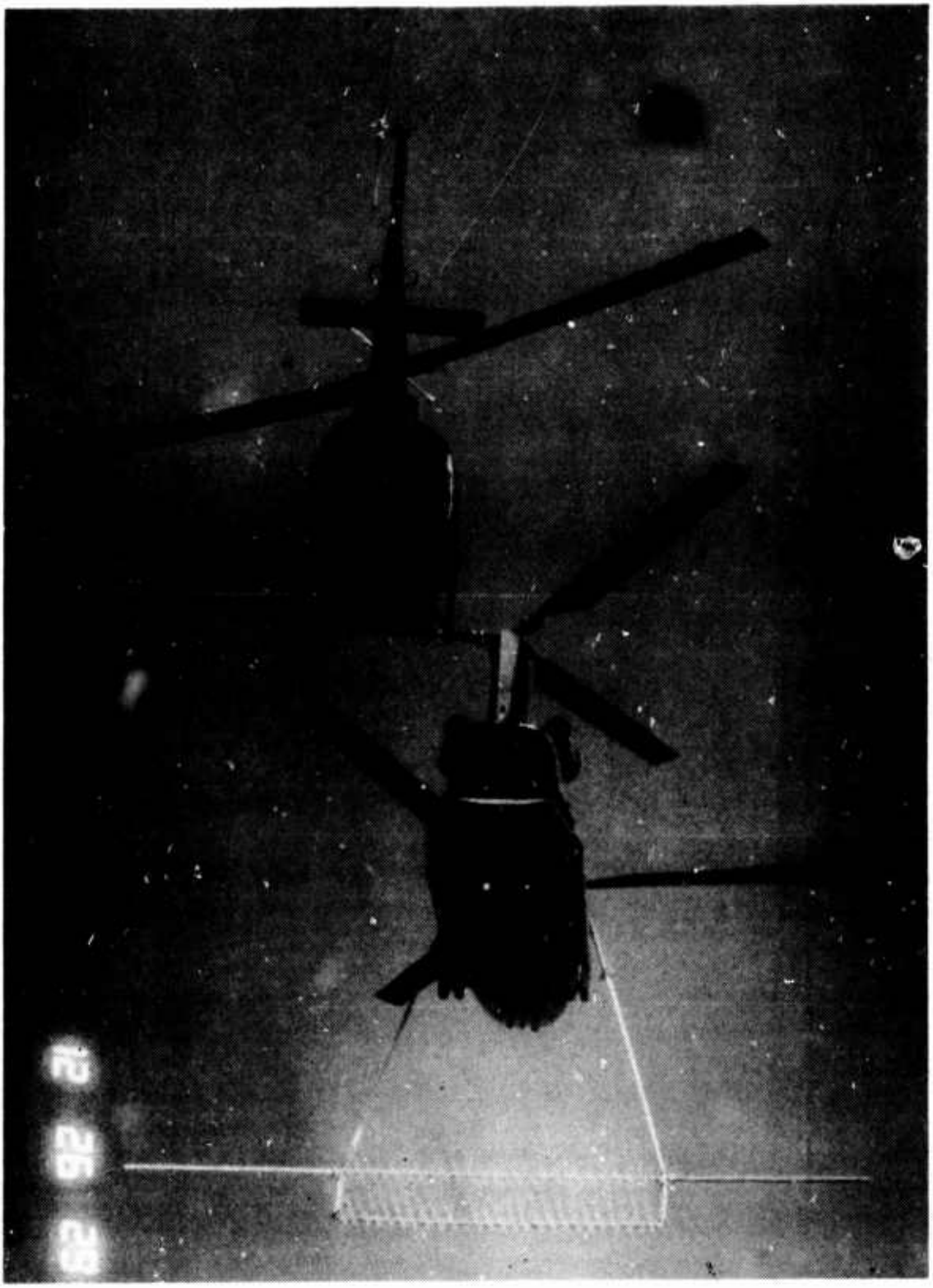

Photo 1. Artificial Icing Environment

Photo 2. Deice Cycle

Photo 3. Deice Cycle

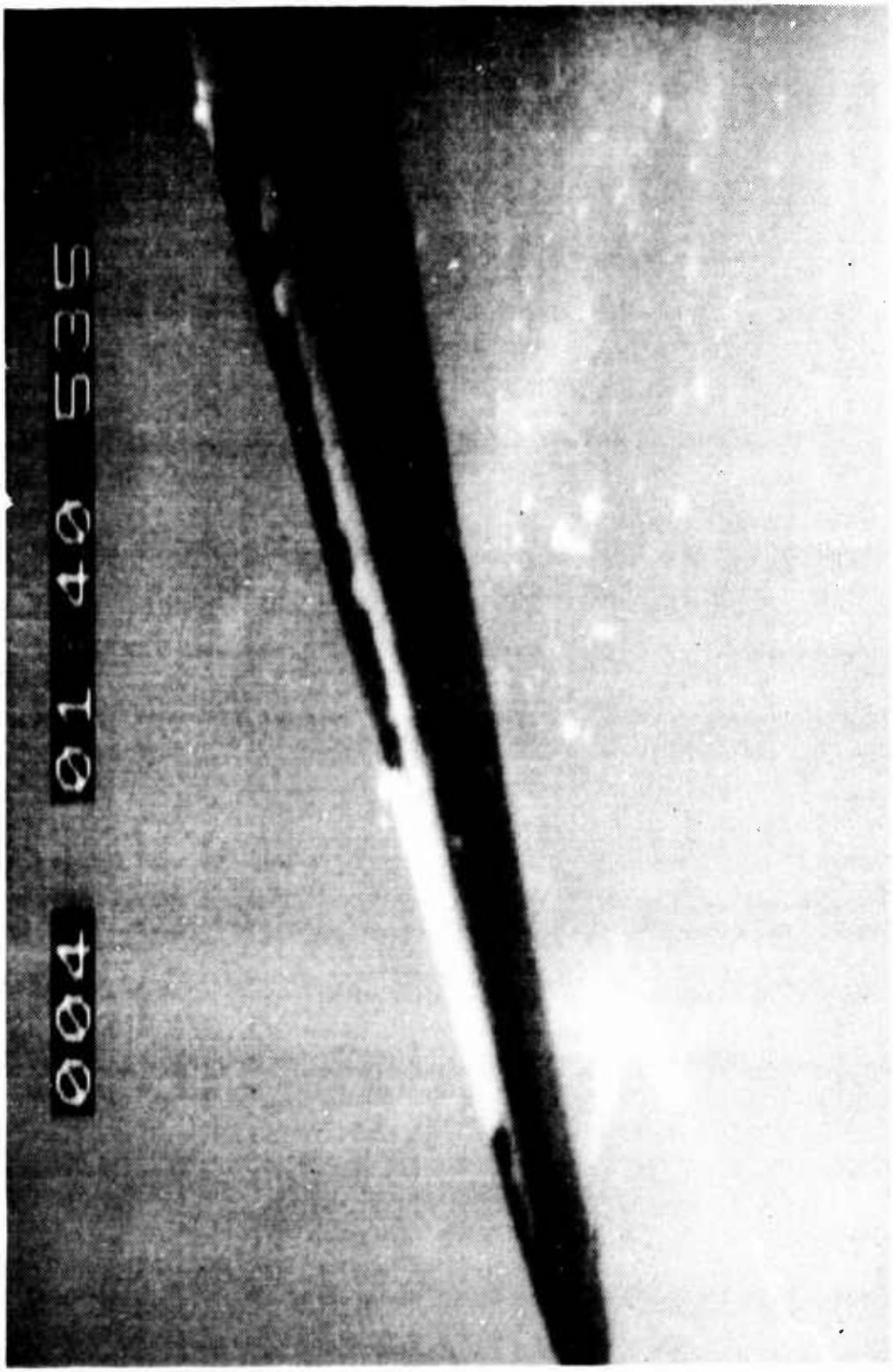

Photo 4. Deice Cycle

Photo 5. Deice Cycle

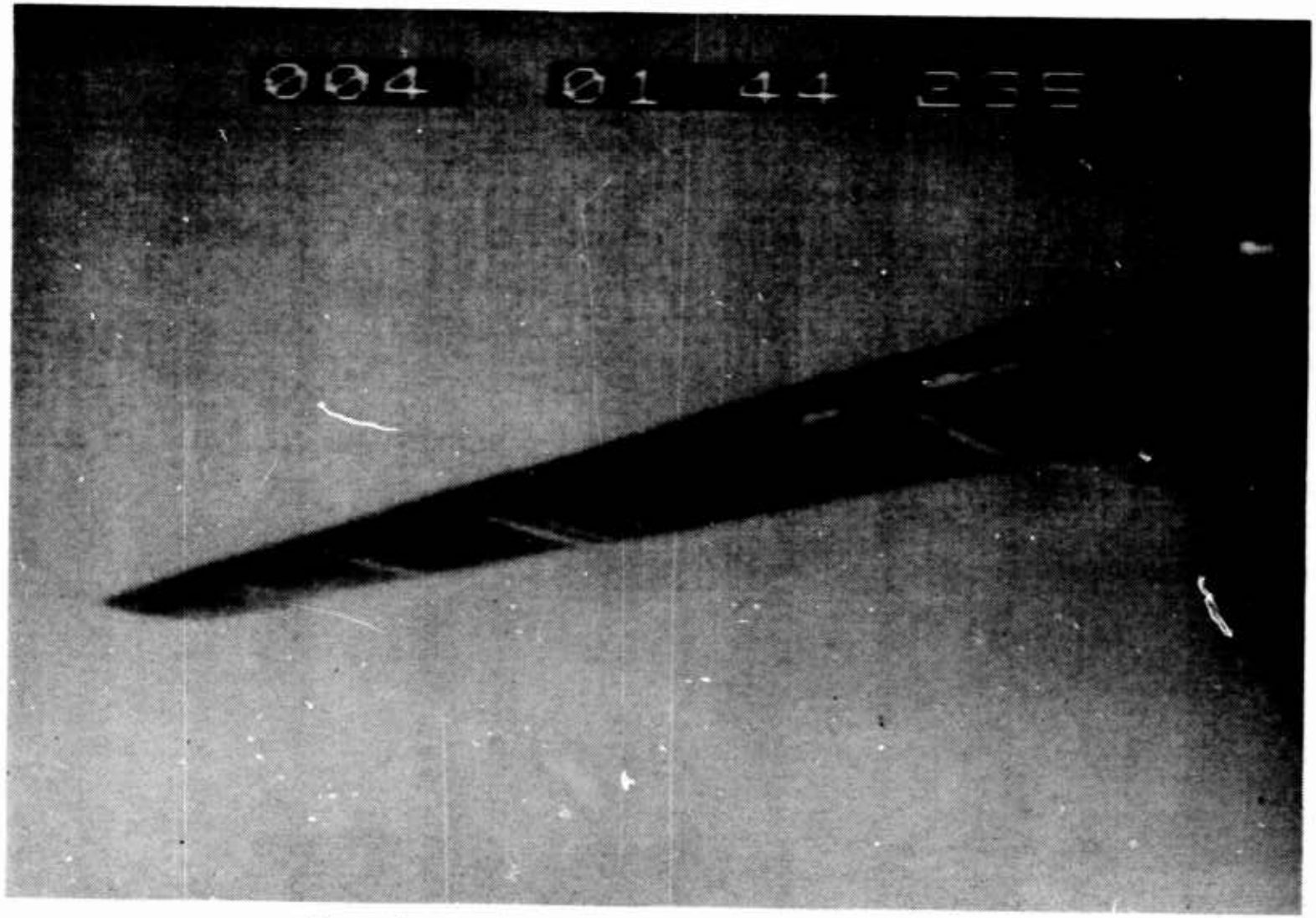

Photo 6. Ice Remaining after Single Deice Cycle

Photo 7. Ice Remaining after Successive Deice Cycle

Photo 8. Self Shedding of Tip

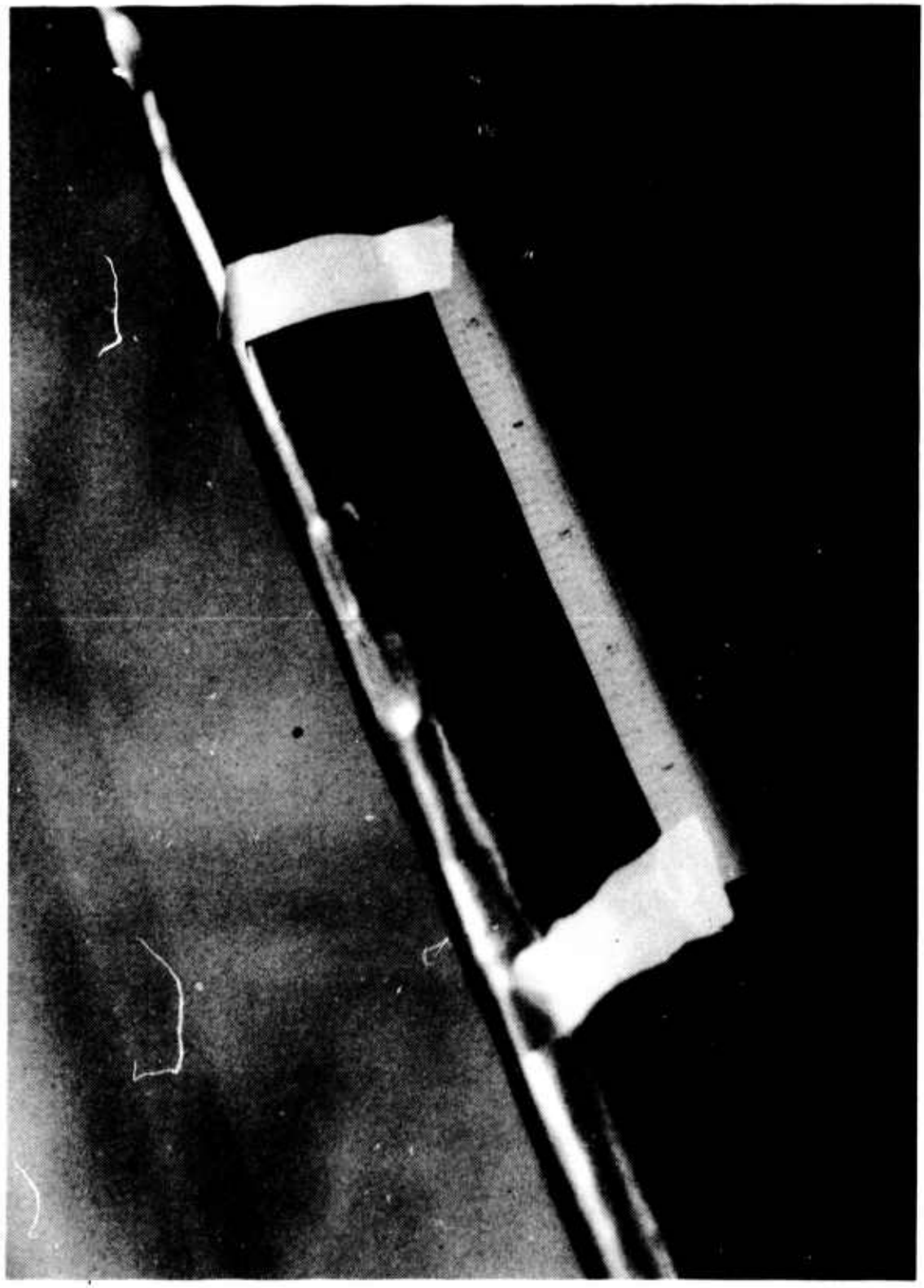

Photo 9. Debonding of Noninflatable Section

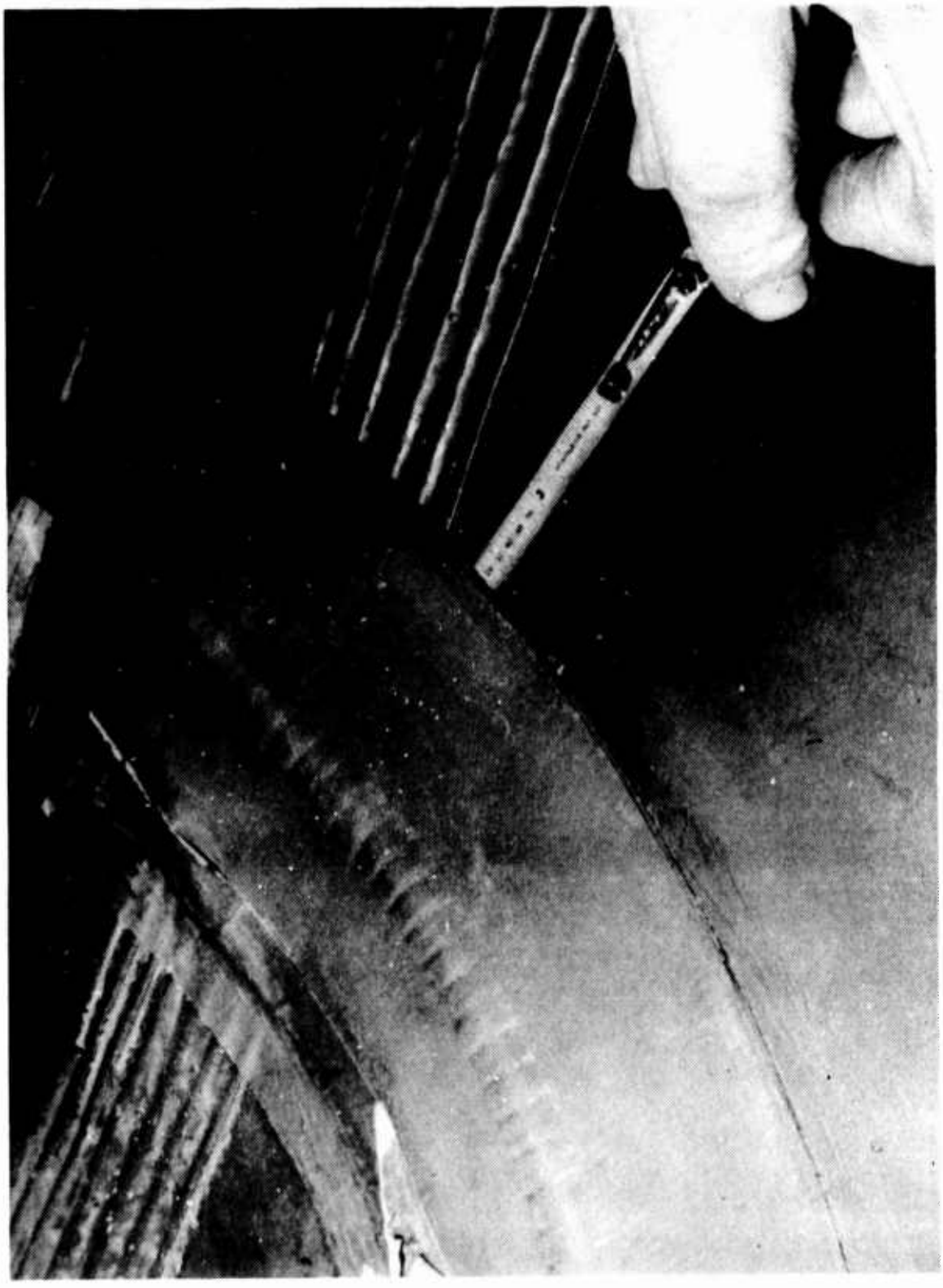

Photo 10. Debonding of Hose and Flap Assembly

Photo 11. Rupture of Inflatable Section

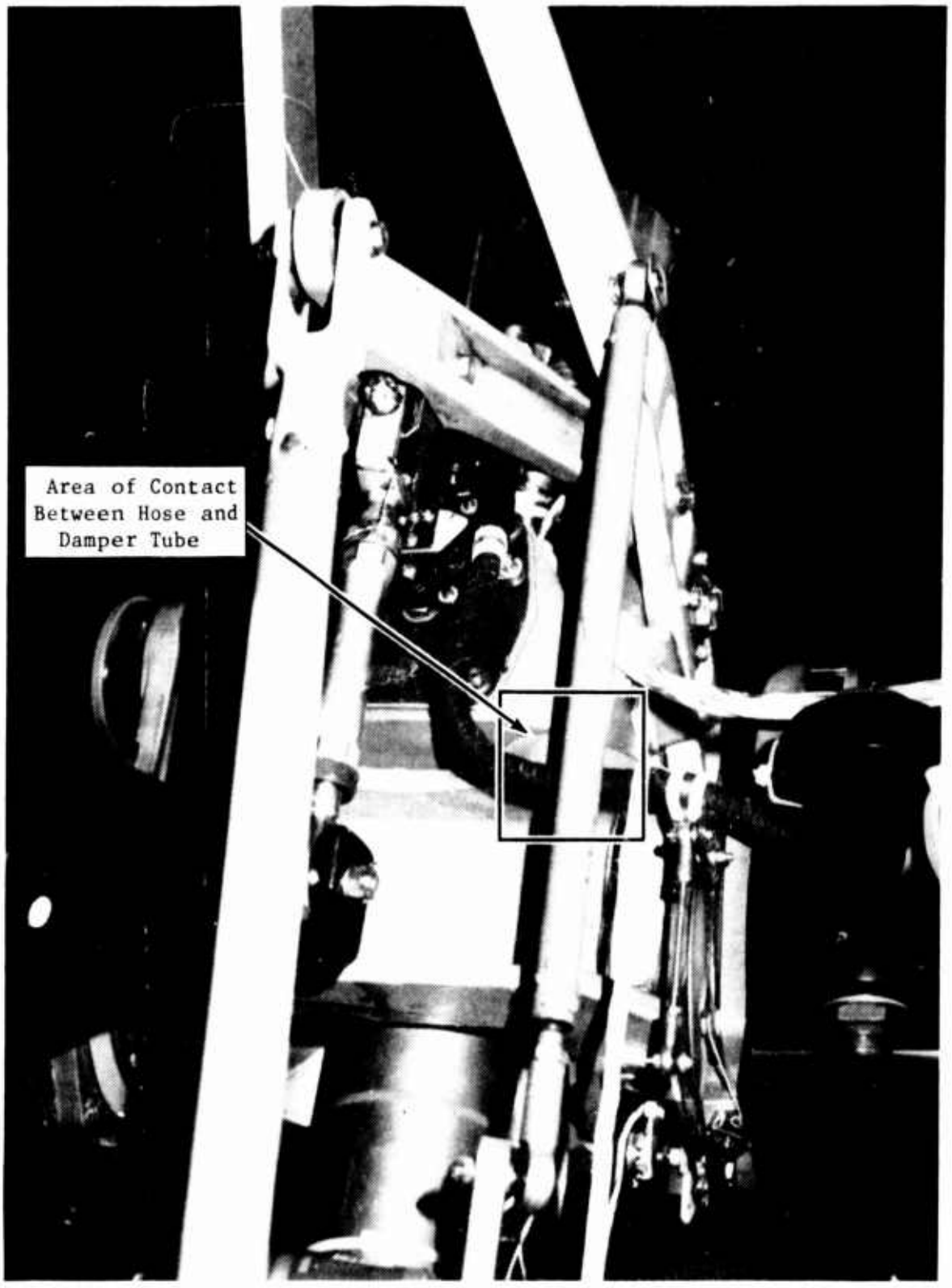

Photo 12. Hose Assembly and Damper Tube

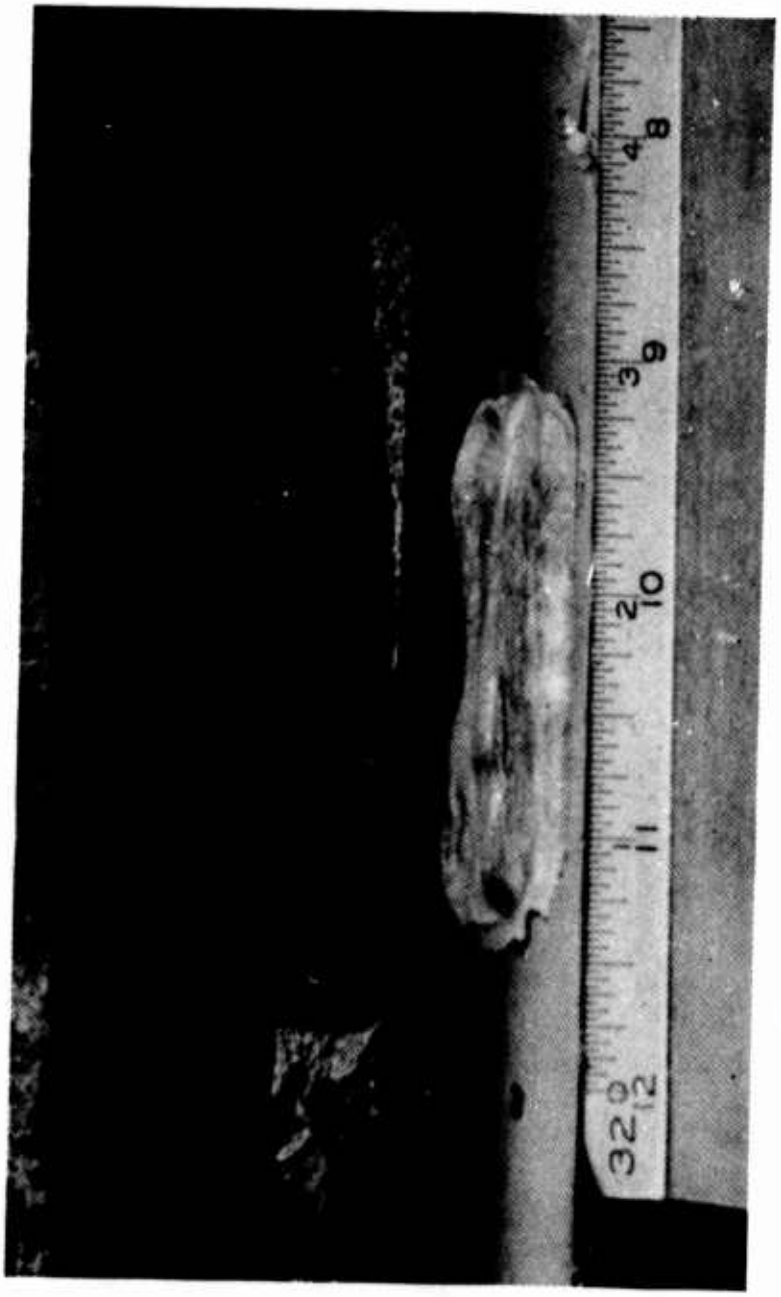

Photo 13. Abrasion of Damper Control Tube

Photo 14. Lumps in Inflatable Section

Photo 15. Depression Created by Missing Manifold Material

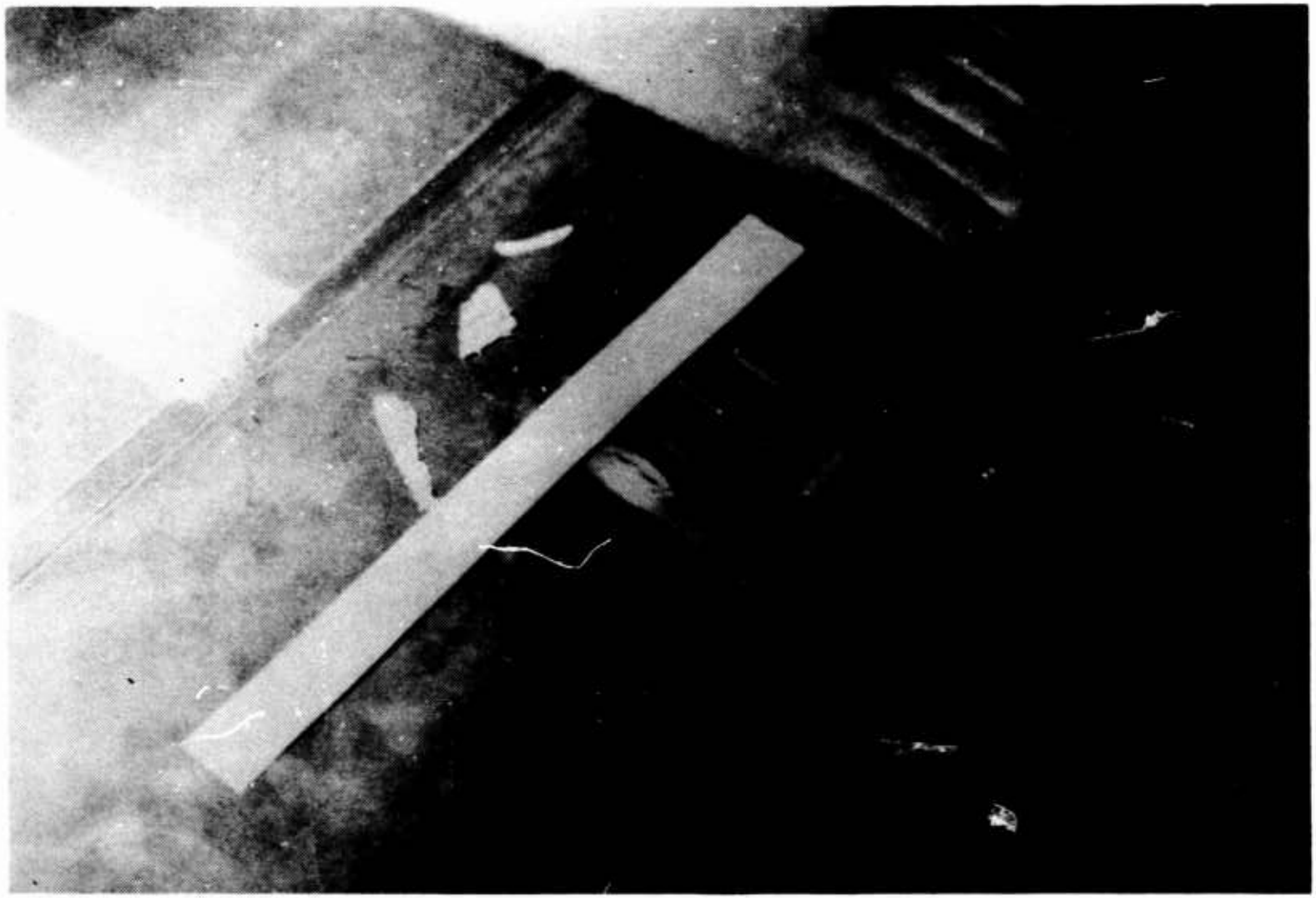

Photo 16. Cuts to Remove Manifold Material

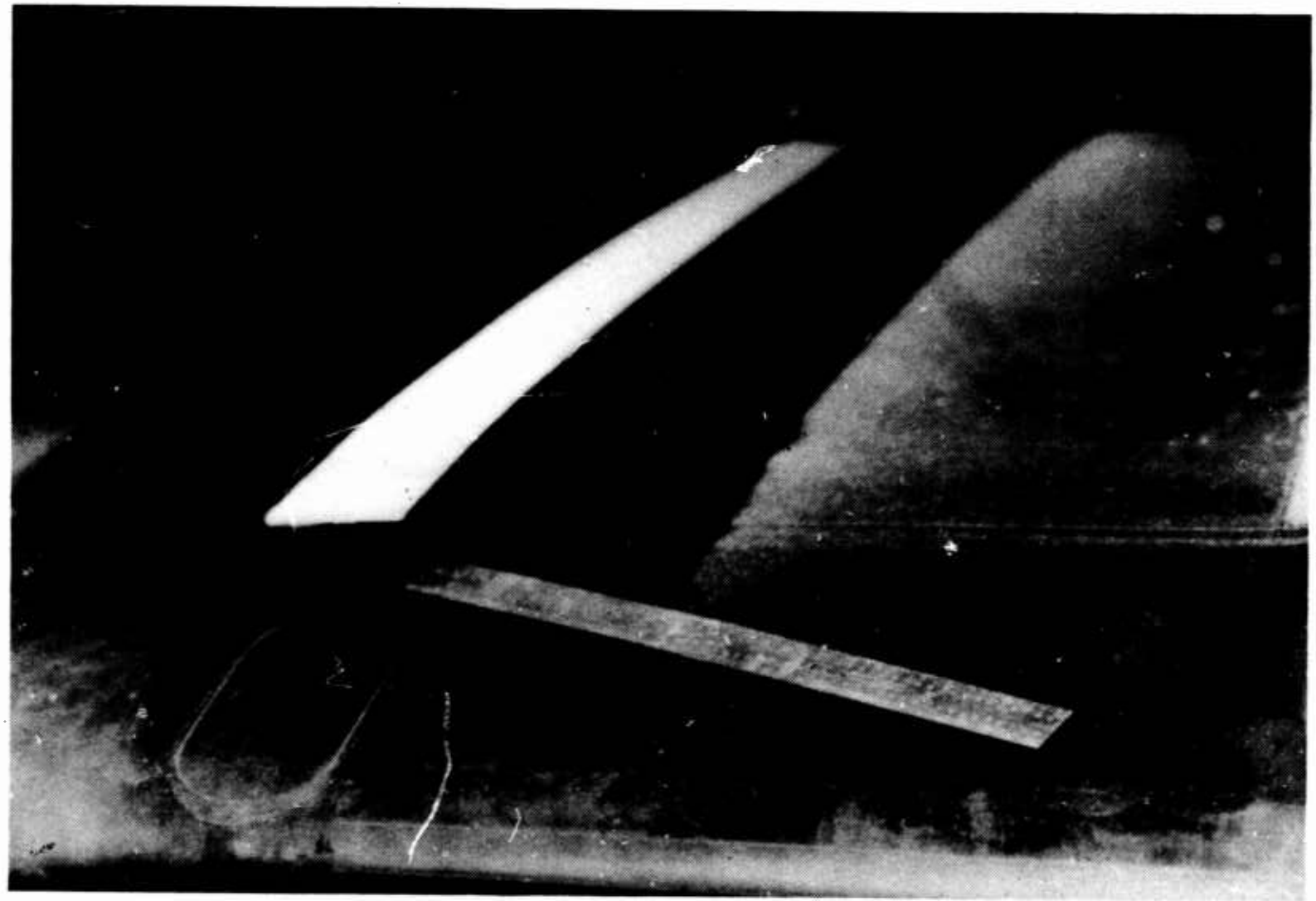

Photo 17. Repaired Cuts

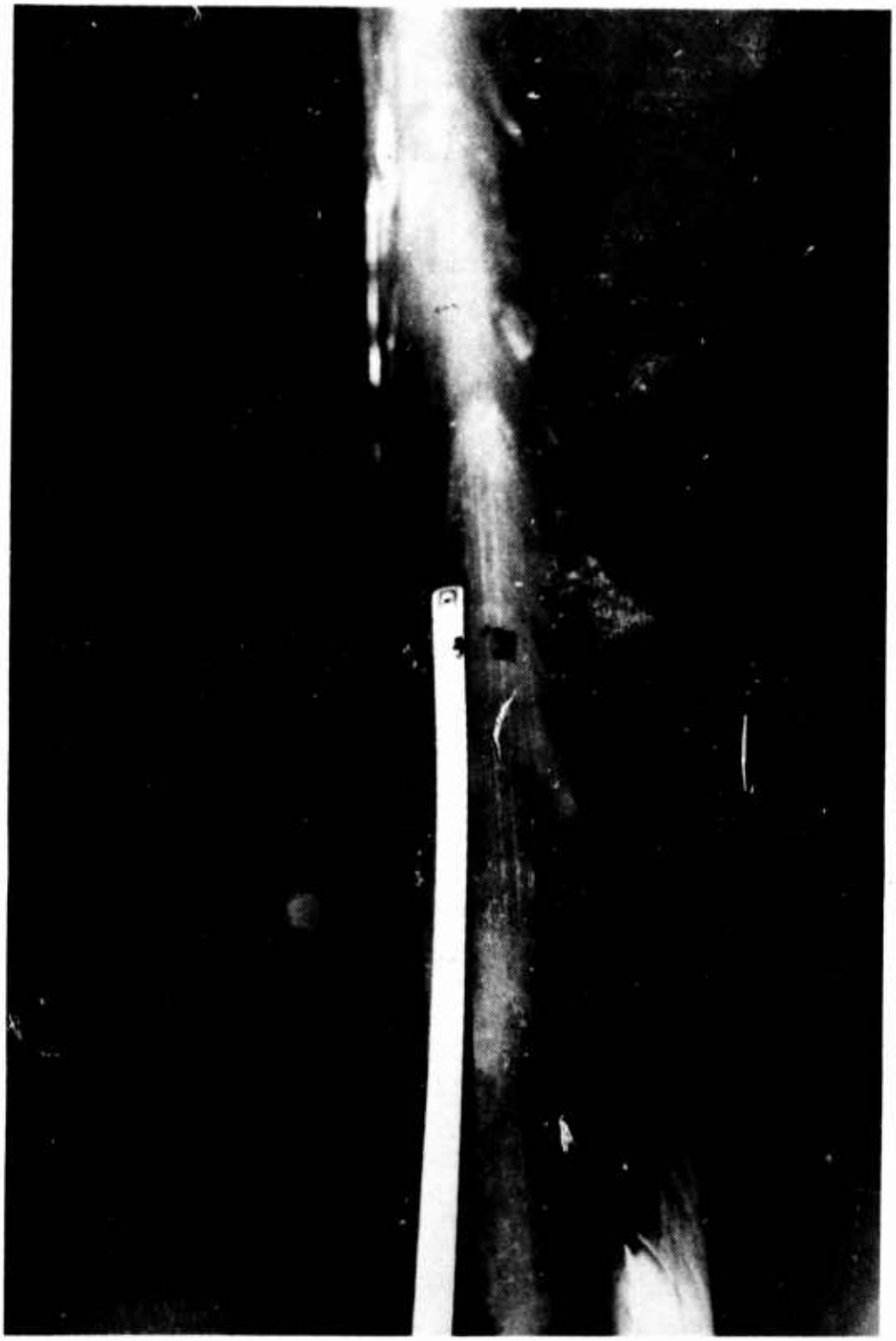

Photo 18. Impact Damage

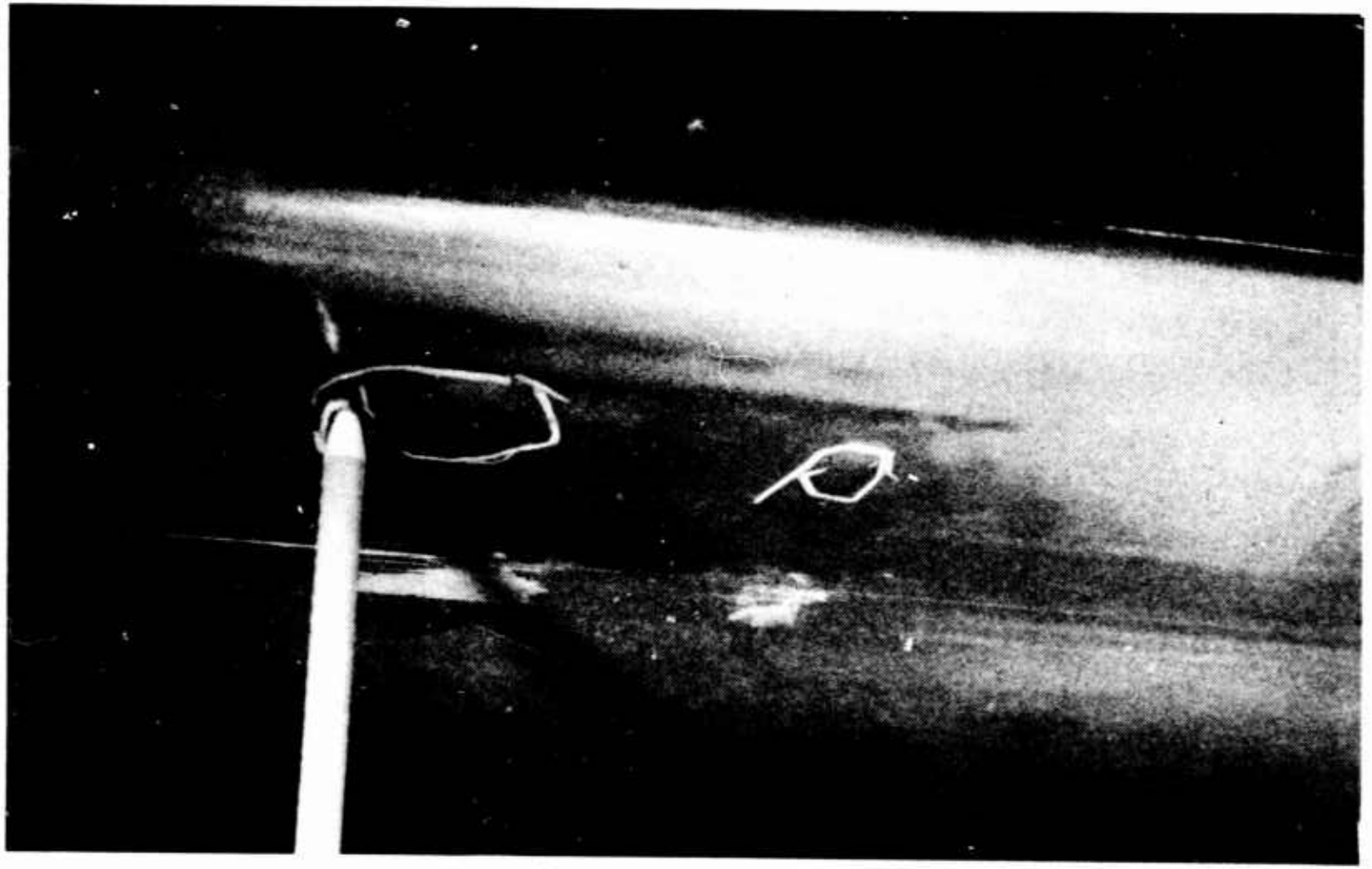

Photo 19. Water Pockets in Deicer

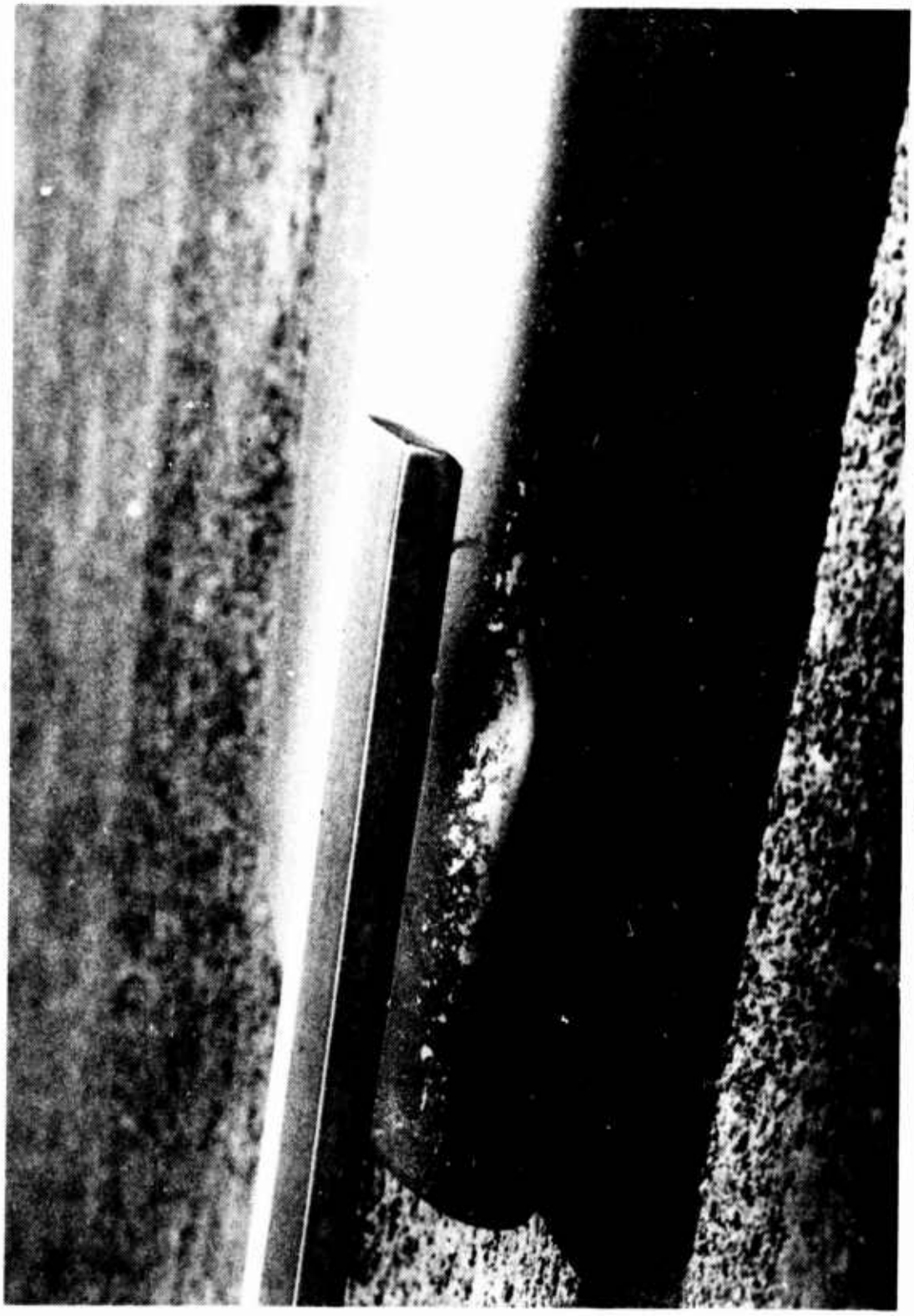

Photo 20. Damage to Tail Rotor Blade

DISTRIBUTION

HQDA (DALO-AV, DALO-FDQ, DAMO-HRS, DAMA-PPM-T, DAMA-RA, DAMA-WSA)	6
US Army Materiel Command (AMCDE-SA, AMCDE-P, AMCQA-SA, AMCQA-ST)	4
US Army Training and Doctrine Command (ATCD-T, ATCD-B)	2
US Army Aviation Systems Command (AMSAV-8, AMSAV-Q, AMSAV-MC, AMSAV-ME, AMSAV-L, AMSAV-N, AMSAV-GTD)	8
US Army Test and Evaluation Command (AMSTE-TE-V, AMSTE-TE-O)	2
US Army Logistics Evaluation Agency (DALO-LEI)	1
US Army Materiel Systems Analysis Agency (AMXSY-RV, AMXSY-MP)	8
US Army Operational Test and Evaluation Agency (CSTE-AVSD-E)	2
US Army Armor School (ATSB-CD-TE)	1
US Army Aviation Center (ATZQ-D-T, ATZQ-CDC-C, ATZQ-TSM-A, ATZQ-TSM-S, ATZQ-TSM-LH)	5
US Army Combined Arms Center (ATZL-TIE)	1
US Army Safety Center (PESC-SPA, PESC-SE)	2
US Army Cost and Economic Analysis Center (CACC-AM)	1
US Army Aviation Research and Technology Activity (AVSCOM) NASA/Ames Research Center (SAVRT-R, SAVRT-M (Library)	3
US Army Aviation Research and Technology Activity (AVSCOM) Aviation Applied Technology Directorate (SAVRT-TY-DRD SAVRT-TY-TSC (Tech Library)	2

US Army Aviation Research and Technology Activity (AVSCOM) Aeroflightdynamics Directorate (SAVRT-AF-D)	1
US Army Aviation Research and Technology Activity (AVSCOM) Propulsion Directorate (SAVRT-PN-D)	1
Defense Technical Information Center (FDAC)	2
US Military Academy, Department of Mechanics (Aero Group Director)	1
ASD/AFXT, ASD/ENF	2
US Army Aviation Development Test Activity (STEBG-CT)	2
Assistant Technical Director for Projects, Code: CT-24 (Mr. Joseph Dunn)	2
6520 Test Group (ENML)	1
Commander, Naval Air Systems Command (AIR 5115B, AIR 5301)	3
Defense Intelligence Agency (DIA-DT-2D)	1
Headquarters United States Army Aviation Center and Fort Rucker (ATZQ-ESO-L)	1
US Army Aviation Systems Command (AMSAV-EA)	1
US Army Aviation Systems Command (AMSAV-EC)	2
US Army Aviation Systems Command (AMSAV-EF)	1
US Army Aviation Systems Command (AMCPM-UH)	2
B.F. Goodrich Company, Aerospace and Defense Division (Mr. Norb Weisend)	4
NASA-Lewis Research Center, M/S 86-7 (Mr. Reinmann)	4
Director, Aviation Applied Technology Directorate (SAVRT-TY-ASR (Mr. Young))	2